2013

Multi-column multi-layer computational model of neocortex

Beata Strack
Virginia Commonwealth University

MULTI-COLUMN MULTI-LAYER COMPUTATIONAL MODEL OF NEOCORTEX

A Dissertation submitted in partial fulfillment of the requirements for the degree of Doctor of Philosophy at Virginia Commonwealth University.

by

BEATA STRACK

M. Sc., AGH University of Science and Technology, Poland, 2008

Director: Krzysztof J. Cios

Professor and Chair, Department of Computer Science

Virginia Commonwealth University

Richmond, Virginia

December, 2013

TABLE OF CONTENTS

LIST OF TABLES

LIST OF FIGURES

Abstract

MULTI-COLUMN MULTI-LAYER COMPUTATIONAL MODEL OF NEOCORTEX

By Beata Strack

A Dissertation submitted in partial fulfillment of the requirements for the degree of Doctor of Philosophy at Virginia Commonwealth University.

Virginia Commonwealth University, 2013.

Director: Krzysztof J. Cios

Professor and Chair, Department of Computer Science

We present a multi-layer multi-column computational model of neocortex that is built based on the activity and connections of known neuronal cell types and includes activity-dependent short term plasticity. This model, a network of spiking neurons, is validated by showing that it exhibits activity close to biology in terms of several characteristics: (1) proper laminar flow of activity; (2) columnar organization with focality of inputs; (3) low-threshold-spiking (LTS) and fast-spiking (FS) neurons function as observed in normal cortical circuits; and (4) different stages of epileptiform activity can be obtained with either increasing the level of inhibitory blockade, or simulation of NMDA receptor enhancement.

The aim of this research is to provide insight into the fundamental properties of vertical and horizontal inhibition in neocortex and their influence on epileptiform activity. The developed model was used to test novel ideas about modulation of inhibitory neuronal types in a developmentally malformed cortex. The novelty of the proposed research includes: (1) design and implementation of a multi-layer multi-

column model of the cortex with multiple neuronal types and short-time plasticity, (2) modification of the Izhikevich neuron model in order to model biological maximum firing rate property, (3) generating local field potential (LFP) and EEG signals without modeling multiple neuronal compartments, (4) modeling several known conditions to validate that the cortex model matches the biology in several aspects,(5) modeling different abnormalities in malformed cortex to test existing and to generate novel hypotheses.

CHAPTER 1

INTRODUCTION

One of the great challenges of science is to understand the human brain and make practical use of this knowledge. Although remarkable progress has been made in the field of neuroscience in the last 20 years, producing progressively more information about its function, neural circuits, and underlying biochemical processes, the complexity of neuronal systems still impedes full understanding of the brain. For this reason, computational models are very useful in obtaining additional insights that can be employed either to interpret experimental findings or suggest alternative biological experiments, especially in studying various neurological disorders.

Epilepsy is a neurological disorder that affects millions of patients world-wide, with 30% suffering from chronic, pharmacoresistant seizures. Intractable seizures are particularly common in patients with developmentally malformed cortex. In case of one of the most common malformations, microgyria, a number of neuronal abnormalities have been identified both prior to and after onset of epileptiform activity. The motivation for our research came from recent findings in the rodent model of microgyria (Zsombok and Jacobs,2007), suggesting that the regions surrounding the malformation have a decrease in the number of inhibitory fast-spiking (FS) interneurons (Rosen et al.,1998) but an increase in the number or effectiveness of inhibitory low-threshold spiking (LTS) interneurons (George and Jacobs,2011; Schwarz et al.,2000).

The aim of this research is to develop a multi-layer multi-column computational model of neocortex, based on the activity of known neuronal cell types and connections, including activity-dependent short term plasticity, that provides insight into

the fundamental properties of the balance between vertical and horizontal inhibition in neocortex and its influence on epileptiform activity.

The model, a network of spiking neurons, is validated by demonstrating that it matches the biology in several aspects: (1) laminar flow of activity, (2) columnar flow of activity, (3) LTS neurons function, (4) FS neurons function, (5) different stages of epileptiform activity can be observed.

The model is used to simulate not only conditions that are already investigated in biological experiments, e.g., focal and global lesions of the cortex, but also modifications of the cortex that cannot easily be performed experimentally, e.g., selective changes to functions of inhibitory subtypes. Specifically, the strength of the computational model is to separately evaluate the epileptogenic potential of known abnormalities in malformed cortex, including (1) the focal loss of deep layers, (2) the increase in excitatory afferents to neurons surrounding the malformation, (3) decrease in numbers of interneurons providing intercolumnar inhibition, and (4) increase in excitatory inputs to interneurons providing intracolumnar inhibition.

1.1 Contributions

The major contributions of this research are:

- introduction of a multi-layer multi-column model of the cortex with several neuronal types and short-time plasticity,
- modification of the Izhikevich neuron model in order to obtain biologically valid maximal firing rate property,
- generating local field potential (LFP) and EEG signals with detailed description of neuronal connectivity, not by modeling multiple compartments of a neuron,
- modeling several known conditions to proof that the cortex model matches the

biology in selected aspects,

- modeling different abnormalities in malformed cortex and generating novel hypotheses.

This dissertation is organized as follows. Chapter 2 provides biological and computational background of the proposed research and review of the state of the art methods. Chapter 3 contains a description of the components and topology of the network. Chapter 4 presents the results that validate our model as biologically accurate. Chapter 5 contains results of modeling simple lesions of the cortex with our model. Chapter 6 presents results of modeling malformed cortex and imbalanced inhibition. In Chapter 7 we briefly discuss our approach to parallelization of the calculations. The research is summarized in Chapter 8.

CHAPTER 2

LITERATURE REVIEW

This chapter contains discussion of the state of the art in computational neuroscience with emphasis on computational models applied to epilepsy. First, in Section 2.2,the elementary biological notions that are necessary to understand the presented research are introduced: elementary properties of the cortex, basic information about epilepsy, and biological findings that motivated our research. Next, we discuss computational approaches used in computational neuroscience (Section 2.2).

2.1 Biological Background

2.1.1 Basic properties of the cortex

All behavior, whether it is a simple reflex response or a complex mental act, is mediated by the central nervous system which consists of the spinal cord and the brain. The brain is composed of six regions: the medulla, pons, cerebellum, midbrain, diencephalon, and cerebral hemispheres or telencephalon (Amaral,2000).

The cerebral hemispheres, which form the largest region of the human brain, consist of the cerebral cortex, the underlying white matter, and the three deep-lying structures: the basal ganglia, the amygdale, and the hippocampal formation.

Although many life-sustaining functions are mediated by other regions of the brain, the cerebral cortex, which is the thin outer layer of the cerebral hemispheres, is responsible for much of the planning and execution of actions in everyday life and plays a key role in memory, attention, perceptual awareness, thought, language, and consciousness. It is organized in functional layers and the information flows across

the layers in interconnected sets of neurons called columns, or modules. The number of layers and details of their functional organization vary throughout the cortex, but the most typical form of neocortex contains six layers (Figure 1), numbered from the outer surface (pia mater) of the cortex to the white mater (Amaral,2000).

- Layer I is an acellular layer called the molecular layer. It contains dendrites of the cells located deeper in the cortex and axons that travel through or form connections in this layer.

- Layer II is comprised mainly of small spherical cells called granule cells and therefore is called the external granule cell layer.

- Layer III contains a variety of cell types, many of which are pyramidally shaped. This layer is called the external pyramidal cell layer.

- Layer IV, like layer II, is made up primarily of granule cells and is called the internal granule cell layer.

- Layer V, the internal pyramidal cell layer, contains mainly pyramidally shaped cells that are typically larger than those in layer III.

- Layer VI is quite heterogeneous layer of neurons and is thus called the polymorphic or multiform layer. It blends into the white matter that forms the deep limit of the cortex and carries neurons to and from the cortex.

Both horizontal and columnar organizations of the neocortex are vital to its normal operations. Thalamic input to the cortex propagates in a specific laminar fashion (Figure 2), from layer IV to II/III, to V and VI (Douglas and Martin,2004). The focality of this input is maintained by surrounding inhibition provided by basket cells that control horizontal spread of excitation (Trevelyan et al.,2006; Thomson,2003;

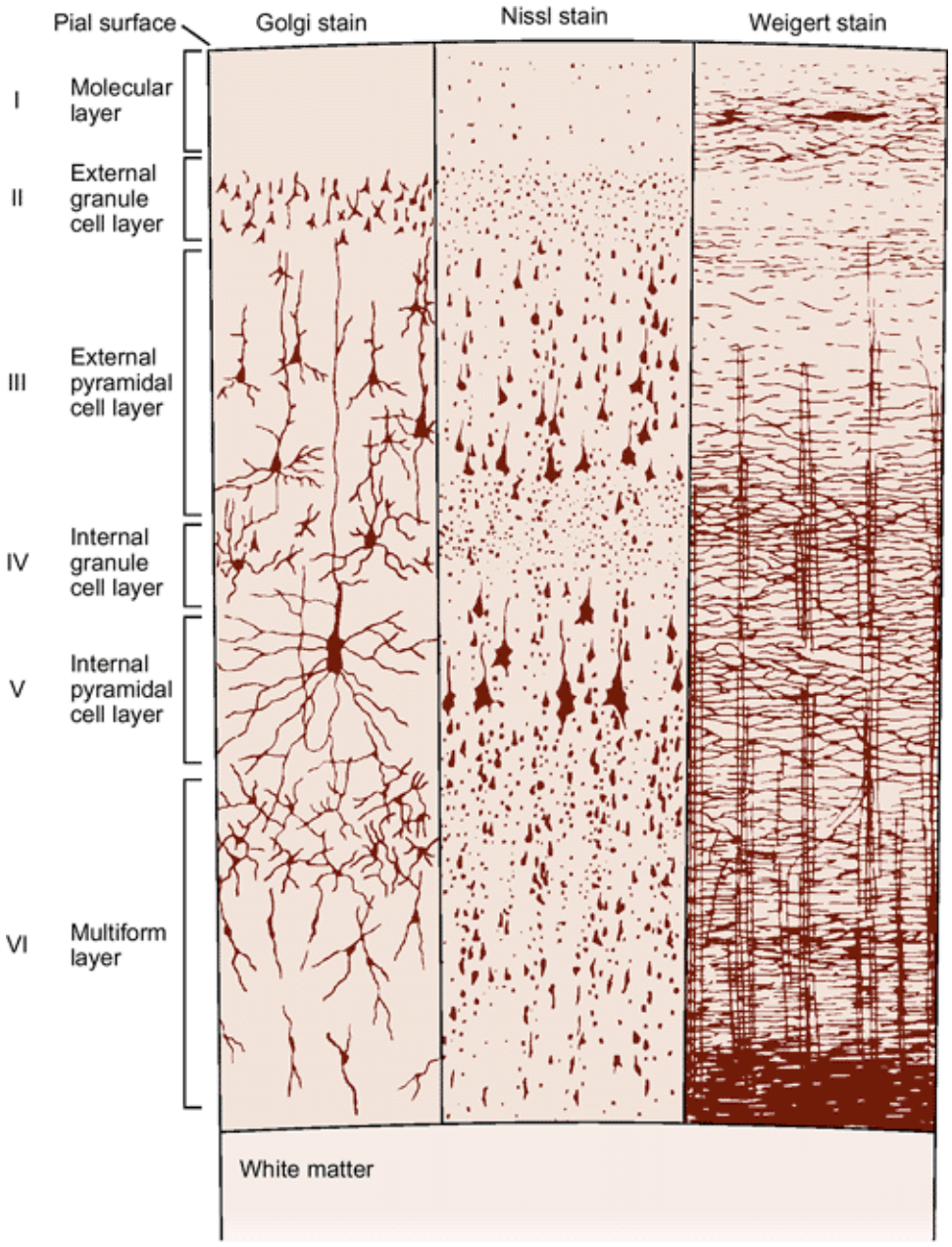

Fig. 1. The laminar organization of the cerebral cortex. Different methods of staining reveal different aspect of the cortex structure: Golgi stain shows cell bodies and dendric trees, the Nissl stain shows cell bodies and proximal dendrites, a Weighert stain for myelinated fibers shows axons. From (Kandel et al.,2000)

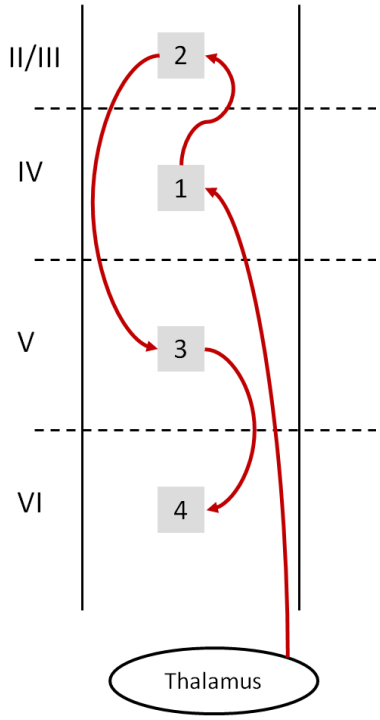

Fig. 2. Schematic representation of the flow of the thalamic input through the cortical layers.

Douglas and Martin,2004). This function of fast-spiking (FS) parvalbumin-containing inhibitory interneurons is in contrast to that of interneurons with a bipolar morphology (Kubota and Kawaguchi,1994; Kawaguchi and Kubota,1996; Wang et al.,2004) that allows for simultaneous inhibition in different layers but within a cortical column. Some bipolar interneurons contain somatostatin and have low threshold spiking (LTS) characteristics (Kawaguchi and Kondo,2002; Monyer and Markram,2004). These two inhibitory cell types vary not only in their morphology, but also in their membrane properties, synaptic inputs, as well as their postsynaptic targets (Monyer and Markram,2004; Bacci et al.,2003; Bacci et al.,2005; Kawaguchi,1993; Thomson et al.,1996). FS cells have horizontally projecting axons, mostly synapse on pyramidal somata, receive strong thalamocortical input, and are responsible for controlling

horizontal spread of excitation, while LTS cells do not receive thalamocortical input, have vertically projecting axons, and synapse mostly on dendrites of pyramidal cells. Because of this variation, significant changes in the effectiveness of LTS interneurons are expected to produce substantially different network effects than altering FS interneuron characteristics. Under certain disease conditions, these two interneuron subtypes are in fact differentially affected (Binaschi et al.,2003; Robbins et al.,1991; Kuruba et al.,2011; Hof et al.,2002; Miettinen et al.,1993; Trotter et al.,2006).

2.1.2 Epilepsy

Epilepsy is a neurological disease that is characterized by the recurrence of seizures. It is the third most common neurological disorder in the world (Hauser and Hesdorffer,1991) with about 2.5 million people diagnosed with epilepsy in the U.S and 50 million world-wide. Any disturbance of the normal neuronal activity due to illness, brain damage, or abnormal brain development can provoke seizures and subsequently lead to chronic epilepsy. Although a number of new antiepileptic drugs have been introduced, about 30% of patients are still pharmacoresistant (Kwan and Brodie,2006).

The term 'epilepsy' refers to a variety of neurological syndromes and disorders. It involves mechanisms, most often nonlinear, taking place at subcellular (i.e., membrane ion channels and neurotransmitter receptors), cellular (neurons), tissular (networks of neurons) and regional (networks of networks) scales within systems where short- or long-term plasticity also plays a crucial role (Wendling,2008). Epileptic phenomena emerge at different temporal scales: the duration of epileptic spikes is typically approximately a few hundred milliseconds, seizures can last from a few seconds up to several minutes, whereas the frequency of seizures can vary from a few per day up to a few per month in uncontrolled epilepsies (in pharmaco-controlled cases, there may

be years between seizures).

A seizure is a "transient occurrence of signs and/or symptoms due to abnormal excessive or synchronous neuronal activity in the brain" (Fisher et al.,2005). An additional aspect of the clinical definition of a seizure is the involvement of the cerebral cortex to distinguish seizures from excessive or synchronous activity elsewhere in the brain.

Intractable seizures are particularly common in patients with developmentally malformed cortex. For one of the most common malformations, the microgyria (Barkovich,2010; Blumcke et al.,2009; Golden and Harding,2010), a number of neuronal abnormalities have been identified both prior to and after the onset of epileptiform activity (Jacobs et al.,1999c; Jacobs et al.,1999b; Jacobs et al.,1999a; Jacobs and Prince,2005; Zsombok and Jacobs,2007). Our research is motivated by findings in the rodent model of microgyria (George and Jacobs,2011), suggesting that the regions surrounding the malformation have a decrease in the number of fast-spiking (FS) interneurons (Rosen et al.,1998) but an increase in the number or effectiveness of low-threshold spiking (LTS) interneurons (George and Jacobs,2011; Schwarz et al.,2000).

Interneuron subtypes have been shown to be selectively affected in other animal models of epilepsy as well as in human tissue (Buckmaster and Dudek,1997; Trotter et al.,2006). For this reason, it is necessary to evaluate FS and LTS interneurons individually. Patients with malformation-associated epilepsy often also have other neurological and cognitive dysfunctions, including mental retardation and dyslexia. Thus an understanding of the interaction between these inhibitory subtypes will be useful not only for microgyria-associated epilepsy, but for cortical dysfunction in general.

2.2 Computational modeling in epilepsy

2.2.1 Survey of approaches and results

Computational neuroscience, which can be considered a branch of system biology (Gilbert et al.,2006), combines mathematical modeling, knowledge discovery, data mining, and simulation. Although there have been some attempts to model the whole brain (Markram,2006), most models are designed for a specific applications, for instance, analysis of a particular process or a disease.

One part of computational neuroscience is modeling in epilepsy (Soltesz and Staley,2008). Diverse approaches to this field can be divided into two main groups (Wendling,2008): stochastic and deterministic. The most common stochastic approaches are Poisson (Milton et al.,1987) and Markov models (Albert,1991; Haut et al.,2005; Sunderam et al.,2001), both used for modeling seizure occurrence times, and Monte Carlo models used mainly to model the flow of molecules and ions in the synapses (Ullah and Wolkenhauer,2007).

Deterministic models, although may use some probabilities, are determined by a set of equations, parameters, and initial conditions. These approaches can be divided into two main groups (Wendling,2008): microscopic and lumped.

The 'microscopic' approach relies on detailed modeling of the structure and functions of neuron cells. The theoretical basis for development of this approach was the adaptation of the equations proposed by Hodgkin and Huxley, which was the first mathematical model to explain the voltage-dependence of ion channels (Hodgkin and Huxley,1952). Many models of neurons has been developed since then: from very simple single compartment units (Lovelace and Cios,2008; Franaszczuk et al.,2003; Izhikevich,2004; Swiercz et al.,2007), to complex, multi-compartmental models (Traub et al.,2005b; Traub et al.,2005a). Detailed modeling can be performed at different scales

starting at the cellular level (Lytton and Sejnowski,1992; Spampanato et al.,2004) and ending at the brain level (Izhikevich and Edelman,2008). Although the 'microscopic' apprach is very successful (Lytton,2008), it has a few limitations. In spite of the fact that the ever increasing computational power allows for simulating networks consisting of a large number of cells (Hereld et al.,2005; Hereld et al.,2007; Markram,2006; Migliore et al.,2006; Drongelen et al.,2005; Drongelen et al.,2007), one limitation of this approach is high computational complexity. Another limitation is the requirement of detailed knowledge on the brain's neural circuits, which makes it difficult to determine the parameters of the model. Thus, such models are often simplified in order to be useful. Additional tools that can be used with this approach are graph theory methods which have been used in the analysis of network structures (Lim et al.,2011b; Strogatz,2001; Watts and Strogatz,1998), e.g., for detecting the presence of hubs and their role in distributing seizure activity (Morgan and Soltesz,2008).

The 'lumped' approach was developed to simulate the dynamics of large ensembles of neurons and typically used a single-state variable to approximate their activity, e.g., to generate EEG signals (Silva et al.,1974). Depending on the model, a large ensemble can be interpreted to be a minicolumn, column, a Brodmann area, a thalamic nucleus, etc. (Freeman,1978; Silva et al.,1974; Silva et al.,1976). Since epilepsy often involves relatively large areas of the brain, researchers often use the second approach (Chakravarthy et al.,2007; Deco et al.,2008; Ermentrout and Saunders,2006; Silva et al.,1976; Suffczynski et al.,2004; Wendling,2008).

Computational models have been successfully used to understand different aspects of epileptiform activity, for example, the transition from interictal to ictal activity in EEG (Suffczynski et al.,2005).

2.2.2 Assessment of existing methods

The aim of our research is to study how a malformation of the cortex affects the initiation of epileptiform activity. In other words, to model changes to vertical and horizontal inhibition, which are mostly provided by LTS and FS neurons, respectively, and then test how this imbalance influences epileptiform activity. This problem has not been studied computationally before, and no currently existing model can be used for this purpose. Specifically, we are not aware of another cortical model with the two interneuron subtypes (LTS and FS neurons) that preserves the multi-layer, multi-columnar structure which is crucial for analysis of a flow of activity in normal or malformed cortex.

Inhibitory neurons have been modeled, for example in simulations of thalamocortical oscillations (Borgers et al.,2005; Bush and Sejnowski,1996; Traub et al.,1989; Traub et al.,1999, Traub et al.,2003; Traub et al.,1997; Whittington et al.,2000), but these models focus on inhibitory neurons in general, without distinguishing their subtypes. Specific inhibitory subtypes are used in models of one or several layers within one column (Cunningham et al.,2004; Traub et al.,2005b) or in large scale simulations (Izhikevich and Edelman,2008; Markram,2006; Suffczynski et al.,2001), but in these models either only global activity is the subject of analysis or they do not preserve the structure important for modeling vertical and horizontal inhibition surrounding a cortical malformation. The model described here was designed to simulate this scenario. We have already shown (Strack et al.,2013b) that our computational model generates results consistent with biological findings in conditions of either global or focal loss of layers.

The computational multilayer model presented here is a network of spiking neurons that consists of multiple cortical columns and employs the two inhibitory sub-

types, along with a detailed description of neural connections within and between layers and columns. In addition, the network includes a synapse model that allows for modeling short-time plasticity. Parameters of connections, namely, the probability of a connection, maximal amplitude, half-width of postsynaptic potential (PSP), and latency to peak of PSP, differ according to the types and location of the interconnected neurons. This allows the model to mimic several details of neuronal connections with the use of a simple neuron model.

Although there exist popular software packages, such as Neuron, Genesis, or NeuroConstruct, that allow for network modeling (Brette et al.,2007; Barela et al.,2006; Lytton et al.,1998; Lytton and Sejnowski,1992; Drongelen et al.,2005; Yang et al.,2002), we developed a new software that allows us to control the network complexity, the level of details, and the structure of the network. Our model uses descriptions of the neuronal connectivity in terms of probabilities of connections from dual cell patch clamp experiments. Importantly, the model also allows for changing structure of the selected columns. Changing the connectivity patterns and structure is crucial to our simulations but is either not possible or very difficult to achieve using the existing software packages.

CHAPTER 3

COMPUTATIONAL MODEL

We introduce here a computational multilayer model of multiple cortical columns that employs

- two inhibitory and two excitatory neuron subtypes,
- a detailed description of neural connections both within and between layers and columns,
- a synapse model that allows for modeling short-time plasticity.

Parameters of connections, such as their probability, maximal amplitude, half-width of Post Synaptic Potential (PSP), and latency to peak of PSP, differ according to types and location of interconnected neurons. This allows the model to mimic details of neuronal connections with use of a simple neuron model without multiple compartments.

The model was designed with emphasis on the following aspects:

- biologically accurate laminar and columnar flows of activity,
- normal function of LTS and FS,
- ability to generate different stages of epileptiform activity with increasing levels of inhibitory blockade.

Having all the above characteristics, this computational model can be further employed to examine properties of developmentally malformed cortex in which the inhibitory subtypes may be differently affected.

The model has been designed to be consistent with biological data regarding probabilities of connections, synapse strengths, PSP characteristics, and the number of neurons taken from published reports (Thomson and Lamy,2007). In particular, the network is built mostly from studies of paired intracellular recordings between neuronal types (Beierlein and Connors,2002; Beierlein et al.,2003), and data from Jacobs lab at VCU. The parameters of connections are gathered in Table 4 in Appendix B. As one can see, not every connection is described in the literature.

In this chapter we describe in detail the most important components of the model, starting with its structure and connectivity in Section 3.1, and ending with description of the synapse and neuron models in Sections 3.2 and 3.3, respectively. In Subsection 3.3.1 we describe how we modified the neuron model to prevent firing with larger frequencies than biologically feasible.

3.1 Spatial structure of the network

The network's topology accounts for spatial structure with five columns and four layers, however, the number of columns and layers can be easily modified. The model is consistent with the rat somatosensory cortex as follows (compare with Section 2.1):

- layer II/III - an association layer, consists of regular spiking (RS), low-threshold spiking (LTS), and fast spiking (FS) neurons.
- layer IV - the input layer (thalamus projects into this layer), contains FS and LTS neurons, as well as spiny stellate (SS) neurons, modeled as RS neurons.
- layer V - an output layer, consists not only of RS, LTS, and FS neurons but also of intrinsically-bursting (IB) neurons.
- layer VI - also generates cortical outputs and consists of RS, FS and LTS neurons.

Numbers of every neural type in each layer are shown in Table 1. Although not every aspect of cellular intrinsic properties and connectivity have been biologically examined for the mammalian neocortex, hundreds of studies have provided many required details (Connors and Telfeian,2000; Lubke and Feldmeyer,2007; Markram et al.,2004; Thomson,2003; Thomson and Deuchars,1997; Thomson et al.,2002; Voges et al.,2010; Watts and Thomson,2005). Biologically verified information was used for:

- the relative numbers of neurons within different layers (DeFelipe et al.,2002),
- the total number of GABAergic neurons in specific layers (Ren et al.,1992),
- the percentage of parvalbumin (PV)-stained neurons (FS) (Ren et al.,1992),
- the percentage of SS-immunostained neurons (LTS) (Miettinen et al.,1993; Mizukawa et al.,1987),
- the percentage of intrinsically-bursting (Connors and Gutnick,1990; Connors et al.,1982).

While there are other types of GABAergic neurons (Kawaguchi and Kondo,2002; Kubota and Kawaguchi,1994; Kubota and Kawaguchi,1997; Monyer and Markram,2004), they are in much smaller numbers, with far less known about their connectivity. Because PV- and SS-immunostained neurons make up the majority of GABAergic neurons in neocortex (Kubota and Kawaguchi,1994), we restricted our model to these two inhibitory types. The model is scaled to 5% of neurons in one column of the cortex but it preserves the ratio of each type of neurons. The total number of neurons in one column is thus 788, which gives the total of $3,940$ neurons and over $400,000$ synapses in five columns.

The spatial size of the network is also consistent with the rat somatosensory cortex, namely, the distance between the centers of columns is $400\mu m$ and the heights

Table 1. Parameters used to generate neurons of different types and the distribution of neural types across layers.

	Parameters of the neuron model					Average Number/Percentage per layer			
	a	b	c	d	Max. firing rate	Layer II/III	Layer IV	Layer V	Layer IV
RS	0.02	0.2	-5	$5-8$	160Hz	169/79%	83/73%	84/52%	230/84%
IB	0.02	0.2	-5	$2-4$	300Hz	-	-	28/17%	-
FS	$0.08-0.1$	$0.175-0.20$	-65	2	350Hz	30/14%	20/18%	33/21%	27/21%
LTS	$0-0.02$	$0.225-0.25$	-65	2	212Hz	16/7%	11/9%	15/10%	15/5%

of the layers are: $400\mu m$, $200\mu m$, $600\mu m$, and $600\mu m$, for layers II/III, IV, V and VI, respectively. When a neuron is placed in a particular layer, its spatial coordinates are chosen randomly with a uniform distribution within this layer.

The crucial aspect of designing any network is to properly design its topology. Connection between the neurons depends on the probability of connection, amplitude, short-term plasticity parameters, and the shape of the PSP. In this work, they are based on data published in the literature (Table 4 in the Appendix B). Probabilities of connections vary not only with the types of neurons but also with the columns and layers where the neurons are located. In this way, each cell type is connected in a unique way to the other cell types (Figure 3).

The probabilities define the spatial structure of the network, e.g., the degree distribution (the number of connections) or shapes of dendric trees of neurons (Figure 4). Synapses between the neurons are characterized by their strengths, which are set using the data shown in Table 4 in Appendix B. The strength of a connection was calculated as a weighted average of published results (PSP amplitudes), with weights being inverses of the reported variances. This was done to take into account the fact that values reported in different reports had different standard deviations due to different sample sizes and methods used.

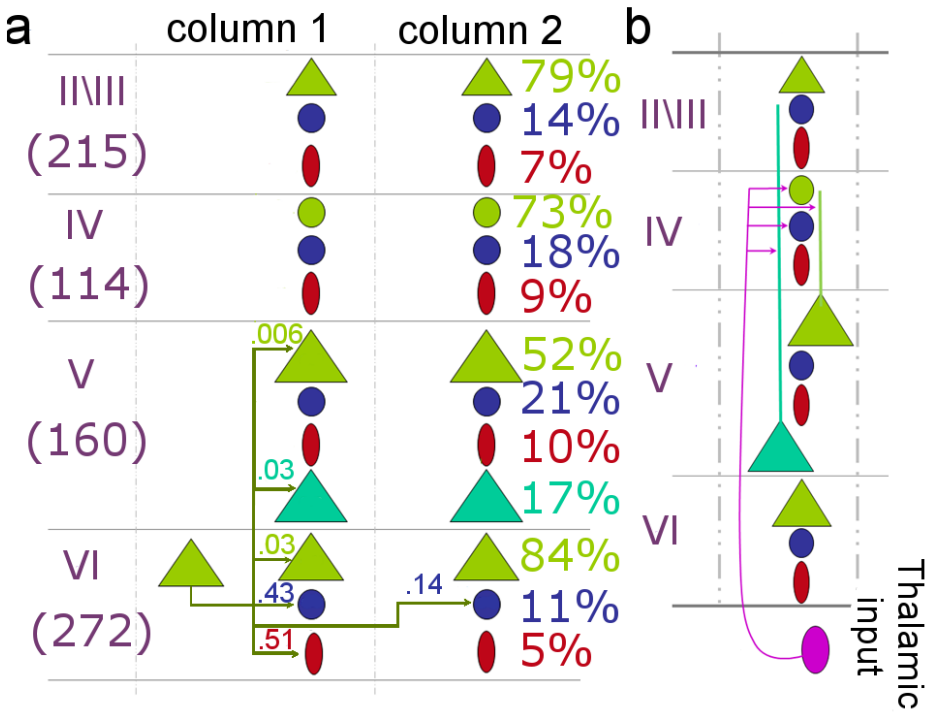

Fig. 3. Example of connectivity. (a) RS neurons (light green triangles) in layer six connect with different probabilities to LTS neurons (red ellipses) in layer VI, IB neurons (dark green triangles) in layer V, other RS neurons in layers V and VI, and FS neurons (blue circles) in layer VI within the same and adjacent columns; (b) Thalamic cell is connected to RS and FS cells in layer IV and to RS and IB cells in layer V.

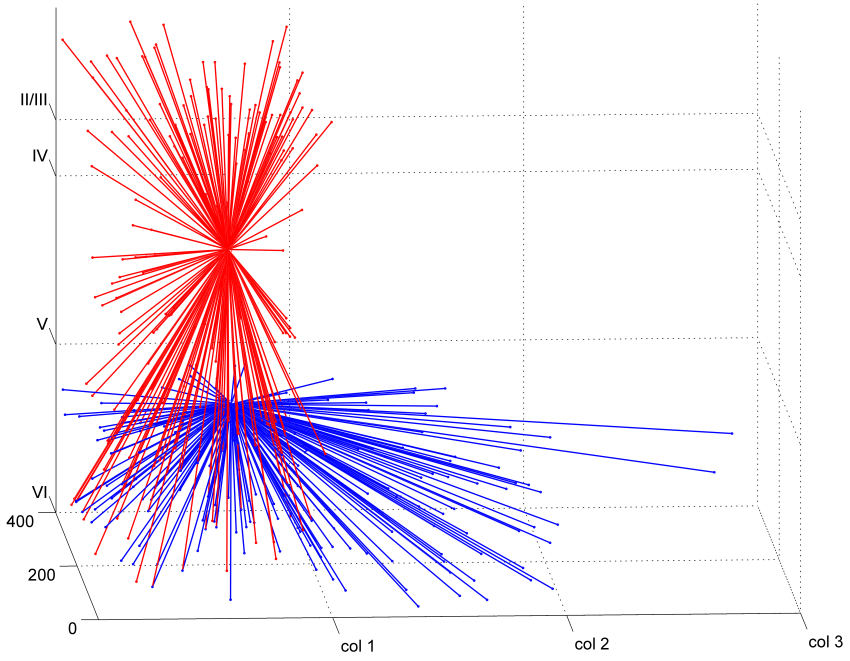

Fig. 4. Connections from an LTS neuron in layer V (red) and FS neuron in layer VI (blue). Both neurons were chosen randomly. It is evident that the structure of connections is vertical in case of the LTS neuron and horizontal in case of the FS neuron

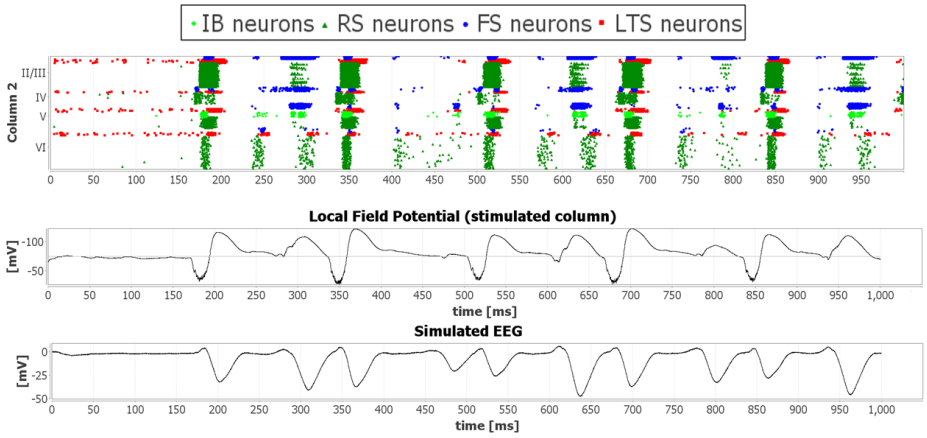

Fig. 5. Example of output generated from our simulator. Top: Spike pattern of neurons in one column: red dots represent LTS neurons, blue - FS neurons, green - RS neurons and light green IB neurons. Each dot represents a spike of a given neuron (y-axis) at a particular time (x-axis). Cells are arranged by layers within the column and by type within a layer; Middle: Local field potential calculated for this column; Bottom: EEG calculated for the entire network.

The thalamic input is modeled as a single cell connected to the selected cells within a single column and is provided to RS and FS neurons in layer IV, and to RS neurons in layer V. This is consistent with the processes that take place in rat somatosensory cortex.

The activity of the network is visualized as (a) a pattern of spikes, (b) an artificially generated local field potential (LFP), and (c) EEG (Figure 5). The spike pattern provides insight into how each neuron behaves and how single neuron responses contribute to the overall network activity. The computational EEG is generated by summation of the excitatory (EPSP) and the inhibitory (IPSP) postsynaptic potentials of all excitatory pyramidal cells in layers III and V, across all columns (Cosandier-Rimele et al.,2010). Local field potentials are calculated by adding the voltage of excitatory pyramidal cells in layers III and V in a single column. This

enables examination of the overall collective activity of the network.

3.2 Short-term plasticity and synapses

Short-time plasticity is an inherent dynamic of synapses resulting in different responses of postsynaptic neurons for different temporal patterns of pre-synaptic spikes. Specifically, the postsynaptic response can be smaller (depression) or larger (facilitation) than the previous one (Figure 6).

Research reported in (Abbott and Nelson,2000; Gilson et al.,2009; Legenstein et al.,2005; Richardson et al.,2005; Sussillo et al.,2007; Tsodyks et al.,2000) indicates that nonlinear synapses are necessary for the synchronous behavior of the network and various learning mechanisms. Therefore, including short-term plasticity is crucial for accurate modeling of network activity under a variety of conditions.

There exist well-accepted models (Morrison et al.,2008) of fast synaptic dynamics (short-term plasticity), in particular, the phenomenological model of Tsodyks and Markram (Tsodyks et al.,1998) and the model of Abbot et al. (Abbott et al.,1997). We have used the first of these models because it accounts for different synapse behaviors reported in the literature, e.g., short term dynamics of neocortical synapses in layer VI (Beierlein and Connors,2002), the depressing connection between layer II/III RS neurons (Feldmeyer et al.,2006), and facilitating connection from RS to LTS neurons in layer IV (Beierlein et al.,2003).

The model consists of four differential equations:

$$\begin{cases} x' = \frac{z}{\tau_{rec}} - ux\delta\left(t - t_{pres}\right) \\ y' = -\frac{y}{\tau_I} + ux\delta\left(t - t_{pres}\right) \\ z' = \frac{y}{\tau_I} - \frac{z}{\tau_{rec}} \\ u' = -\frac{u}{\tau_{fac}} + U(1-u)\delta\left(t - t_{pres}\right) \end{cases} \tag{3.1}$$

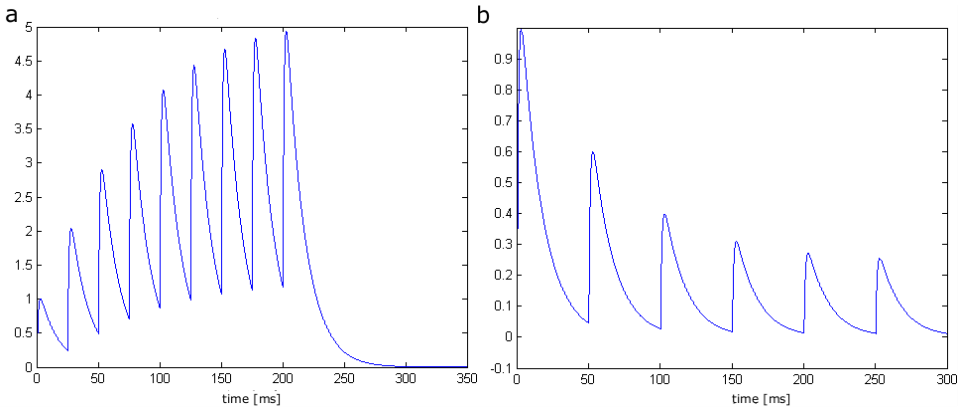

Fig. 6. Post-synaptic potentials generated with presence of short-term plasticity. (a) Example of a facilitating synapse. PSP generated as a response to a trial of nine pre-synaptic spikes with 40 Hz frequency. STP parameters: $\tau_I = 3.0$, $\tau_{rec} = 150$, $\tau_{fac} = 200$, $U = 0.02$ (b) Example of a depressing synapse. PSP generated as a response to a trial of six pre-synaptic spikes with 20 Hz frequency. STP parameters: $\tau_I = 3.0$, $\tau_{rec} = 350$, $\tau_{fac} = 0.0000001$, $U = 0.5$.

Here x, y, and z are the fractions of the synaptic resources in the recovered, active, and inactive states, respectively, t_{pres} is the time of the pre-synaptic spike, τ_I is the decay constant of the postsynaptic current, and τ_{rec} represents the recovery from the synaptic depression. The variable u is the fraction of the available resources used by the pre-synaptic spike. It increases with each pre-synaptic spike (this change is described by constant U) and decays accordingly to τ_{fac}.

These equations can be solved using exact integration technique, since between consecutive pre-synaptic spikes the system can be integrated linearly (Morrison et al.,2008).

The synapse behavior, e.g., the rate of facilitation or depression, varies not only with types of pre- and post-synaptic neurons but also with the layers where neurons are located. We gathered data from many published reports and chose the parameters in the model to reflect the reported behavior (Table 4, Appendix B).

When the pre-synaptic neuron fires the input to the post-synaptic neuron, the Post Synaptic Potential (PSP) is calculated as

$$PSP(t) = wy(t)C_{norm}\left(e^{-t/\tau_1} - e^{-t/\tau_2}\right) \tag{3.2}$$

where w is the weight of the connection, y is the fraction of active resources in the synapses calculated according to (3.2), τ_1 and τ_2 are decay constants, and C_{norm} is a normalizing constant. The values of τ_1, τ_2, and C_{norm} are chosen to match the shape of PSP reported in the literature for a particular connection (Table 4, Appendix B).

3.3 Neuron model

A simple neuron model introduced by Izhikevich (Izhikevich,2003) is used since it realistically mimics spike patterns of different neuron types while being computationally simple (Izhikevich,2004).It has been already used in a wide range of applications, e.g. modeling of multisensory processing (Lim et al.,2011b; Lim et al.,2011a), racing car controllers (Yee and Teo,2011), character recognition (Bhuiyan et al.,2009), and in large scale simulations of the thalamocortical circuits (Izhikevich and Edelman,2008). There are also multiple hardware circuit implementations of this model (Van Schaik et al.,2010; Demirkol and Ozoguz,2011).

The Izhikevich neuron model is a two dimensional system of nonlinear ordinary differential equations of the form

$$\begin{cases} v' = 0.004v^2 + 5v + 140 - u + I \\ u' = a(bv - u) \end{cases} \tag{3.3}$$

with the condition

$$\text{if } v > 30, \text{ then } v = c, u = u + d, \tag{3.4}$$

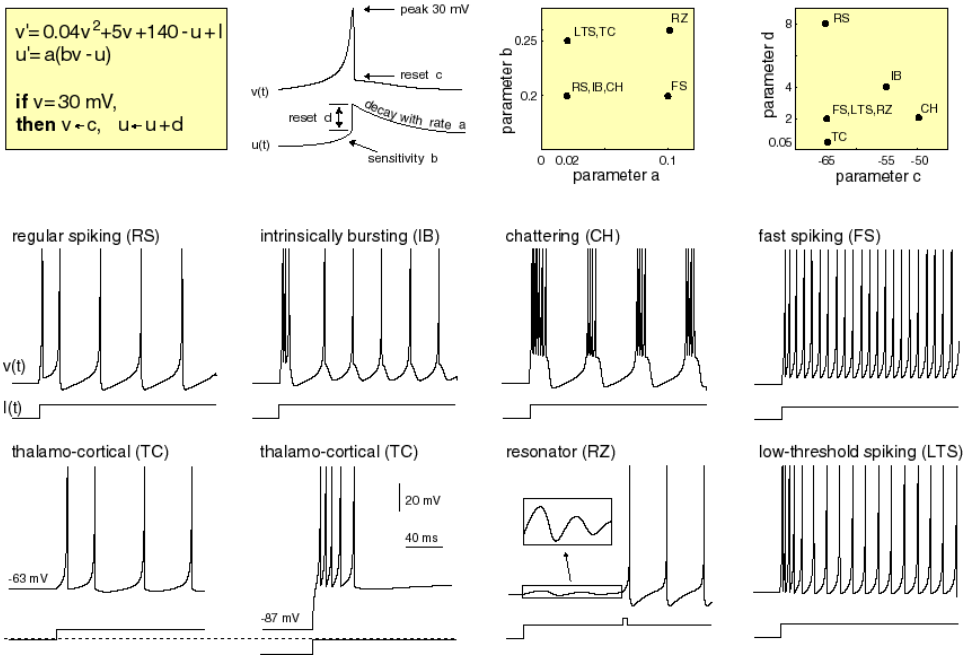

Fig. 7. Known types of neurons correspond to different values of the parameters a, b, c, d in the model described by equations (3.3), (3.4). RS and IB are cortical excitatory neurons. FS and LTS are cortical inhibitory interneurons. Each inset shows a voltage response of the model neuron to a step of dc-current $I = 10$ (bottom). This figure is reproduced with permission from www.izhikevich.com. Electronic versions of the figure and reproduction permissions are available at www.izhikevich.com

where v represents the membrane potential of the neuron and u is a membrane recovery variable (both are functions of time), a, b, c, and d are dimensionless parameters (Figure 7), and I is the value of the input to the neuron. The membrane potential v has an mV scale and the time has an ms scale in this model.

Depending on the values of parameters in equations (3.3) and (3.4) this model can mimic the spike pattern of different types of neurons (Figure 7). Similar quadratic models have been introduced (Latham et al.,2000; Hansel and Mato,2001) but the Izhikevich model seems to be the most frequently used. One of the reasons is that it has been clearly demonstrated (Izhikevich,2004) that various spiking patterns can be

easily obtained by different settings of the parameters a, b, c, and d.

Parameters used for generating types of neurons used in our network are shown in Table 1 and are consistent with the values previously published (Izhikevich,2003). To achieve heterogeneity in the neurons' dynamics, some parameters have been fixed and some generated from a uniform distribution on a given interval.

The value of input (I in equation (1)) represents all summed inputs provided to the neuron at a given time (I = I(t)), including post-synaptic potentials or direct stimulation. In addition, white Gaussian noise is provided to all neurons (independently) for two main reasons. First, to take into account that each neuron receives more connections than modeled. Large sum of independent inputs can be approximated by the Gaussian distribution (by the central limit theorem), so adding this kind of noise is a way to simulate additional distant connections. Second, with absence of any stimulus, biological networks exhibit spontaneous activity. This kind of activity does not occur in artificial networks without presence of noise.

The fact that various compartments of a neuron are not modeled is compensated by the use of realistic PSP shapes, timings, STP, and biologically measured strengths of connections, as described in the previous sections. For example, the fact that LTS and FS neurons likely terminate along different parts of the somato-dendritic axis of pyramidal neurons is reflected in the network by different average amplitudes and half-widths of the generated IPSPs. In this way, without a separate compartment, we are still able to model the difference in synaptic connectivity to dendrites versus somata.

3.3.1 Modification of the Izhikevich neuron model

Although it is a very popular neuron model, it obviously is only a simplification of real neural cell dynamics and therefore it is necessary to understand its limitations

before it can be used. One of its limitations, is the fact that the model can produce spikes with arbitrarily high frequency, which is not a biologically feasible behavior. Note that this issue is not unique to this neuron model, e.g., the firing rate of the leaky integrate-and-fire neuron model is proportional to the value of input (Dayan and Abbott,2001).

Since in the Izhikevich model the change in the voltage v depends linearly on input, the frequency of generated spikes is not bounded. A spike is always generated when condition in equation (3.4) is satisfied. In cases of a powerful input (I in equation (3.3)), the neuron can spike arbitrarily fast. Such pre-synaptic neuron spiking with high frequency causes large changes in the amplitude of PSP in the post-synaptic neuron (Figure 8), which can result in a cascade of biologically unfeasible and numerically unstable activity. This can be even further amplified if the network includes a model of frequency-dependent plasticity (short term dynamics).

The relationship between the simulated firing rate and the input amplitude is shown in Figure 9. We consider four different neuron subtypes: regular spiking (RS), intrinsically bursting (IB), fast-spiking (FS), and low-threshold spiking (LTS) neurons.

It is well known that FS neurons fire at frequencies much higher than RS or LTS neurons. Observed maximum rates of FS neurons range from 300-500 Hz (McCormick et al.,1985; Agmon and Connors,1992; Connors and Gutnick,1990; Kawaguchi and Kondo,2002). It is also well known that due to their ability to burst, IB cells fire at much higher frequencies than RS cells. Observed maximum rates of intraburst frequencies range from 300-500 Hz (Connors and Gutnick,1990; Chagnac-Amitai and Connors,1989b; Schwindt and O'Brien,1997). Maximum rates for RS and LTS cells have been reported in the ranges of 150-200 and 200-250 Hz, respectively (McCormick et al.,1985; Agmon and Connors,1992; Connors and Gutnick,1990; Kawaguchi and

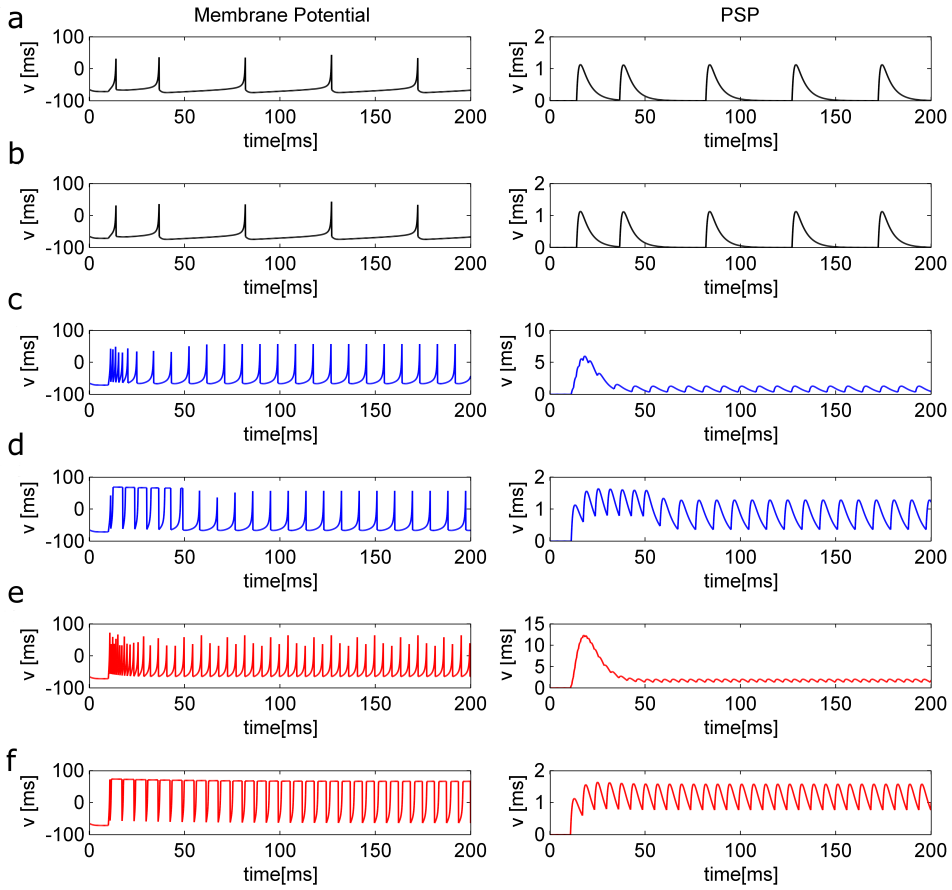

Fig. 8. Comparison of membrane voltage of a pre-synaptic neuron (left column) and PSP in the post-synaptic neuron (right column) generated with use of the original Izhikevich neuron model (panels a, c, and e) and with our modification (b, d, and f). The pre-synaptic neuron is an RS cell depolarized with currents of different amplitude: 10 (black), 50 (blue), and 100 (red). In the last two cases, the maximal firing frequency of RS neurons (160 Hz) is exceeded resulting in large increase in PSP amplitude. This issue is fixed with our modification (compare c and e with d and f, respectively). STP parameters: $\tau_I = 3.0$, $\tau_{rec} = 10$, $\tau_{fac} = 10$, $U = 0.1$. Parameters of the RS neuron: $a = 0.02$, $b = 0.2$, $c = -65$, $d = 8$.

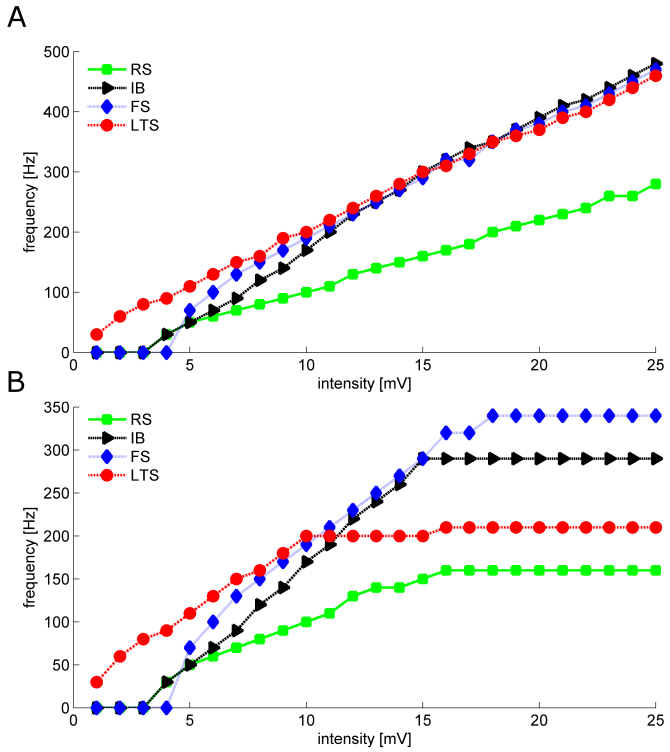

Fig. 9. Frequency of spikes versus intensity (amplitude) of the input of the original (A) and modified (B) Izhikevich neuron model. Maximal firing frequencies were assumed to be 160 Hz, 300 Hz, 350 Hz, and 212 Hz for RS, IB, FS, and LTS neurons respectively. The following parameters were used to generate different neuron types: RS: $a = 0.02$, $b = 0.2$, $c = -65$, $d = 8$, IB: $a = 0.02$, $b = 0.2$, $c = -55$, $d = 4$, FS: $a = 0.1$, $b = 0.2$, $c = -65$, $d = 2$, LTS: $a = 0.02$, $b = 0.25$, $c = -65$, $d = 2$. Frequency was averaged over 100 ms of stimulation.

Kondo,2002; George and Jacobs,2011). We set the maximum rates of IB, RS, FS, and LTS to 300, 160, 350, and 212 Hz, respectively.

Network approach to computational brain modeling requires a careful choice of all components of the network to make sure that they are not only biologically correct and computationally stable by themselves, but also in a network. Moreover, it is crucial to realize what range of activity is going to be modeled and foresee possible issues for computational stability of the network. This is especially critical when modeling epileptiform or synchronous activity that can result in excitation greater than under normal conditions.

Figure 9A shows that using the standard Izhikevich model, the maximal firing frequency is exceeded for all considered neuron types with an input in the range of $I = 10\text{-}16$. Such input level is not unusual under normal conditions and is surely exceeded in scenarios with extremely powerful excitation, e.g., simulations of inhibitory blockade (biologically achieved for example by application of bicuculline (Chagnac-Amitai and Connors,1989a; Hwa and Awoli,1989)) where the strength of inhibitory neurons is decreased, or situations of synchronous activity of excitatory neurons which generate synchronized input to post-synaptic neurons.

To address this problem, we prevent the generation of an action potential if the time from the previous spike (inter-spike interval, ISI) is shorter than given by the maximum firing frequency for that neuronal subtype. In this case, the membrane voltage is reset to 30 mV for computational stability. In other words, equation (3.4) is replaced by

$$\text{if } v \geq 30 \text{ and } t - t_{prev} \geq \tau_{min}, \text{ then (spike generated)}$$

$$\begin{cases} v & \leftarrow & c \\ u & \leftarrow & u + d, \end{cases} \tag{3.5}$$

else if $v \geq 30$, then (no spike)

$$v \leftarrow 30,$$

where t_{prev} is time of the previous spike and τ_{min} is inter-spike interval in milliseconds given by the maximum firing frequency.

Since the modification imposes an absolute refractory period, it enforces an upper bound on the maximum firing frequency of a neuron. The impact of this modification on the firing rates of different neuron models is shown on Figure 9B. The frequency increases with increasing amplitude of input until it reaches the predefined firing frequency, which is more biologically feasible behavior than in the original neuron model (Figure 9B).

3.3.1.1 Network dynamics

To illustrate the importance of the maximum firing rate in a network dynamics, we use an artificial network introduced in Izhikevich,2003. It consists of 800 regular spiking (RS) neurons and 200 fast-spiking (FS) neurons, thus keeping the ratio of excitatory to inhibitory neurons of $4:1$. All neurons are interconnected with the strengths of synaptic connections chosen randomly from the interval $(-1, 0)$ in case of inhibitory connections, and from the interval $(0, 0.5)$ for excitatory connections. In addition to the synaptic input, each neuron receives a noisy input with Gaussian distribution (mean value of zero, variance of five and two for excitatory and inhibitory neurons respectively). We will refer to this network as the original network.

We compare this network with one with the modified neuron model (see Figure 10). The maximum firing frequency is 160 Hz and 350 Hz for RS and FS neurons respectively, as described above. To achieve heterogeneity, we vary these frequencies $\pm 10\%$. Two different scenarios were tested: increasing the input to neurons and

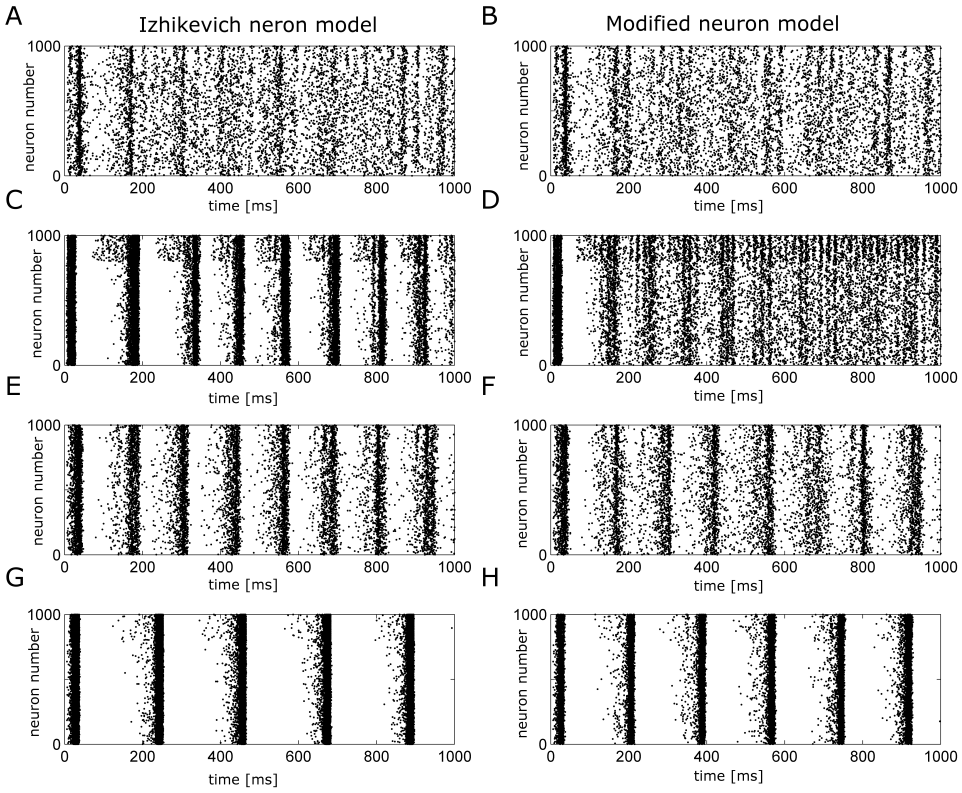

Fig. 10. Comparison of spike activity of two networks across different scenarios. The horizontal axis is time and the vertical axis is the neuron number, with each dot representing a single action potential and each row the activity from one neuron. The network is taken from (Izhikevich,2003) and consists of regular-spiking (neuron numbers 1-800) and fast-spiking (neuron numbers 801-1000) neurons. (A-B) The original (left) and modified (right) networks with a normal level of activity. (C-D) The variance of the noisy input increased to the value of two for all neurons. (E-F) 20% inhibitory blockade. (G-H) 50% inhibitory blockade.

blocking the inhibitory synapses. Results of these simulations are shown in Figure 10. All simulations were calculated with a time step of 1 ms.

First, the input to the neurons was artificially increased by changing the mean value of the noise to two for all neurons. Note that this change was quantitatively bigger for FS than for RS neurons (change to 40% and 67% of the initial variance for these types, respectively). Interestingly, although the network with modified neuron model (Figure 10D) is less synchronized than the original network (Figure 10C), there is still some synchrony. Indeed, analysis of artificially generated EEG (see Figure 11), which was computed as a sum of all inputs to the excitatory neurons (Cosandier-Rimele et al.,2010), shows that the modified network exhibits oscillations with frequency of 43 Hz that corresponds to the gamma band, contrary to the original network that oscillates with 10 Hz frequency. This result is consistent with findings that increased input to FS neurons results in generating gamma oscillations (Traub et al.,2005b).

Secondly, we kept the level of input as in the original network but we blocked inhibitory neurons, that is reduced their strengths by 20% and 50%. We see that in the case of 20% inhibitory blockade the network with the modified neuron model (Figure 10F) is less synchronized than the original network (Figure 10F). With higher inhibitory blockade the network is synchronized (Figure 10H) but with slightly different frequency compared to that in the original network (Figure 10G). This described that this modification strongly impacts network behavior. In (Strack et al.,2011) and (Strack et al.,2013b) we presented a multi-column, multi-layer cortex model that uses the modified neuron model. We demonstrated that under inhibitory blockade conditions the network generates local field potentials (LFP) that are comparable with those experimentally measured.

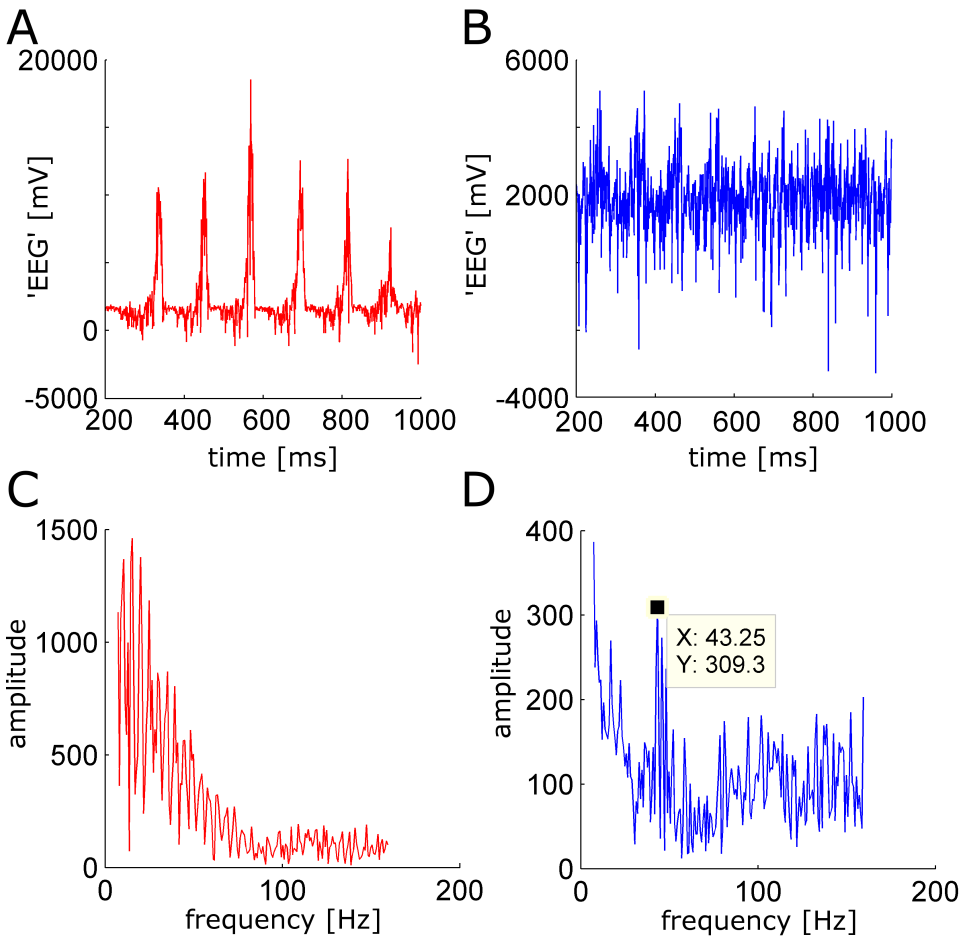

Fig. 11. Comparison of frequencies generated with use of the original (red) and modified (blue) neuron models in case of increased input to the network (compare Figure 2C-D). (A-B) artificial EEG generated for both networks. (C-D) Amplitude of Fourier transform of both signals.

CHAPTER 4

VALIDATION OF THE MODEL

Validating computational models, especially the ones of epilepsy, is not a straightforward task (Soltesz and Staley,2008) mostly because the same kind of activity, e.g., a seizure, can be caused by different underlying processes. With the current state of knowledge, it is not possible to build a comprehensive model of the cortex that matches biology in each and every detail.

Thus, it is important to validate a model by assuring that it replicates known biological behaviors that are crucial for particular applications of the model. We validate our model on the following aspects that are critical for the functioning of a normal multi-layer multi-columnar cortex:

1. proper laminar flow of activity,
2. columnar organization with focality of inputs,
3. LTS neurons function properly, that is
    (a) enhancement of their input produces local 1 Hz oscillations,
    (b) reduction of their activity does not induce epileptiform activity, since they perform a primarily modulatory function,
    (c) blockade of their function does not cause spread of activity to adjacent columns, since their output is intracolumnar,
4. FS neurons function properly, that is

(a) when they are blocked within one layer, activity in that layer spreads to adjacent columns

(b) when activity in these neurons is increased, a gamma rhythm is induced in the network

5. different stages of epileptiform activity (interictal-like and ictal-like) can be observed with either increasing levels of inhibitory blockade, or enhancement of NMDA receptors.

In this chapter we present results of our simulation experiments. In Section 4.1 we present results of validation of the proposed model and discuss them in Section 4.2. All simulations were performed on a network consisting of five columns with a time step of 0.1 ms, second column is stimulated, and Gaussian noise with zero mean and standard deviation of eight is added to the network (unless indicated otherwise). All results were evaluated by a neuroscience expert.

4.1 Results

We sought to validate that the designed model emulates the biology in terms of the following characteristics:

4.1.1 Laminar- and Columnar- selective flow of activity

In order to determine whether the proper laminar flow of activity occurs, we examined the timing of activity in different layers after thalamic input (activation of the selective thalamic cell, see Fig 3). Thalamic input to one column resulted in activity occurring first within layer IV, followed by activity in layer II/III, and then in layers V and VI, similar to what was shown biologically (Douglas and Martin,2004). In addition, the excitation occurs most prominently within the stimulated column. Al-

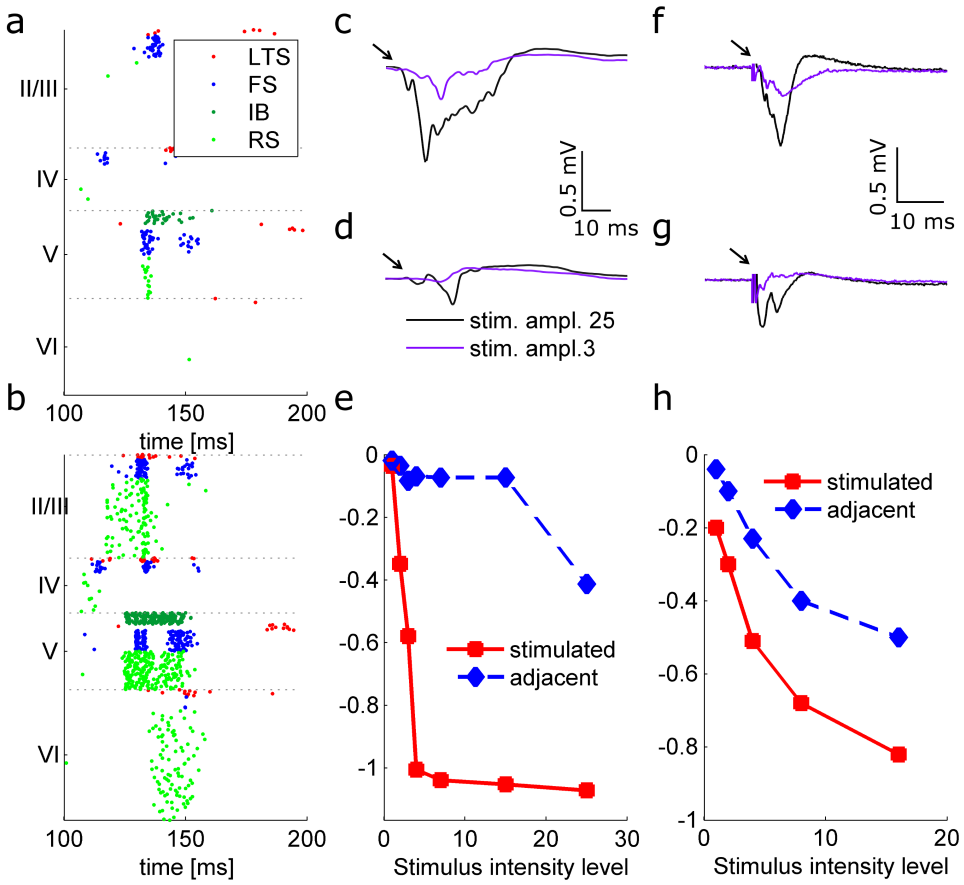

Fig. 12. Laminar and columnar flow of activity. (a-b) Spike pattern of activity in an adjacent (a) and the stimulated (b) columns as a response to stimulus with amplitude 3. (c-d) Computational Local Field Potentials (LFP) in the stimulated (c) and an adjacent (d) column as a response to two different levels of input. (f-g) Biological LFP in the stimulated column (f) and 0.5 mm away (g) as a response to two stimulus levels. (e-h) Peak negativity of LFP vs. intensity of the stimulus. Computational results (e) were obtained by averaging 10 simulations.

though a weak excitation passes intracortically to the adjacent columns, it is damped by surrounding inhibition. The LFPs also demonstrate and confirm this focal nature of the input. The computational LFP matches the typical biological LFP in terms of shape, and in the increasing peak negativity with the increasing stimulus intensity (Fig. 12c-e,h). This is true for both the stimulated and the adjacent column. The simulations demonstrate that inhibition and excitation are properly balanced within and between columns.

4.1.2 LTS neuronal function

Depolarization of LTS neurons with a 1 Hz oscillatory input within one column results in synchronization of adjacent FS and pyramidal cells (Fig. 13a-b) that does not spread laterally into the adjacent columns. This is typical of what is observed biologically after application of metabotropic glutamate agonists (Beierlein et al.,2000; Long et al.,2005).

Since LTS neurons provide only modulatory inhibition, selective blockade of these cells would not be expected to result in a spread of activity within or between columns. Blockade of a neural cell was modeled by decreasing strengths (amplitudes) of all outgoing connections. When all LTS cells within two columns were blocked by 50%, there was little change in the computational LFP, as expected (Fig. 13c-d). Blockade by 80% slightly decreased the latency of the evoked LFP in the blocked column, and increased the amplitude of a late component of the computational LFP (Fig. 13c-d). Little change was observed in the column adjacent to that stimulated even with 80% blockade of the LTS cells in both columns.

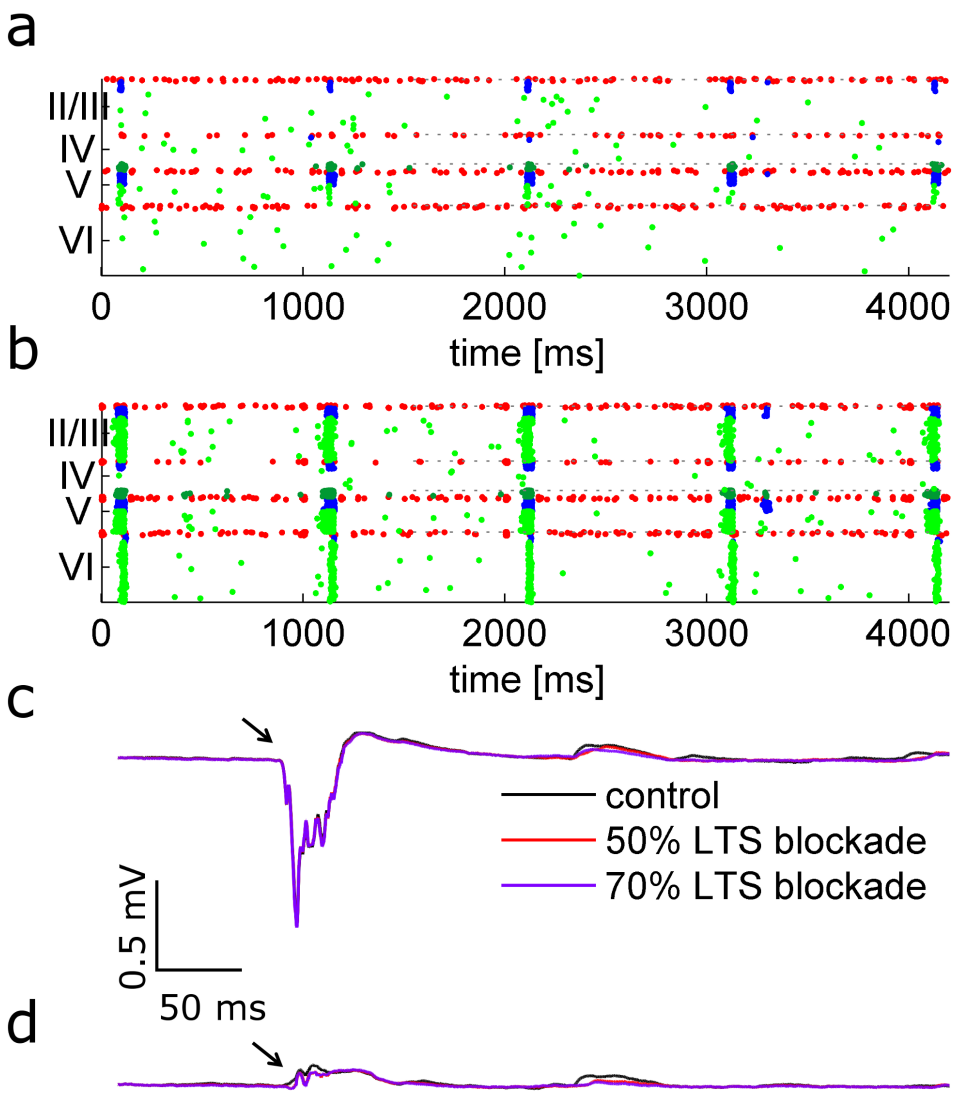

Fig. 13. LTS neuronal function (a-b) LTS cells (red) were depolarized with input of 1Hz frequency causing synchronization of RS (green) and FS (blue) neurons. The depolarizing current of value 5 was given to column 2 only (b) and does not cause oscillations in adjacent columns (a). (c-d) Local Field Potentials (LFP) in the stimulated (c) and an adjacent column (d) with different levels of LTS neuron blockade.

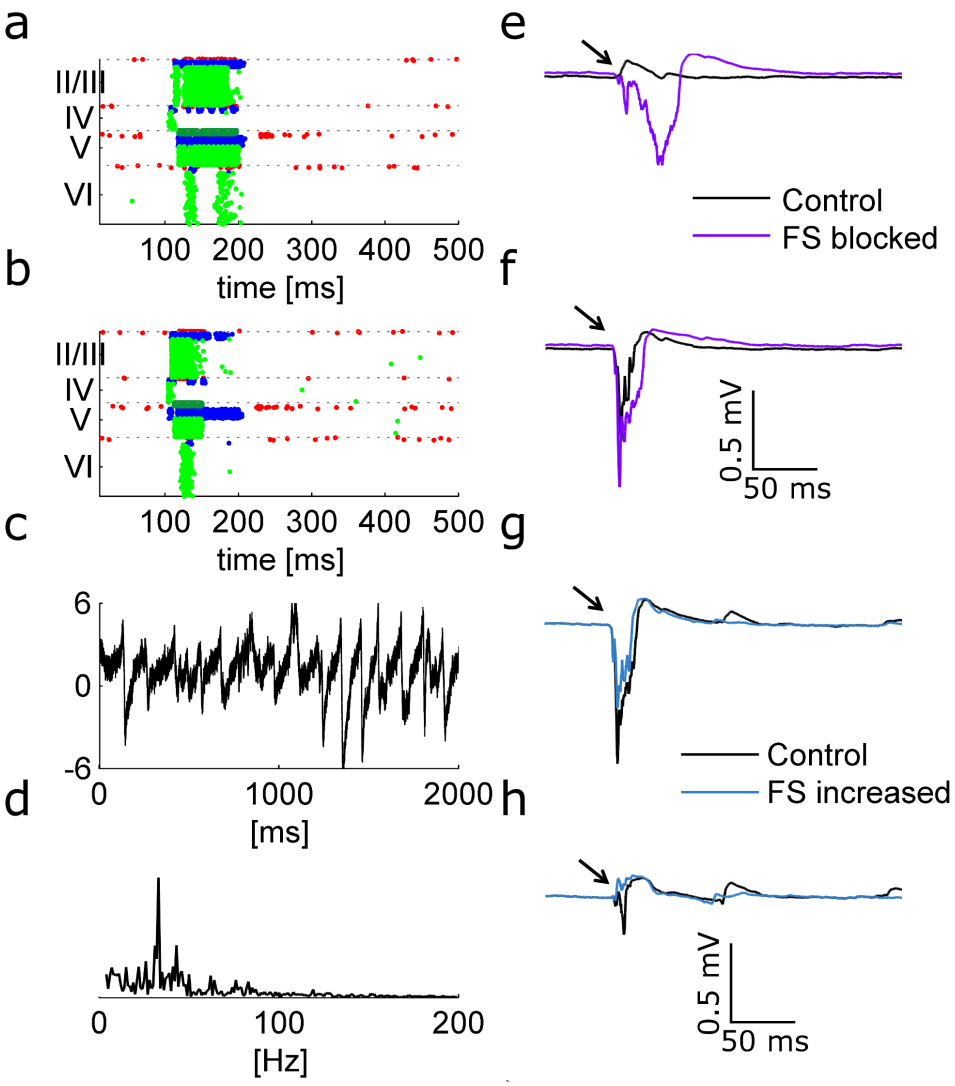

Fig. 14. FS neuronal function. (a-b) Result of blockade of FS cells in layer III by 50%: activity in the stimulated (a) and an adjacent column (b). The amplitude of stimulus is 8. (e-f) LFP in the case of blockade (purple) is compared to the control case (black) both in stimulated (e) and an adjacent (f) column; (c-d) Gamma oscillations resulting from applying constant depolarizing currents (2 mV to RS neurons in layer III and IV, 3 mV to all LTS and IB neurons and RS neurons in layer V, 6 mV to RS neurons in layer VI, and 4 mV to all FS neurons): EEG (c) and its Fourier transform (d) with a peak at 33 Hz. The depolarizing inputs were: 2-6 for RS cells, 3 for LTS and IB cells, and 4 for FS cells (g-h) Results of strengthening FS cells to 200% their amplitude. LFP in the stimulated (g) and adjacent (h) column. The amplitude of stimulus is 25.

4.1.3 FS neuronal function

FS neurons provide inhibition that controls horizontal spread of excitation within the cortex (Thomson,2003; Douglas and Martin,2004). Simulation of increased strength of FS neurons within layer III showed that the computational LFP decreased in duration and amplitude (Fig. 14g). In addition, the response in the column adjacent to that stimulated was reduced, demonstrating an increased focality (Fig. 14g-h). In contrast, when the strength of the FS neurons was selectively reduced, activity spread laterally within the cortex (Fig 14a-b). Reduction or increase of the effectiveness of inhibitory synapses was achieved by decreasing or increasing weights of the synapses connecting inhibitory neurons to other cells.

The cortical and thalamocortical oscillations in the gamma frequency ($30 - 80$ Hz) are well studied. They occur, for instance, in pharmacologically isolated networks of inhibitory interneurons and it has been shown that the interneurons that drive the gamma oscillations are the FS cells (Traub et al.,1997; Whittington et al.,1995). Applying constant depolarizing currents that effectively increase the function of FS cells results in persistent gamma oscillations in the computational EEG as shown in Fig 14c-d. The values of the current where: 2 mV to RS neurons in layer III and IV, 3 mV to all LTS and IB neurons and RS neurons in layer V, 6 mV to RS neurons in layer VI, and 4 mV to all FS neurons.

4.1.4 Generation of interictal-like and ictal-like epileptiform activity

Three sequential effects of decreasing levels of GABAA receptor blockade can be observed by looking at the evoked field potentials. First, the short latency evoked field increases in duration, reflecting a greater excitatory postsynaptic response. Second, longer but variable latency, polyphasic, all-or-none fields are evoked that are

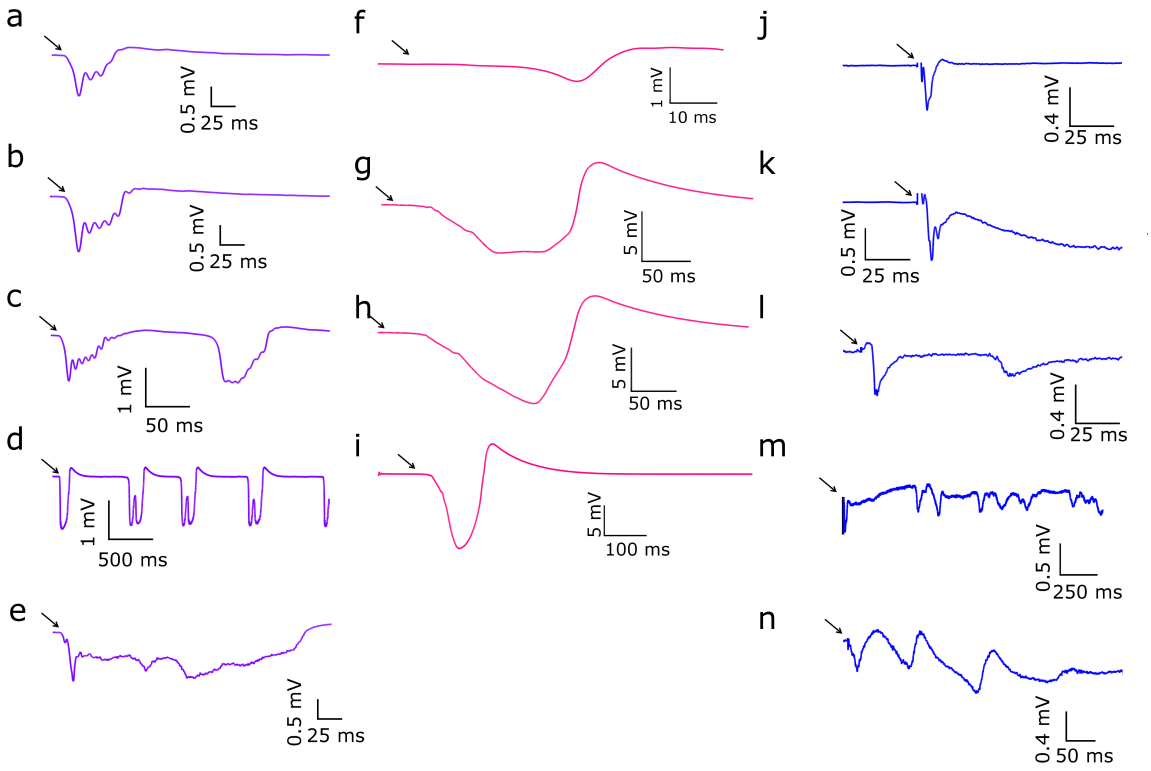

Fig. 15. Different stages of inhibitory blockade (a-e) Computational local field potentials (LFP) for the stimulated columns in different conditions: control (a), increasing levels of inhibitory blockade (b-d): 20, 30, and 90% respectively, and simulation of enhancement of NMDA receptors (e). Amplitude of input was 8 mV; (f-i) Computational local field potentials (LFP) for the stimulated columns in the network without modification of the neuron model with increasing levels of inhibitory blockade 0 (control), 20, 30, and 90% respectively. Amplitude of input was 3 mV; (j-n) Biologically measured LFP: control (j), increasing levels if bicuculline (k-m), and enhancement of NMDA receptors (n).

similar to interictal-like epileptiform activity. Third, repetitive sharp ictal-like waves are produced both spontaneously and in response to stimulation. All three levels could be simulated with increasing reductions in all inhibitory synapses within the computational network (Fig. 15a-d). Examples of network activity visualized as spike plots are shown in Fig. 32-34 in Appendix C.

The computational LFP generated under these conditions is similar to that produced biologically with application of the GABAA antagonist, bicuculline (Fig. 15j-m). Under these conditions, a single stimulation pulse resulted in long trains of excitation and propagation across columns.

However, result obtained in the network with original Izhikevich neuron model (without our modification, see Section 3.3) do not match biology (Fig. 15f-i). Blockade if inhibitory neurons results only in increase of the amplitude and duration of the LFP. ALthough there is spread of activity to the adjacent columns (not shown), there is no repetitive activity.

Epileptiform activity can also be induced in cortical slices acutely by activation of NMDA receptors with application of a bathing medium without the addition of MgCl2 (Robinson and Kawai,1993; Zhang et al.,1995). Computationally, enhancing NMDA receptors was modeled by increasing the late component of the EPSC (Fig. 15e and n), since NMDA receptors account for the late part of the EPSP. Specifically, the value of τ_2 in equation (3.2) was increased by a factor of two (Figure 16).

4.2 Discussion

In this chapter we presented a model of neocortex that allows for selective modulation of the powerful inhibition that maintains the boundaries on focal excitation, separately from the form that provides simultaneous modulatory inhibition to several layers within a column. A unique characteristic of this model is the multi-

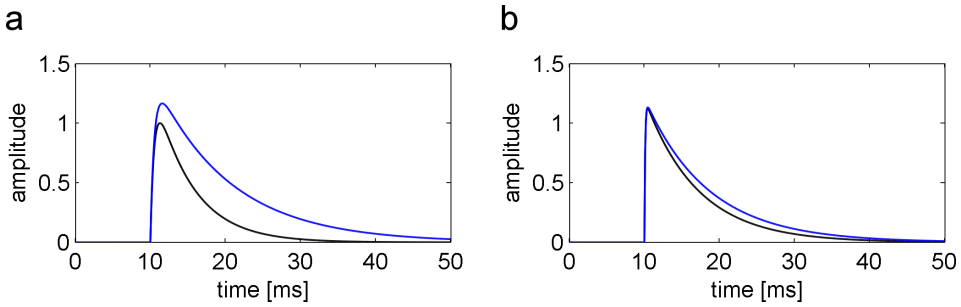

Fig. 16. Simulation of NMDA receptor increase. (a-b) Post Synaptic Potential (PSP) before (black) and after (blue) increasing its half-width. (a) PSP for connection between RS and FS neurons in layer III. (b) PSP for connection between RS neurons in layer IV.

column multi-layer construct. This allows for a better understanding of the processes that propagate across columns, as well as those that create inter-laminar synchrony. This model can specifically be used to probe questions about mechanisms underlying epileptiform activity induced in a malformed cortex.

When creating a computational model of neocortex, there are a number of questions that should be asked. First, how much detail is necessary in order to answer the specific questions proposed. High level models do not account for shapes of synaptic input, while more complex models use multiple compartments for individual neurons but limit the size of the network that can be modeled within a reasonable computation time. In this work we used the best aspects of each model, allowing for simulation of different EPSC shapes (necessary for instance to model NMDA inputs) but still having fast computing since. Since the main goal here is to understand how alteration of specific interneuron subtypes affects the development of propagating excitatory activity, multiple compartments are not necessary.

Another critical question is: which aspects of function are necessary to test to demonstrate that the computational model performs close to the biological network.

Clearly the individual units from which the network is composed must be tested. We adopted the Izhikevich neuron model that has been used and tested in many studies to create neuronal subtypes with specific firing patterns. We have confirmed this unique firing pattern in response to depolarization and added a crucial modification that prevents 'runaway' firing (Strack et al.,2013a). Without this modification, the neurons would fire at much higher frequencies than those occurring biologically. In addition, we have confirmed two other critical aspects of connectivity: (1) the correct form of short-term plasticity on the synaptic inputs that the cell receives; and (2) the correct amplitude and probability of outputs to specific cell types, as shown by paired intracellular recordings. We have also demonstrated that their synaptic inputs and outputs produce the biologically demonstrated result. For LTS neurons, this includes a modulatory inhibitory output that spans the layers but remains confined within a column. For FS interneurons, this includes a powerful inhibition that is primarily within a single layer.

One goal of this work was to determine connectivity patterns that generate network epileptiform activity. The other aspects of function necessary to test are those that contribute to patterns of activity under both conditions of normal network function and hyperexcitability, or seizure-like, function. We demonstrated that thalamic input produced the expected laminar and columnar pattern, namely, layer IV to II/III to V and VI, within a single column, without spread to other columns or activation of epileptiform activity. Yet, when conditions that produce epileptiform activity were simulated (blockade of inhibitory receptors, or increased function of NMDA receptors) the network undergoes the same pattern of changes that are observed biologically. For instance, application of low levels of bicuculline to the bathing medium of a cortical slice block GABAA receptors and produce enhancement of the short latency evoked field potential (Chagnac-Amitai and Connors,1989a; Connors,1984). This is also ob-

served in our model with 20% inhibitory blockade. With increasing levels of bicuculline in the biological slice, interictal epileptiform activity occurs, the characteristics of which are a varied but typically long latency after the stimulus, variable form, and all-or-none event (Chagnac-Amitai and Connors,1989a; Connors,1984). This means that the amplitude of the interictal event does not vary with stimulus intensity. In our model, we observe the same characteristics at 30% inhibitory blockade. Ultimately, with either strong GABAA blockade or removal of magnesium from the bathing solution, ictal-like events can be generated in cortical slices. These events typically have a sharp onset and are repetitive (Robinson and Kawai,1993; Zhang et al.,1995). In our model we observe these same characteristics at 90% level of inhibitory blockade or enhancement of NMDA receptors equivalent to the removal of magnesium from the slice bath solution.

Computational models have commonly been used to understand different aspects of epileptiform activity. For instance, the macroscopic approach, which involves modeling larger population of neurons instead of separate cells, provided many valuable insights, including modeling of EEG and the transition from interictal to ictal activity (Suffczynski et al.,2005). However, when the goal is to model the influence of connectivity, specific neural subtypes, or synaptic properties on epileptiform activity, network models are more appropriate. Although the network approach has been successfully combined with experimental studies (Cunningham et al.,2004; Traub et al.,2005b), there are several areas that have not been studied computationally, such as how malformation of the cortex affects the propagation of epileptiform activity. The model described here was designed to simulate this scenario.

CHAPTER 5

MODELING LESIONS IN THE CORTEX

The laminar organization of the neocortex is vital to its normal operation. The neocortex consists of several layers that differ in thickness, number of neurons and their types, the types of input they receive, and the ways that input is processed. Analyzing flows of activity in vertical and horizontal brain tissue slices have been a significant source of knowledge about neuronal connections in the brain. In particular, there is a wide range of studies that compare different aspects of connectivity between superficial and deep layers (Telfeian and Connors,1998; Telfeian and Connors,2003; Ichinose and Murakoshi,1996). However, focal or global loss of layers has not been modeled using computational models, even in those that preserve laminar structure of cortex (Traub et al.,2005b).

In this chapter we focus on analyzing the spread of activity with different levels of inhibitory blockade in superficial and deep layers using our multi-layer multi-columnar model of neocortex.

The simulations were performed using time step of 0.1 ms on a network consisting of five columns with added white noise with variance of eight. Inhibitory blockade was modeled by decreasing the weights of all inhibitory connections. The amplitude of the stimulus was 8 mV, however, simulations with stimulus amplitude in the range $7-19$ mV were also performed and the results were consistent through all amplitudes.

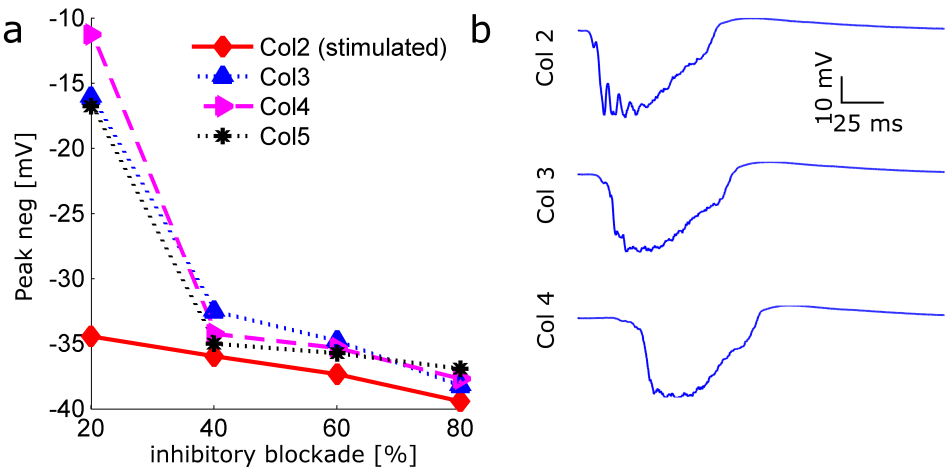

Fig. 17. Spread of activity in the intact network. (a) Peak negativity vs. level of inhibitory blockade in different columns. Results averaged from two simulations. (b) Local field potentials in stimulated column (column 2), one column away (column 3), and two columns away (column 4) in conditions of 70% inhibitory blockade.

5.1 Results

5.1.1 Spread of activity in the intact network

First, different levels of inhibitory blockade within the whole network where simulated. As expected, without inhibitory blockade, or with low levels of blockade, there is little spread to adjacent columns in response to stimulation within a single column. This can be seen from the peak negativity (excitation) of the LFP plotted as a function of the level of inhibitory blockade (Figure 17). However, with 40% blockade, activity in the adjacent column is near that within the stimulated column and continues to propagate horizontally across the columns. These results confirm the well known function of inhibition in limiting horizontal spread within neocortex (Chagnac-Amitai and Connors,1989a).

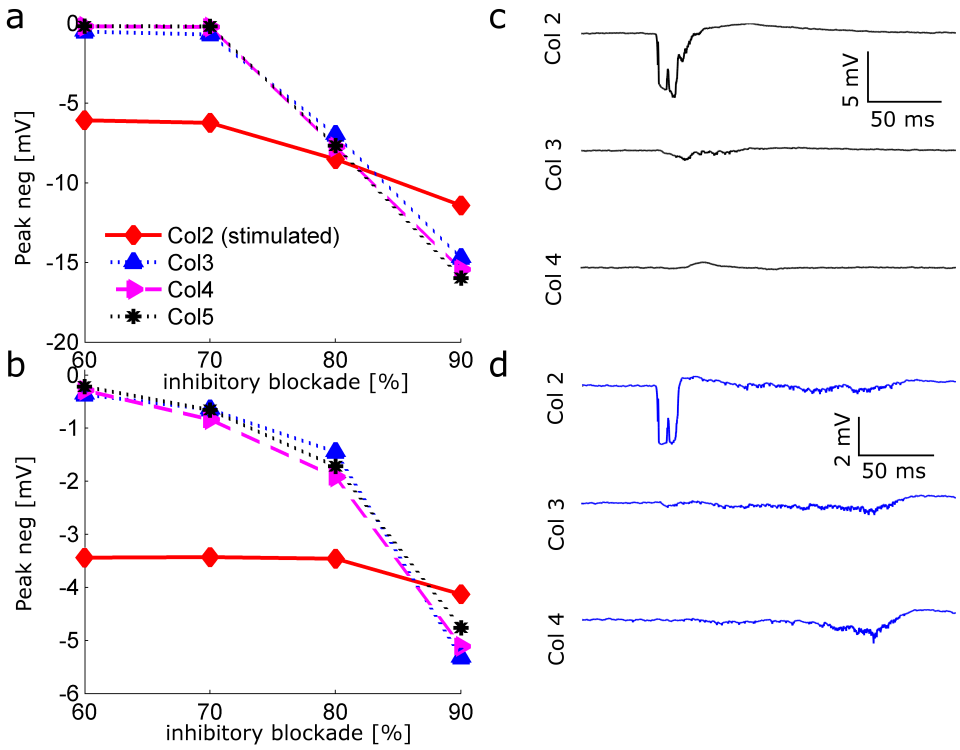

Fig. 18. Horizontal spread of activity through individual layers after removal of other layers in all columns (global lesion). (a-b) Peak evoked negativity from computed LFP after stimulation of column 2 under various levels of inhibitory blockade. Cortical strips of only layer III (a) or layer V (b) were modeled as created experimentally from biological tissue after cut of coronal slices (Telfeian). Average of 2 simulations shown. (c-d) Local field potentials produced after stimulation of column 2 under condition of 70% inhibitory blockade for layer III (c, black) and layer V (d, blue). Activity in columns 3 and 4 is a result of propagation across the laminar strip. Propagation to columns 3 and 4 occurs for both layer III and layer V strips.

5.1.2 Global horizontal cuts

Second, all layers but one were removed across all columns and the remaining layer (forming a strip) was stimulated focally in the second column. Different levels of inhibitory blockade were applied.Propagation in a strip of layer III (Fig. 18a,c) and a strip of layer V (Fig. 18b,d) was investigated.

Comparing Figures 18a and b with Figure 17a we notice that the activity spreads faster with the increase of the inhibitory blockade level in the intact network (with all layers) than in a single layer. In the whole network with 40% blockade, the activity in adjacent columns is comparable to the stimulated column, whereas in network consisting of only one layer these levels of activity do not become similar until the blockade reaches 80-90%. In addition, LFPs in the lesioned network are shorter and of lower amplitude when compared with the intact network.

At high levels of inhibitory blockade (80-90%), activity propagates across columns for both the layer III and layer V strip. Importantly, in the case of 70% blockade some spreading is noticeable within layer V, but not within layer III. This result is consistent with what was reported for the biological network in (Telfeian and Connors,1998).

5.1.3 Focal loss of layers

Next, either superficial (III and IV) or deep (V and VI) layers were removed within column 3 only, leaving remaining layers to bridge columns 2 and 4. To determine if activity could spread across the bridge, stimulation was applied focally within column 2.

Little propagation is observed with 20-40% blockade, but with 60% blockade, the spread is strong for the deep but not the superficial layer bridge (Figure 19a,b). Moreover, LFPs show that for the deep layer bridge, the activity in column number

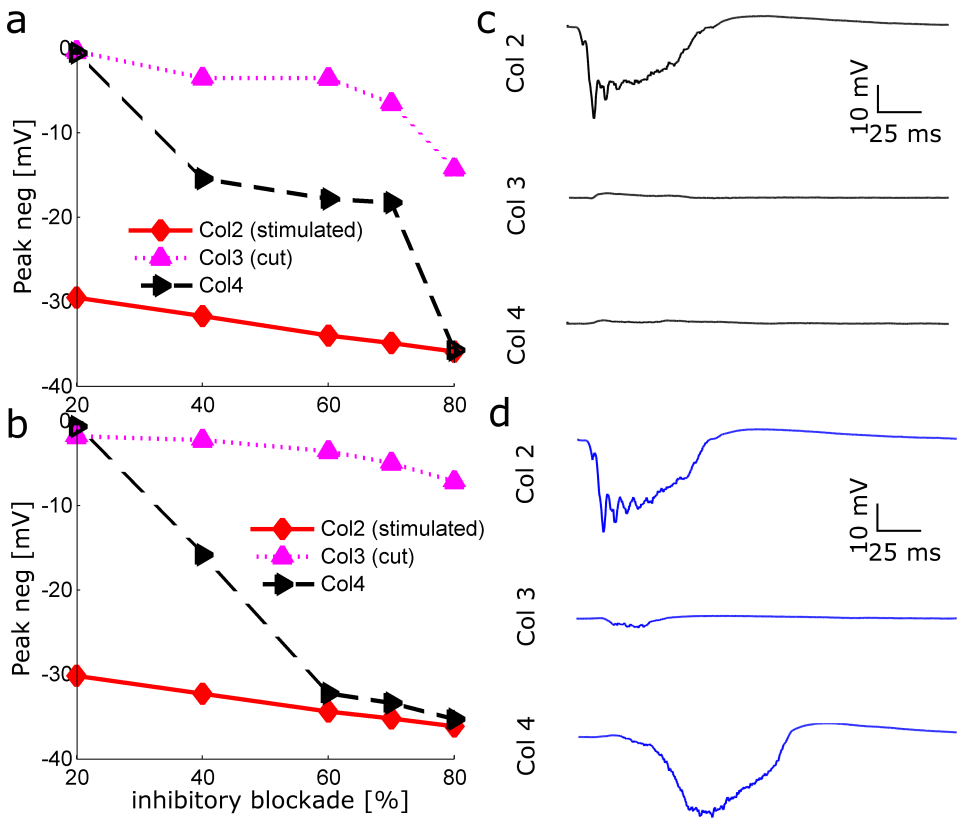

Fig. 19. Propagation through superficial versus deep cortex measured by creating bridges of tissue within column 3 (focal lesions). (a-b) Peak evoked negativity from computed LFP after stimulation of column 2 under various levels of inhibitory blockade when only superficial (a) or deep (b) layers remain within column 3. Average of 2 simulations shown. Larger LFPs are produced from propagation across the deep layer bridge. (c-d) Local field potentials produced after stimulation of column 2 under condition of 60% inhibitory blockade for the superficial (c, black) and deep(d, blue) layer bridge. A greater amount of propagation occurs with the deep layer bridge.

four (two columns away from the stimulation) is comparable to that in the intact network (see Figure 19b). This supports the idea that layer V may be more susceptible to activity propagation when all columns are intact. It has been suggested that this is true biologically due to IB cells that have horizontal projections (Chagnac-Amitai et al.,1990) and are more active during epileptiform activity relative to the RS cells (Chagnac-Amitai and Connors,1989a). Within our model, we also find that with 40% inhibitory blockade and all layers intact, the average RS firing rate is 12 spikes/sec, while that of IB cells is 26.

Finally, as was true for the global lesion, with high levels of inhibitory blockade, both superficial and deep layer bridges can support spread and propagation of excitatory activity across columns (Figure 19a,b).

5.2 Conclusions

We have examined the propagation of activity across the computational multi-layer, multi-columnar cortex. As expected and previously shown biologically, with all layers and inhibition intact, stimulation within one column remains focal. As shown biologically, and within our computational model, even low level blockade of inhibition allows the horizontal propagation of activity across columns (Chagnac-Amitai and Connors,1989a; Chagnac-Amitai et al.,1990). We also showed here that deep layers are distinct from superficial layers in this ability. While both superficial and deep layers can support the propagation of activity at high levels of inhibitory blockade, the threshold at which the propagation succeeds is lower for deep layers. In addition, the deep layer response looks most similar to that produced when all layers are intact, further suggesting that the deep layers are normally a significant pathway for propagation under conditions of reduced inhibition.

All of these results are consistent with biological findings from cortical slices

under similar conditions of creating strips and laminar bridges (Telfeian and Connors,1998; Telfeian and Connors,2003). Importantly, this model is the first, to the best of our knowledge, to use multiple layers, multiple columns, and short term plasticity for the computational study of activity propagation.

CHAPTER 6

STUDY OF INHIBITION INFLUENCE ON EPILEPTIC SEIZURES

When the vertical or horizontal organization of the cortex is altered during development, several neurological and cognitive abnormalities occur. Study of a biological model of a 4-layered microgyria associated with epileptiform activity has demonstrated a number of cellular and synaptic anomalies. It is currently not known what influence each of these changes has on overall network function.

Importantly, our computational model allows to study these potentially epileptogenic mechanisms in isolation. In this chapter the role of FS and LTS neurons in modulating network activity is examined, and we show effects of a malformed structure with some of the known alterations in cellular function and connectivity.

Section 6.1 describes how the modifications to the network are performed. Results and their discussion are presented in section 6.2.

6.1 Methods

6.1.1 Simulated conditions

Several different modifications are performed on the network structure and properties of neurons.

Malformation: Deep layers (IV,V, and VI) are removed within one column. All connections that have their pre- or post-synaptic neurons in the removed area are lost.

Rewiring of connections: Connections that have lost their post-synaptic target in the malformed column are rewired to the same cell type in one of the adjacent

columns (chosen randomly). Cells that have lost a pre-synaptic connection from the malformed column receive a connection from the same type of cell in one of the columns adjacent to malformation (randomly). The synaptic amplitude of these rewired connections can be selectively modified. The length of the connection is adjusted to the distance between the new interconnected neurons. Figure 20 illustrates the process of rewiring connections.

Reduction of FS neurons: Number of FS neurons can be selectively reduced in any column. It does not affect the probabilities of connections since only the number of neurons changes.

Replacement of FS neurons with LTS neurons: Number of FS neurons is reduced but they are replaced with LTS cells. This change affects only the number of neurons, the probabilities of connections remain exactly the same as in the intact network.

Enhanced excitation to LTS neurons: Increased excitation to LTS neurons in a particular column is done by duplicating excitatory connections to LTS neurons in layers IV, V, and VI. The duplicated connections have the same pre- and post-synaptic neurons and the same synaptic weight as the original connection. The length of the new connection is randomly chosen in the range of $100 - 150\%$ of the length of the original connection. If the excitation to LTS neurons is to be increased N times, each connection is duplicated $N-1$ times. If the column has already increased excitation to all neurons (rewiring), it is taken into account (on average, rewiring results in 1.5 increase of excitatory connections to LTS neurons) so that the final number of excitatory connections is increased N times.

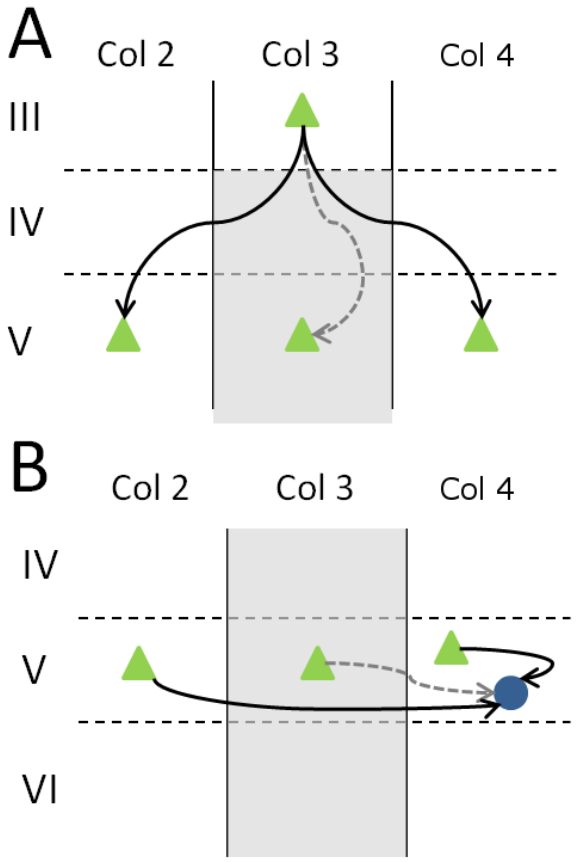

Fig. 20. Example of rewiring of connections. Shaded area represents the malformation (removed layers). Green triangle represents a regular-spiking (RS) neuron, blue circle represents fast-spiking (FS) neuron. (A) Lost connection (dashed gray line) from an RS neuron in layer III to an RS neuron in layer V within col 3 is rewired to RS neuron in layer V in either column 2 or column 4. (B) Lost connection from the malformed area (gray dashed line) is rewired to originate either in column 2 or column 4.

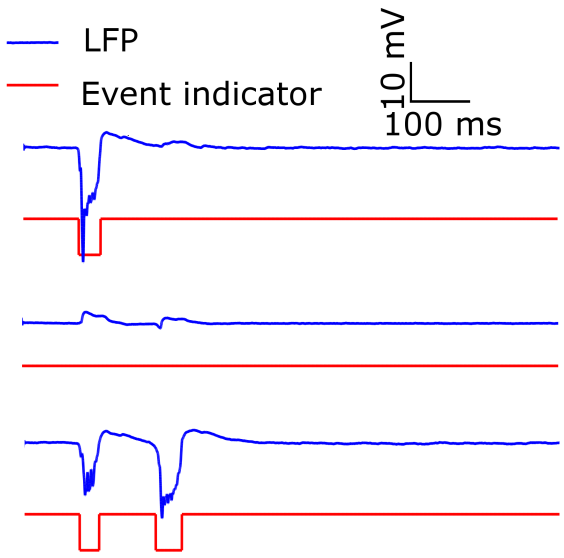

Fig. 21. Example of event detection in three local field potentials (LFP). The red line indicates the duration of event.

6.1.2 Event detection

To asses the amount of epileptic activity, event detection in local field potential (LFP) needs to be implemented. It is done using a simple threshold method. The parameters of detection (threshold, minimum time) were adjusted based on a sample of 10 LFP (2000 ms each) and expert labeling of events.

First, the average μ_{10} and standard deviation σ_{10} are calculated from the first 10 ms of the signal. The potential event is detected if the value of normalized signal (subtracted μ_{10}) is greater than $8\sigma_{10}$ and it is considered to last till the value drops to $0.4\sigma_{10}$. Only events lasting longer than 10 ms are considered. An example of event detection is presented in Figure 21.

6.1.3 Simulations

Each condition was simulated 30 times and the results were averaged. In each simulation, column 2 was stimulated at 100 ms with thalamic input of amplitude 8.

We defined a short latency spread as activity spreading to either column 1 or 4 within first 250 ms of simulation (column 3 was the malformed column). Late activity epileptiform is defined as any event occurring later than 250 ms, and repetitive spiking is a series of at least two late events.

6.2 Results and discussion

When 50% of connections are rewired, there is not much increase of activity even with increase of the amplitude of rewired connections (Figure 22). Figure 23 shows number of seeds (experiments) that exhibit different types of epileptiform activity with 50% and 100% of connections rewired. When 100% of connections are rewired, there is more activity in the network than with 50% rewiring (p value < 0.001 in z-test for each pair-wise comparison).

We also explored the effect of decreasing number of FS neurons in columns 2-4 combined with these conditions: (1) malformation only, (2) malformed cortex and replacement of the missing FS neurons with LTS neurons, (3) malformed cortex with rewired connections, and (4) malformed cortex with rewired connections and missing FS neurons replaced with LTS neurons. Figure 24 shows results of these simulations.

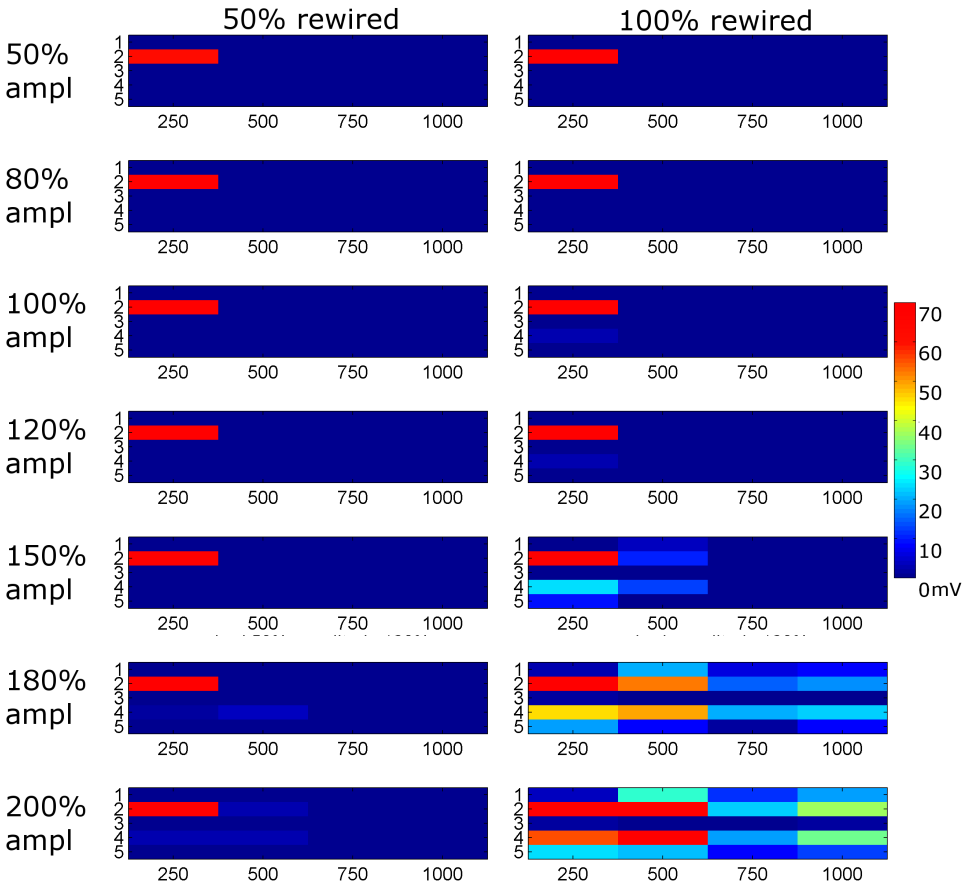

Fig. 22. Spatio-temporal patterns of activity after rewiring (Left) Connections are rewired with 0.5 probability (50% rewired). (Right) Connections are rewired with 1.0 probability. Color coding shows area of computed LFP for time period ending in number indicated on x-axis ($250 = 0-250$ ms, $500 = 250.1-500$, etc) and averaged across 30 seeds (experiments). Area was calculated only for the detected events.

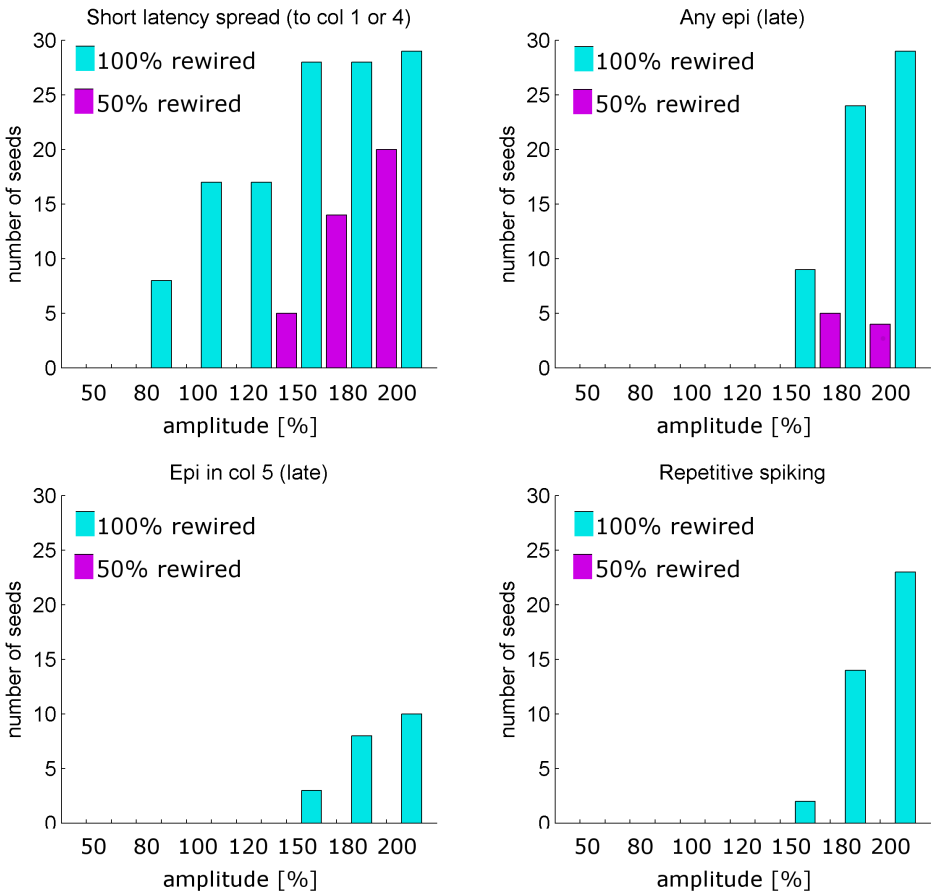

Fig. 23. Number of experiments with different amplitudes of rewired connections (50% rewired connections in purple, and 100% in blue) that exhibit different types of epileptiform activity: short latency (in first 250 ms) spread to adjacent columns, late activity in column 5, repetitive spiking, any kind of late (later than 250 ms) activity.

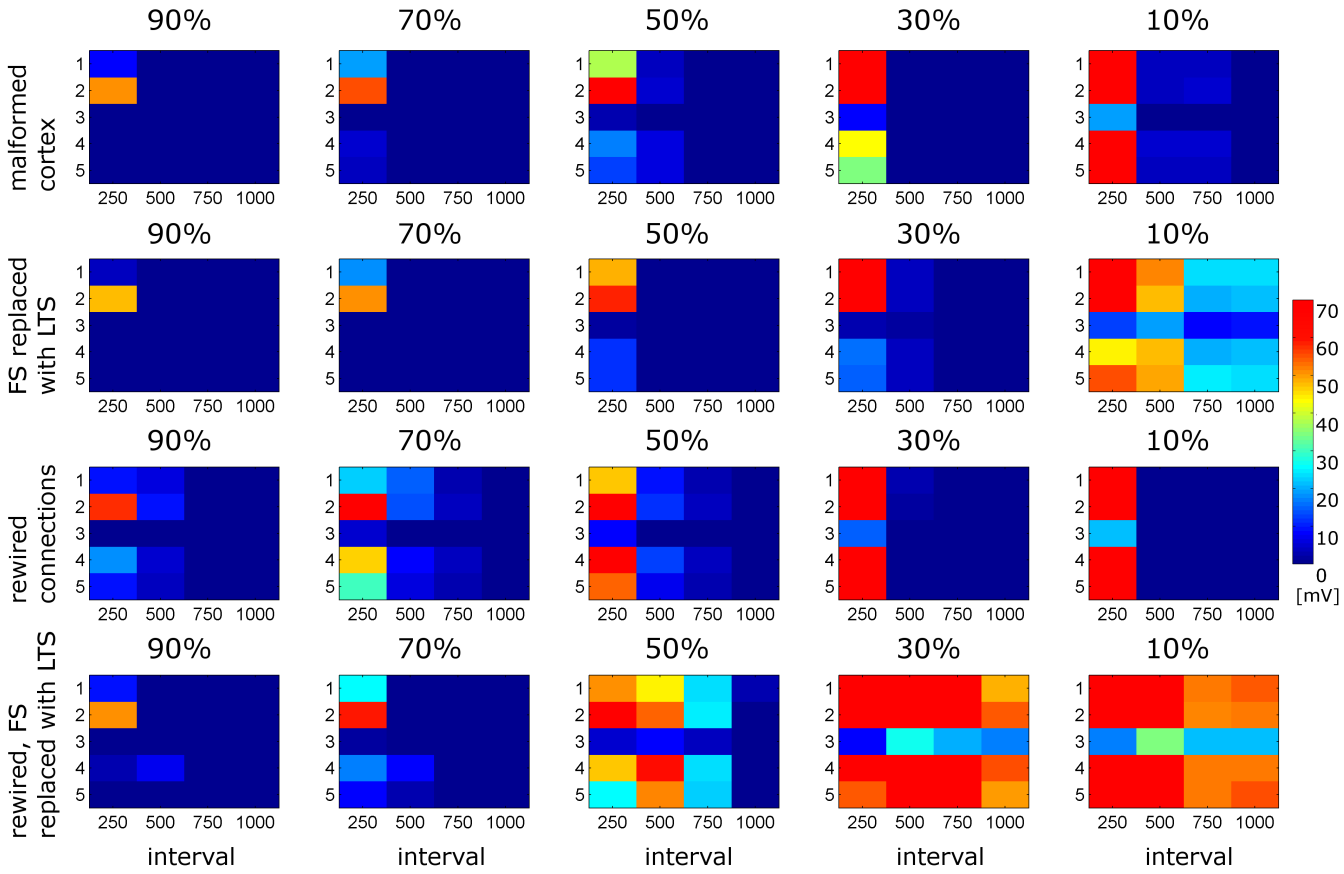

Fig. 24. Spatio-temporal patterns of activity in network with reduced number of FS neurons to different levels: 90%, 70%, 50%, 30%, and 10%, and under different conditions (in rows). Color coding shows area of computed LFP for time period ending in number indicated on x-axis (250 = 0 − 250 ms, 500= 250.1 − 500, etc) and averaged across 30 seeds (experiments).

Figure 25 shows the results of increasing number of excitatory connections to LTS neurons surrounding the malformation. Increasing excitatory input to LTS cells alone does not induce epileptiform activity, however, when performed in a network with increased excitation (rewired connections) it results in enhanced activity for 3X and 5X increase. This suggests that increasing excitatory input to inhibitory LTS cells can induce epileptiform activity.

Figure 26 shows activity of the network for combinations of conditions that were simulated (Table 2). Number of simulations of each condition (different seeds) that produce different type of epileptiform activity are shown in Figure 27. Representative examples of network activity for each condition are presented in Appendix C.

We observe that focal removal of deep layers alone does not change the network excitability. Rewiring connections results mostly in short-latency spread of activity to the adjacent columns. However, increasing the amplitude of the rewired connections (Figure 22) results in late epileptiform activity.

Comparing conditions F (reducing the number of inhibitory FS cells to 70% in cols 2-4) and H (increasing excitatory input to LTS cells by 3X) leads to interesting results. In condition F, there is more short latency spread (p value = 0.001 for z-test for equality of proportions), while condition H results in more late epileptiform and repetitive activity (p value < 0.001 for z-test for equality of proportions). There is no significant difference in the number of simulations that resulted in late spread activity to column 5 (p value = 0.13 for z-test for equality of proportions). These results suggest that the biologically demonstrated increase in excitatory input to LTS cells likely contributes to generation of epileptiform activity in malformed cortex.

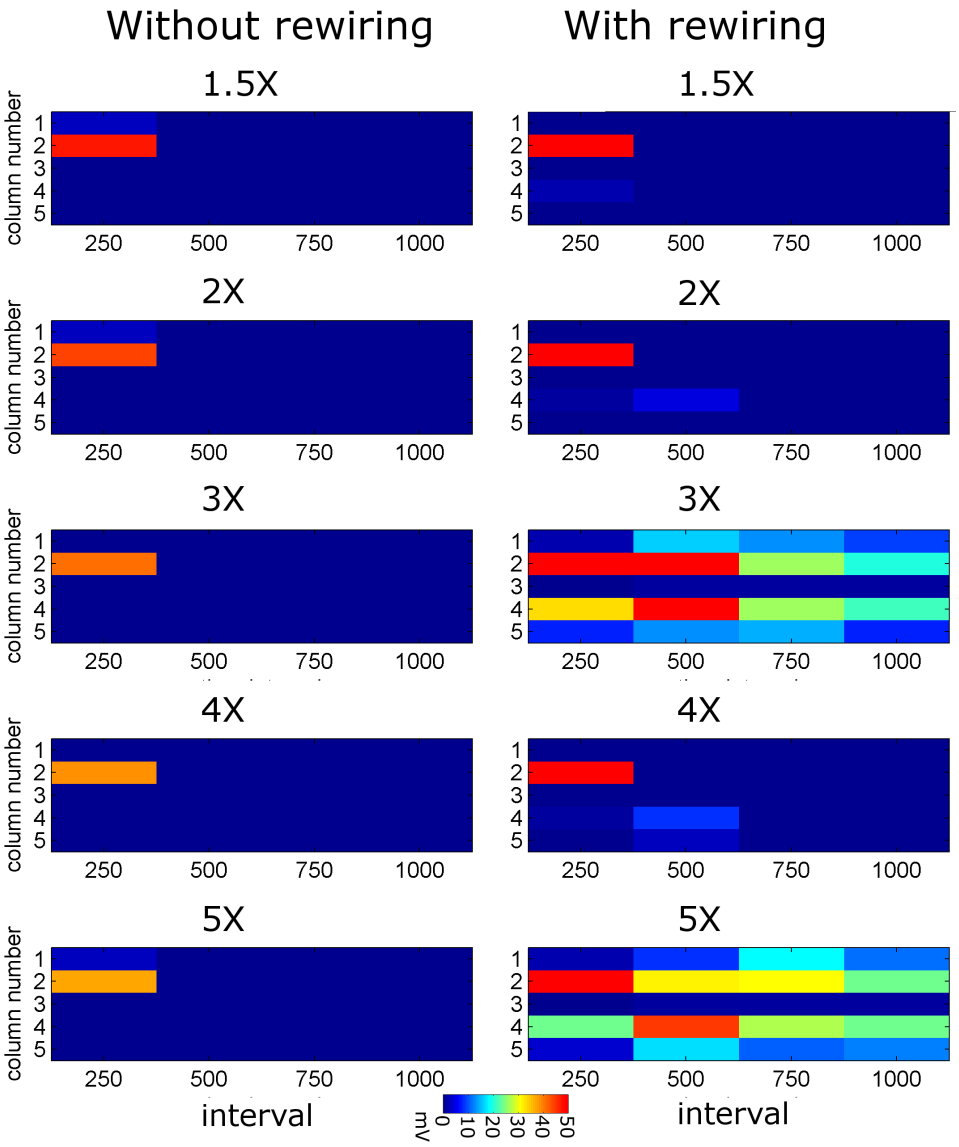

Fig. 25. Spatio-temporal patterns of activity in network with rewired connections and increased levels of excitation to LTS neurons. Color coding shows area of computed LFP for time period ending in number indicated on x-axis (250 = 0 − 250 ms, 500= 250.1 − 500, etc) and averaged across 10 seeds (experiments). Area was calculated only for the detected events.

Table 2. List of simulated conditions.

Condition	Description
A	Normal (intact) cortex with all columns and layers
B	Malformed cortex - removed layers IV-VI in column 3
C	Malformed cortex with reduction of the number of FS neurons to 70% in columns 2-4
D	Malformed cortex with rewired connections
E	Malformed cortex with 3x increased excitation to LTS neurons in columns 2-4
F	Malformed cortex with rewiring and reduction of the number of FS neurons to 70% in columns 2-4
G	Malformed cortex with rewiring and 30% of FS neurons replaced with LTS neurons in columns 2-4
H	Malformed cortex with rewiring and 3x increased excitation to LTS neurons in columns 2-4
I	Malformed cortex with rewiring, 3x increased excitation to LTS neurons and 30% of FS neurons replaced with LTS neurons in columns 2-4

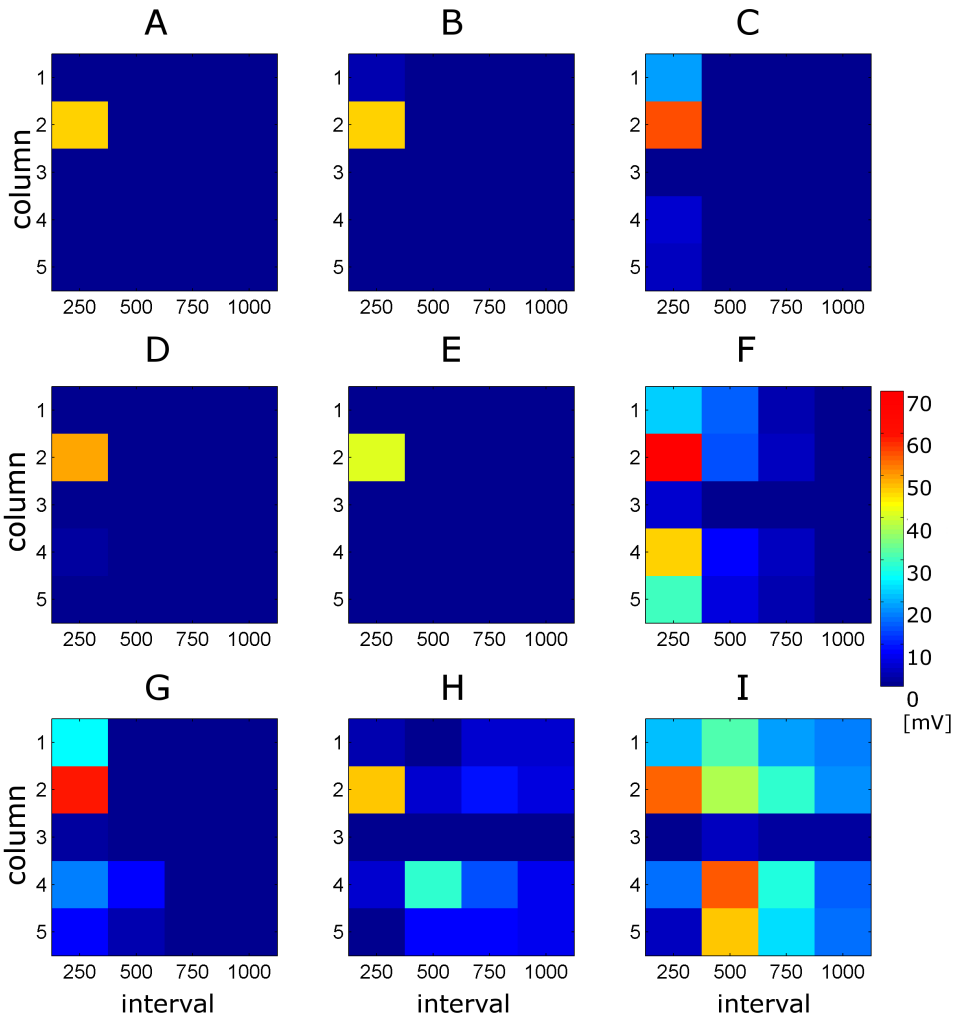

Fig. 26. Spatio-temporal patterns of activity under various conditions (see Table 2). Color coding shows area of computed LFP for time period ending in number indicated on x-axis (250 = 0-250 ms, 500= 250.1-500, etc) and averaged across 10 seeds (experiments). The area was calculated only for the detected events.

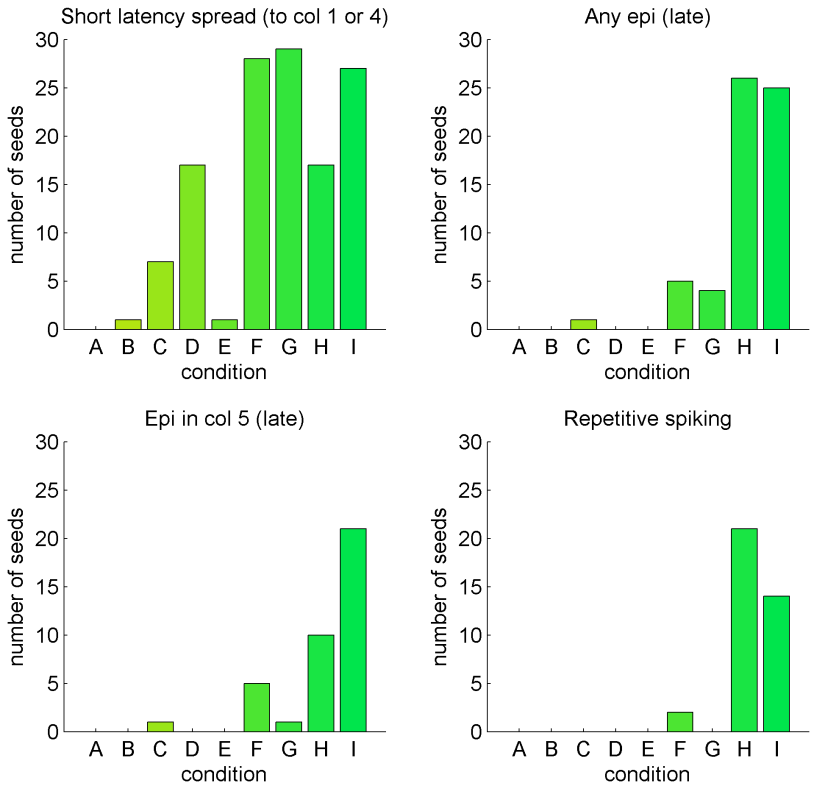

Fig. 27. Number of experiments with given condition (x-axis) that exhibit different types of epileptiform activity: short latency (in first 250 ms) spread to adjacent columns, late activity in column 5, repetitive spiking, any kind of late (later than 250 ms) activity. See Table 2 for the list of conditions.

CHAPTER 7

RUNNING TIME OF SIMULATIONS

In this chapter we present running time analysis of the implemented model. In Section 7.1 we discuss how the running time depends on the size of the network, the amount of activity, and the total time of simulation. In Section 7.2 we discuss how the simulations are parallelized.

7.1 Running time analysis

With fixed network size and the total time to be simulated, the running time depends on amount of activity in the network, since the number of calculations performed on synapses depends on the number of spikes in the network. The amount of activity in the network depends on several factors: amount of noise, stimulus provided to the network, and settings of the neural connections, that is strength and number of excitatory and inhibitory connections.

Since each column of neurons is connected with at most two adjacent columns, the number of connections increases linearly with the number of neurons. Thus, the simulation time depends linearly on the number of neurons (if all other parameters are kept fixed).

To illustrate these dependencies, several experiments were performed to assess how the running time of a simulation depends on different factors (Figure 28): size of the network measured by the number of columns, amount of activity in the network measured by the level of noise, and total time of simulated activity. We analyze both time of building the network, which include placing the neurons, initializing

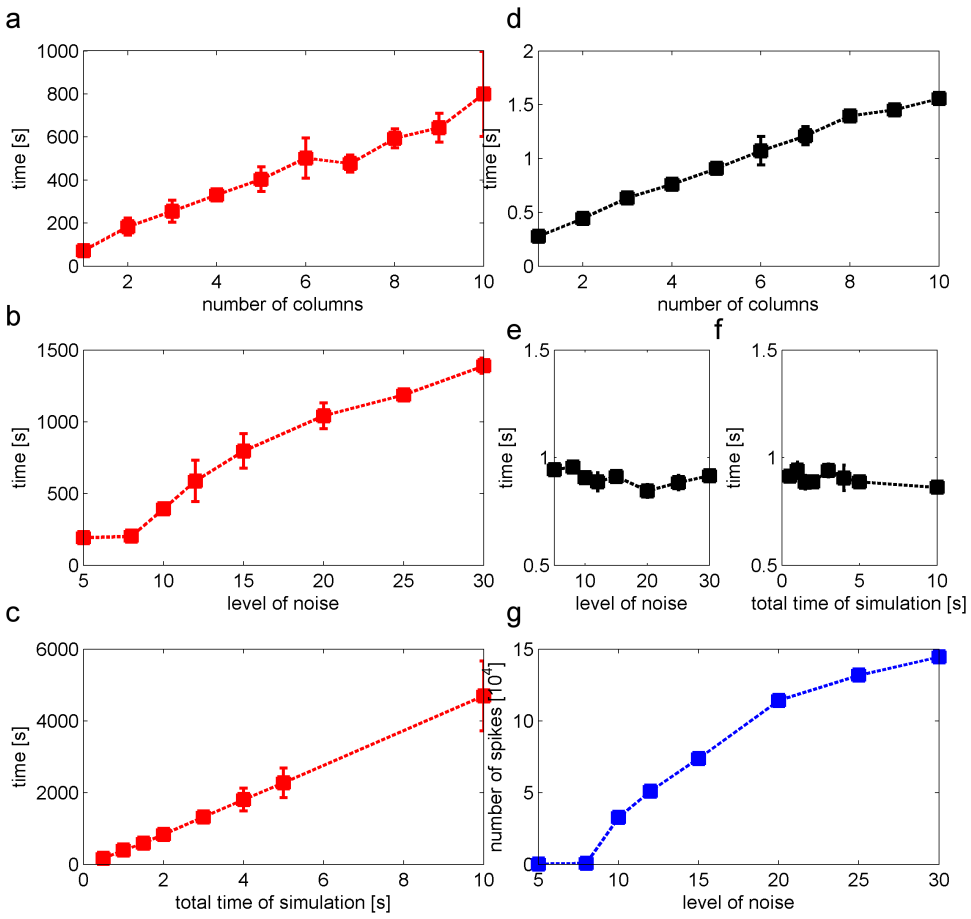

Fig. 28. (a) Time of simulation as a function of the number of columns. One column consists of 788 neurons, the network was provided with a white noise with variance equal to 10; (b) Time of simulation as a function of level of noise, that is the variance of the white noise provided to the network; (c) Time of simulation as a total time of simulated activity. The network was provided with a white noise with variance equal to 10; (d) Time of initialization as a function of the number of columns; (e) Time of simulation as a function of level of noise; (f) Time of simulation as a total time of simulated activity; (g) The level of noise can be understood as a measure of the amount of activity in the network. All times were obtained as an average of three simulations.

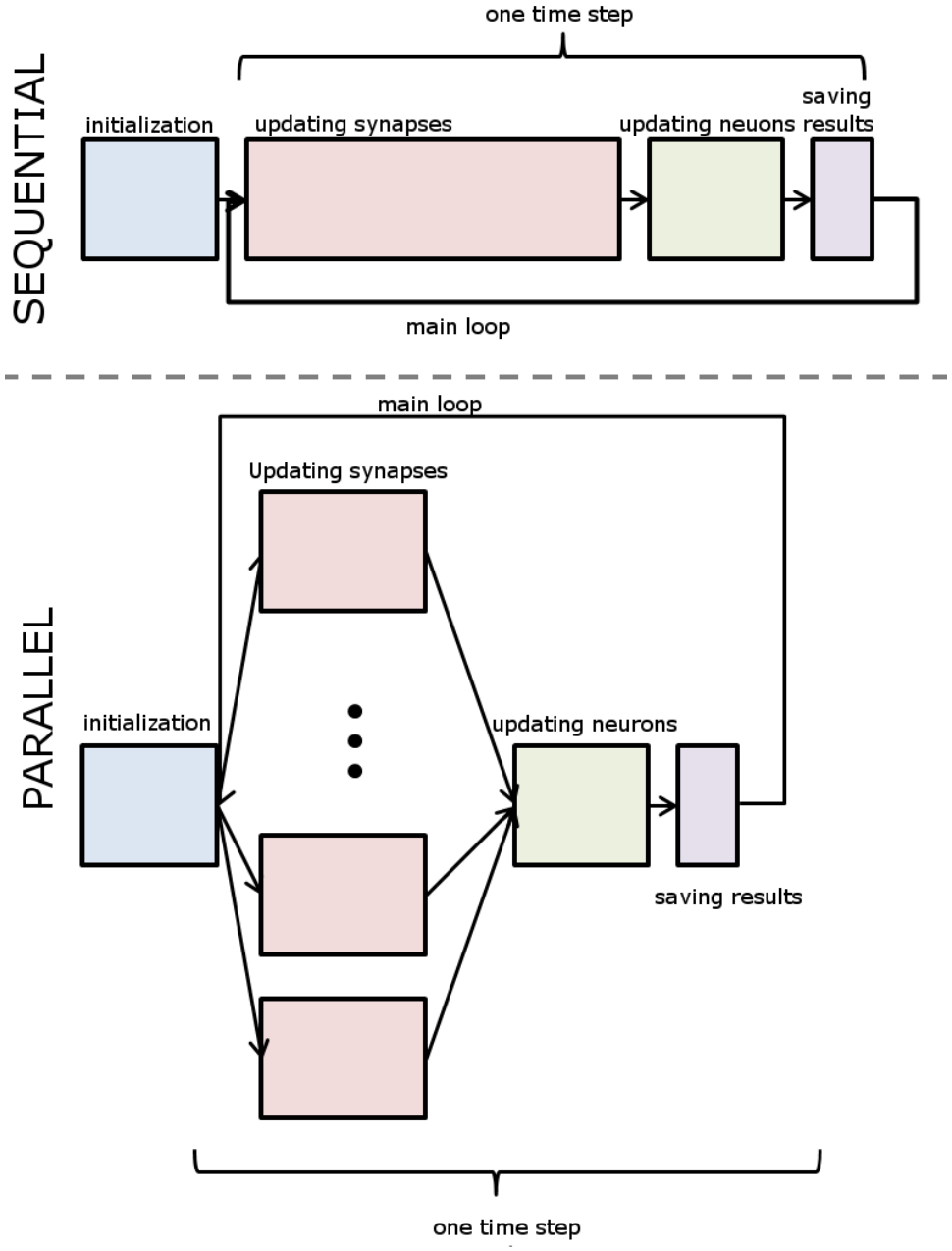

Fig. 29. Diagram of the task flow in sequential and parallel implementations of our network.

connections, and performing network modifications as e.g. removal of some layers, and the actual time of simulation.

All experiments were performed on a PC equipped with Intel^{TM} Core^{TM} i7 CPU 1.80 GHz and 12 GB RAM.

As expected, the time of building the network depends only on the size of the network, while the time of simulation depends on all the analyzed factors. Since the goal is to simulate epileptic seizures, which are cascades of increased activity, the relationship between the simulation time and the amount of activity is the most crucial one. The simulation time varies from minutes in case if single focal input in a normal network to hours in case of inhibitory blockade simulation.

7.2 Parallelization

Parallelization of such a network is not straightforward since the neurons are highly interconnected and it is challenging to isolate independent tasks. Each synapse, on the other hand, is independent on other synapses. In addition, there is 100 times more synapses than neurons in the network and the computations performed on neurons and synapses are comparably expensive. This motivated us to parallelize the calculations of synapses (Figure 29). Each thread updates state of a set of synapses and then, after all synapses are synchronized, neurons are updated in a separate thread. This minimizes the amount of synchronization needed.

Dependency of the running time and the speedup versus the number of threads are presented on Figure 30. The speedup was calculated as

$$S_n = \frac{T_1}{T_n}, \tag{7.1}$$

where T_n is the execution time using n threads (T_1 is the time of the sequential algorithm).

As expected, the time decreases with the number of threads but, since there is significant amount of synchronization performed, the speedup is worse than linear (which is the case of $S_n = n$). Notice that the more activity in the network the more thw speedup.

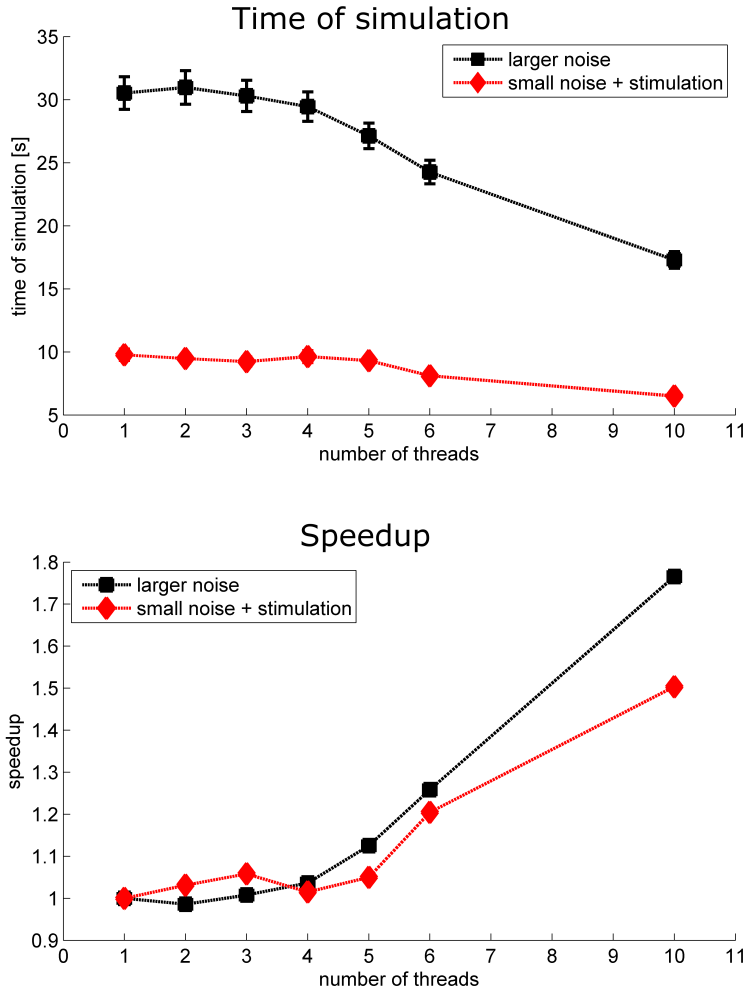

Fig. 30. Comparison of the time of simulation and speedup for two different stimulus configuration. 'Larger noise' refers to simulation with noise of standard deviation of 10, 'small noise + stimulus' refers to simulation with noise of 7 and with stimulated one column with amplitude of 10 for 1 ms (focal input). (Top) Time of simulation versus the number of threads. Each point is an average of 10 simulation (standard error shown as error bars). (bottom) Speedup for both settings.

CHAPTER 8

CONCLUSIONS

A computational model of neocortex that preserves its multi-layer and multi-column structure was developed. It employed four different neuronal types, short-term plasticity, and detailed network connectivity, based on current state of knowledge. The used Izhikevich neuron model was modified to account for the refractory period and thus restricting its maximal firing rate.

The network model was validated by showing that it behaves close to biology in several aspects: focality of the input, ability to generate different stages of epileptiform activity with increased blockade of inhibitory cells, and functions of inhibitory fast-spiking (FS) and low-threshold spiking (LTS) neurons, including generation of gamma oscillations. The model was used for modeling global and focal lesions in the cortex and generated results consistent with biological findings.

Furthermore, the malformed cortex and several neuronal and connectional abnormalities in the area surrounding the malformation were also modeled.

Both horizontal (laminar) and vertical (columnar) organization of the neocortex are vital to its normal operations. When this organization is altered during development, neurological and cognitive abnormalities occur. Study of a biological model of the 4-layered microgyria associated with epileptiform activity revealed a number of cellular and synaptic anomalies. It is currently not known what influence each of these changes has on the overall network function.

Our model allowed investigation of the above mentioned potentially epileptogenic mechanisms in isolation. The results suggested that (1) after rewiring, increasing

excitatory input to LTS neurons was more effective in inducing epileptiform activity than was reducing the number of inhibitory FS cells to 70% within and around the malformation, (2) an increase in the excitatory input to LTS cells contributed to generation of epileptiform activity in the malformed cortex.

Appendix A

ABBREVIATIONS

EEG	Electroencephalography - recording of brain electrical activity (voltage fluctuations) along the scalp
FS	Fast-spiking neurons - inhibitory neurons that can fire periodic trains of action potentials with extremely high frequency practically without any adaptation
GABA	Gamma-aminobutyric acid - an inhibitory neurotransmitter
IB	Intrinsically bursting neurons - excitatory neurons that fire a stereotypical burst of spikes followed by repetitive single spikes
LFP	Local field potential - electrical potential recorded in neural tissue with an electrode
LTS	Low-threshold spiking neurons - inhibitory neurons that can fire high-frequency trains of action potentials, but with a noticeable spike frequency adaptation, and have low firing thresholds
NMDA receptor	Voltage-dependend glutamate receptor - NMDA (N-methyl-D-aspartate) is a selective agonist that binds to NMDA receptors but not to other 'glutamate' receptors
PSP	Post-synaptic potential - a change in the membrane potential of the postsynaptic terminal of a synapse
PV	Parvalbumin - calcium-binding protein
RS	Regular-spiking excitatory neurons - the most typical neurons in the cortex

RVA	Richmond, Virginia
SS	Somatostatin, hormone that regulates the endocrine system and affects neurotransmission
STP	Short-term plasticity - ability of a synapse between two neurons to change in strength depending on the frequency of pre-synaptic spikes; acts in tens of milliseconds to a few minutes
VCU	Virginia Commonwealth University

Appendix B

PARAMETERS OF NEURAL CONNECTIONS

All the parameters of our network are collected in in Table 4.

'D' stands for depressing, and 'F' stands for a facilitating synapse. τ_1, τ_{rec}, and τ_{fac} are the parameter of the short-term plasticity model (equation (3.2) in Section 3.2), U, C_1, C_2 are the parameters of Post-synaptic Potential (equation (3.2) in Section 3.2). The neuron type and location are coded as Ax, where A is the first letter of the neuron type, and x is the number representing layer, e.g., R6 means RS neuron in layer VI.

Some information is available to verify which cell types project horizontally across columns (Chervin et al.,1988; Telfeian and Connors,1998; Telfeian and Connors,2003). In terms of the actual values for probability and strength across columns, they were based on a percentage of the values obtained for the same connection within a column. The percentage was cell-type specific and based on the references cited above.

Table 4.: Parameters of connections.

Connection					**STP**					**PSP**		
pre-synaptic	**pos-synaptic**	**columns away**	**probability**	**strength**	**type**	τ_1	τ_{rec}	τ_{fac}	U	C_1	C_2	**References**
R3	R3	0	0.16	0.49	D	3	100	10-6	0.30	0.5	20	(Bannister and Thomson,2007; Feldmeyer et al.,2006; Hardingham et al.,2010; Holmgren et al.,2003; Kapfer et al.,2007; Mason et al.,1991; Ren et al.,2007; Reyes et al.,1998; Reyes and Sakmann,1999; Thomson and Bannister,1998; Thomson et al.,2002; Yoshimura et al.,2005)
	F3	0	0.36	0.56	D	3	110	10-6	0.20	0.5	5	(Angulo et al.,1999b; Angulo et al.,2003; Blatow et al.,2003; Buhl et al.,1997; Reyes et al.,1998; Thomson and Morris,2002; Thomson et al.,2002)
	L3	0	0.07	0.37	F	3	150	200	0.02	0.1	5	(Ali et al.,2007; Buhl et al.,1997; Kapfer et al.,2007; Porter et al.,1998; Reyes et al.,1998; Rozov et al.,2001; Tamas et al.,1998; Thomson and Deuchars,1997; von et al.,2007)
	R4	0	0.02	0.36						1	12	
	F4	0	0.01	0.05						0.1	5	
	L4	0	0.01	0.05						0.1	5	
	R5	0	0.3	1.13	D	3	100	10-6	0.40	1	18	(Hardingham et al.,2010; Kampa et al.,2006; Reyes and Sakmann,1999; Thomson and Bannister,1998; Thomson and Morris,2002)
	I5	0	0.3	1.13						1	18	
	F5	0	0.15	0.5						0.1	5	
	R3	1	0.08	0.343	D	3	100	10-6	0.30	0.5	20	
	F3	1	0.29	0.45	D	3	110	10-6	0.20	0.5	5	
	R3	2	0.04	0.24	D	3	100	10-6	0.30	0.5	20	
	F3	2	0.23	0.29	D	3	110	10-6	0.20	0.5	5	
F3	R3	0	0.37	-0.83	D	3	100	10-6	0.50	0.3	24	(Blatow et al.,2003; Holmgren et al.,2003; Kapfer et al.,2007; Reyes et al.,1998; Reyes and Sakmann,1999; Thomson et al.,2002; Wang et al.,2002)

	F3	0	0.62	-1.5	D	3	100	10-6	0.50	1	10	(Tamas et al.,1998)
	L3	0	0.34	-1.5	D	3	100	10-6	0.42	1	10	(Tamas et al.,1998)
	R3	1	0.3	-0.7	D	3	100	10-6	0.50	0.3	24	
	R3	2	0.24	-0.6	D	3	100	10-6	0.50	0.3	24	
L3	R3	0	0.54	-0.23	D	3	250	10-6	0.32	0.5	24	(Ali et al.,2007; Angulo et al.,1999a; Fanselow et al.,2008; Kapfer et al.,2007; Rozov et al.,2001; Tamas et al.,1997)
	F3	0	0.53	-0.8	D	3	100	10-6	0.53	1	10	(Reyes et al.,1998)
	L3	0	0.09	-1.5	F	3	600	1000	0.09	1	10	(Reyes et al.,1998)
	R5	0	0.35	-0.2						1	20	
	F5	0	0.53	-0.83						1	10	
	I5	0	0.04	-0.08						1	20	
	R6	0	0.25	-0.2						1	20	
	F6	0	0.53	-0.5						1	10	
R4	R3	0	0.16	1.25						0.5	15	(Ali et al.,2007; Bannister and Thomson,2007; Feldmeyer et al.,2006; Thomson et al.,2002)
	F3	0	0.23	1						0.1	5	
	L3	0	0.02	0.3						0.1	5	
	R4	0	0.1	1.09						0.8	18	(Bannister and Thomson,2007; Beierlein et al.,2003; Feldmeyer et al.,1999; Maffei et al.,2004; Petersen and Sakmann,2000; Tarczy-Hornoch et al.,1998; Thomson et al.,2002)
	F4	0	0.55	1.73	D	3	250	10-6	0.26	0.1	7	(Ali et al.,2007; Beierlein et al.,2003; Tarczy-Hornoch et al.,1998; Thomson et al.,2002)
	L4	0	0.26	0.5775	F	3	20	300	0.01	0.5	15	(Ali et al.,2007; Beierlein et al.,2003; Buhl et al.,1997; Thomson,2003)
	R5	0	0.08	0.53						1	12	(Beierlein et al.,2003; Feldmeyer et al.,2005)
	F5	0	0.1	0.45						0.1	5	
	I5	0	0.08	0.53						1	12	
	R6	0	0.03	0.25						1	12	
	F6	0	0.01	0.1						0.1	5	
	R4	1	0.08	0.872						0.8	18	
	F4	1	0.44	1.038	D	3	250	10-6	0.26	0.1	7	
	F4	2	0.22	0.623	D	3	250	10-6	0.26	0.1	7	
F4	R4	0	0.35	-1.025	D	3	250	10-6	0.26	0.08	20	(Ali et al.,2007; Beierlein et al.,2003; Tarczy-Hornoch et al.,1998; Wang et al.,2002)

	F4	0	0.74	-1.5						1	10	
	L4	0	0.36	-1						1	10	
	R4	1	0.28	-0.82	D	3	250	10-6	0.26	0.08	20	
	R4	2	0.22	-0.61	D	3	250	10-6	0.26	0.08	20	
L4	R3	0	0.1	-0.4						1	20	
	F3	0	0.3	-0.4						1	10	
	R4	0	0.39	-0.839	F	2	70	60	0.09	0.3	25	(Ali et al.,2007; Beierlein et al.,2003; Tamas et al.,1997)
	F4	0	0.62	-0.8						1	10	
	L4	0	0.08	-0.8						1	10	
	R5	0	0.1	-0.4						1	20	
	F5	0	0.3	-0.4						1	10	
	R6	0	0.05	-0.2						1	20	
	F6	0	0.15	-0.2						1	10	
R5	R3	0	0.08	0.9	D	3	100	10-6	0.40	1	12	(Thomson et al.,1996)
	F3	0	0.43	0.86						0.1	5	
	L3	0	0.52	0.5						0.1	5	
	R4	0	0.01	0.48						1	12	
	F4	0	0.43	0.5						0.1	5	
	L4	0	0.51	0.3						0.1	5	
	R5	0	0.087	0.588	D	3	350	10-6	0.50	0.8	15	(Ali,2003; Frick et al.,2007; Gil and Amitai,1996; Hardingham et al.,2010; Kalisman et al.,2005; Le Be et al.,2007; Markram,1997; Markram et al.,1997; Reyes and Sakmann,1999; Thomson and Deuchars,1997; Thomson and Bannister,1998; Thomson et al.,1993; Thomson et al.,2002; Wang et al.,2006)
	F5	0	0.6	0.585						0.1	12	(Ali et al.,2007; Angulo et al.,1999a; Thomson and Deuchars,1997)
	L5	0	0.08	0.4039						0.1	7	(Silberberg and Markram,2007; Thomson and Deuchars,1997; Thomson et al.,1995)
	I5	0	0.087	0.588	D	3	350	10-6	0.50	1	12	
	R6	0	0.03	0.5						1	12	
	F6	0	0.1	0.05						0.1	5	
	L6	0	0.19	0.02						0.1	5	
	R5	1	0.066	0.47	D	3	350	10-6	0.50	0.8	15	
	F5	1	0.275	0.4						0.1	12	
	I5	1	0.07	0.47	D	3	350	10-6	0.50	1	12	

	R5	2	0.049	0.376	D	3	350	10-6	0.50	0.8	15	
	F5	2	0.2	0.17						0.1	12	
	I5	2	0.056	0.376	D	3	350	10-6	0.50	1	12	
F5	R5	0	0.33	-0.8	D	3	60	10-6	0.60	1	15	(Ali et al.,2007; Silberberg and Markram,2007; Thomson et al.,1996; Thomson et al.,2002)
	F5	0	0.62	-1.5	D	3	80	10-6	0.50	1	10	(Pangratz-Fuehrer and Hestrin,2011)
	L5	0	0.34	-1						1	10	
	I5	0	0.1	-0.8	D	3	60	10-6	0.60	1	15	
	R5	1	0.26	-0.64	D	3	60	10-6	0.60	1	15	
	I5	1	0.06	-0.4	D	3	60	10-6	0.60	1	15	
	R5	2	0.21	-0.51	D	3	60	10-6	0.60	1	15	
	I5	2	0.03	-0.2	D	3	60	10-6	0.60	1	15	
L5	R3	0	0.35	-0.83						1	20	
	F3	0	0.53	-0.83						1	10	
	R5	0	0.35	-0.83						1	20	(Thomson et al.,1996)
	F5	0	0.53	-1						1	10	
	L5	0	0.09	-1						1	10	
	I5	0	0.03	-0.08						1	20	
	R6	0	0.25	-0.83						1	20	
	F6	0	0.53	-0.83						1	10	
I5	R3	0	0.08	0.9	D	3	100	10-6	0.4	1	12	
	F3	0	0.43	0.5						0.1	5	
	L3	0	0.52	0.3						0.1	5	
	R4	0	0.01	0.48						1	12	
	F4	0	0.43	0.5						0.1	5	
	L4	0	0.51	0.3						0.1	5	
	R5	0	0.176	0.7	D	3	350	10-6	0.5	1	12	
	F5	0	0.25	0.56						0.1	5	
	L5	0	0.08	0.62						0.1	5	
	I5	0	0.16	1.06						1	12	
	R6	0	0.03	0.6						1	12	
	F6	0	0.1	0.05						0.1	5	
	L6	0	0.19	0.02						0.1	5	
	R3	1	0.04	0.45	D	3	100	10-6	0.40	1	12	

	F3	1	0.21	0.43						0.1	5	
	L3	1	0.25	0.25						0.1	5	
	R5	1	0.15	0.8	D	3	350	10-6	0.5	1	12	
	F5	1	0.15	0.4						0.1	5	
	L5	1	0.06	0.5						0.1	5	
	I5	1	0.112	0.8	D	3	350	10-6	0.5	1	12	
	R3	2	0.02	0.23	D	3	100	10-6	0.4	1	12	
	F3	2	0.09	0.22						0.1	5	
	L3	2	0.13	0.13						0.1	5	
	R5	2	0.06	0.5	D	3	350	10-6	0.5	1	12	
	F5	2	0.032	0.3						0.1	5	
	L5	2	0.05	0.4						0.1	5	
	I5	2	0.078	0.2	D	3	350	10-6	0.5	1	12	
R6	R4	0	0.002	0.23						0.1	15	(Tarczy-Hornoch et al.,1998)
	F4	0	0.05	0.34						0.01	3	
	R5	0	0.018	1.39						0.8	20	(Mercer et al.,2005)
	F5	0	0.15	0.51						0.1	5	
	I5	0	0.018	1.39						1	12	
	R6	0	0.036	0.5	D	3	150	10-6	0.2	0.8	10	(Beierlein and Connors,2002; Mercer et al.,2005)
	F6	0	0.225	0.69	F	2	70	100	0.1	0.1	7	(Beierlein and Connors,2002; West et al.,2006)
	L6	0	0.21	0.16						1	7	(West et al.,2006)
	F6	1	0.18	0.28	F	2	70	100	0.1	0.1	7	
	F6	2	0.14	0.11	F	2	70	100	0.1	0.1	7	
F6	R6	0	0.44	-0.9						1	15	
	F6	0	0.62	-1.5						1	10	
	L6	0	0.34	-1						1	10	
	R6	1	0.35	-0.72						1	15	
	L6	2	0.28	-0.57						1	10	
L6	R3	0	0.35	-0.83						1	20	
	F3	0	0.53	-0.83						1	10	
	R5	0	0.25	-0.83						1	20	
	F5	0	0.53	-0.83						1	10	
	I5	0	0.25	-0.83						1	20	
	R6	0	0.35	-0.63						1	20	

	F6	0	0.53	-0.83						1	10	
	L6	0	0.09	-0.63						1	10	

Appendix C

EXAMPLES OF NETWORK ACTIVITY

In this appendix, we show examples of the network activity in different conditions discussed in previous chapters. Each figure shows the spike pattern of neurons and the generated LFP by column. Column 2 was stimulated at 100 ms with thalamic input of amplitude 8 (focal input) and the network was provided with the noise of amplitude 8.

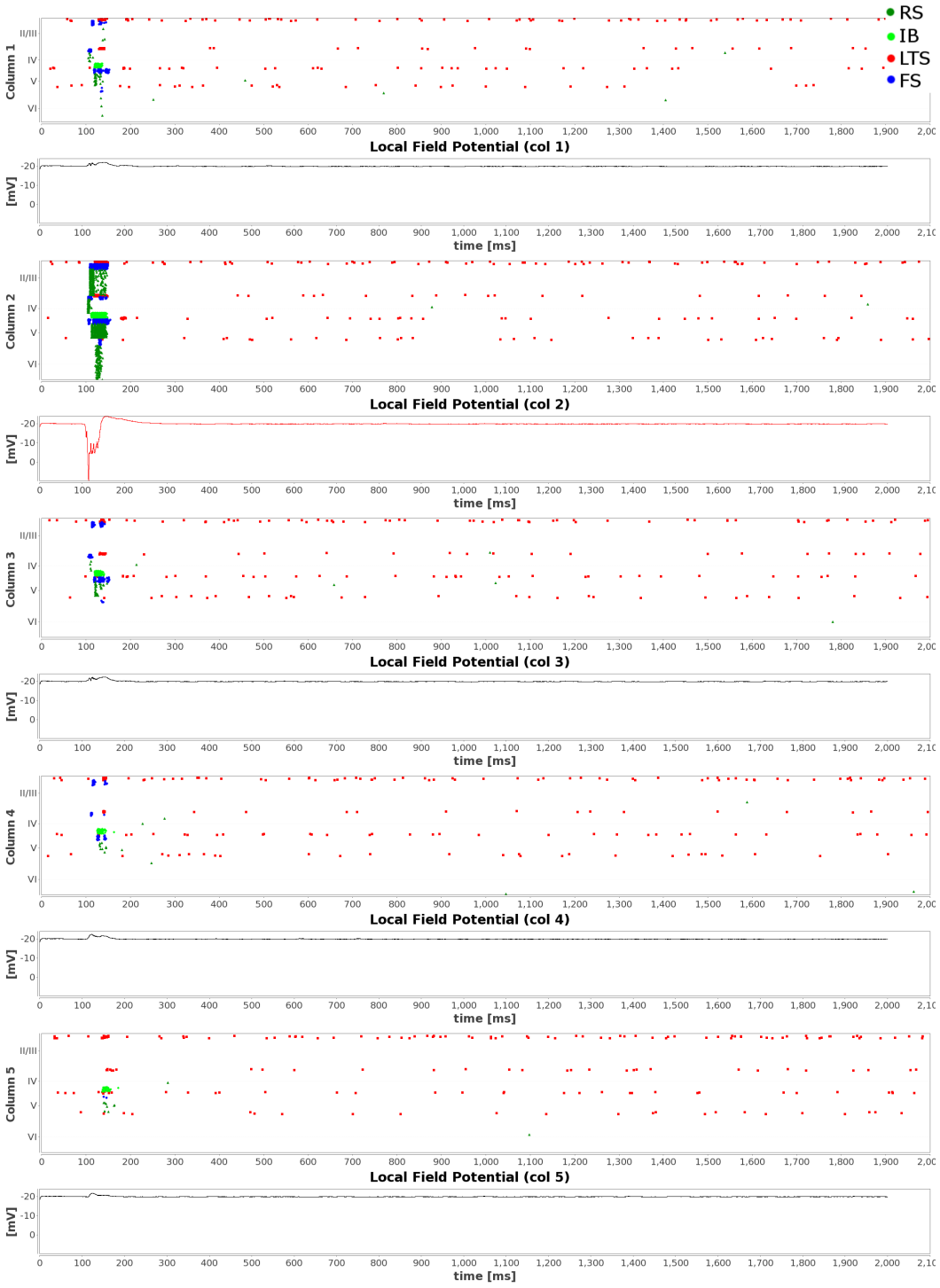

Fig. 31. Modeled condition: focal input to intact network

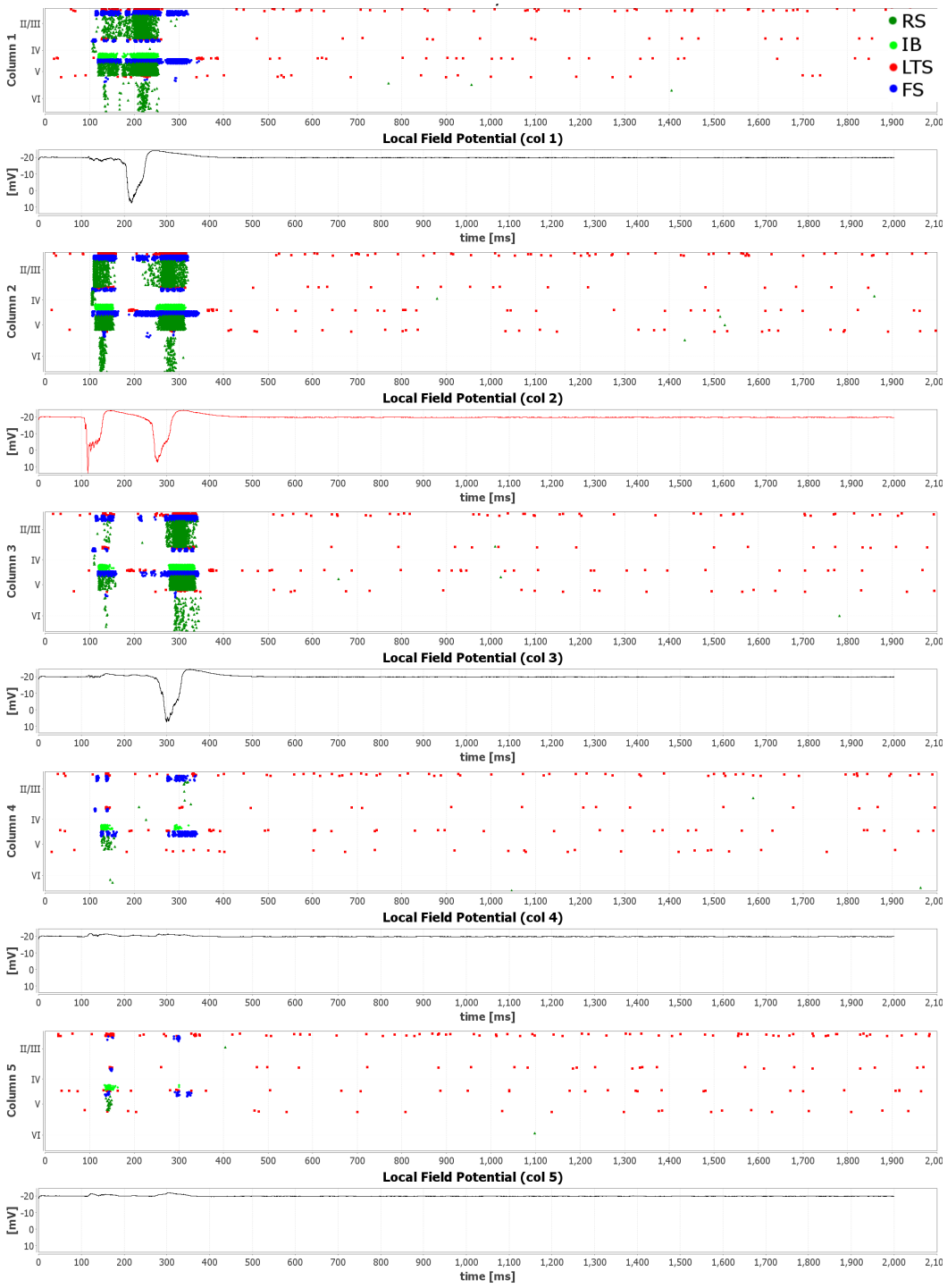

Fig. 32. Modeled condition: 10% of the inhibitory neurons, focal input to intact network.

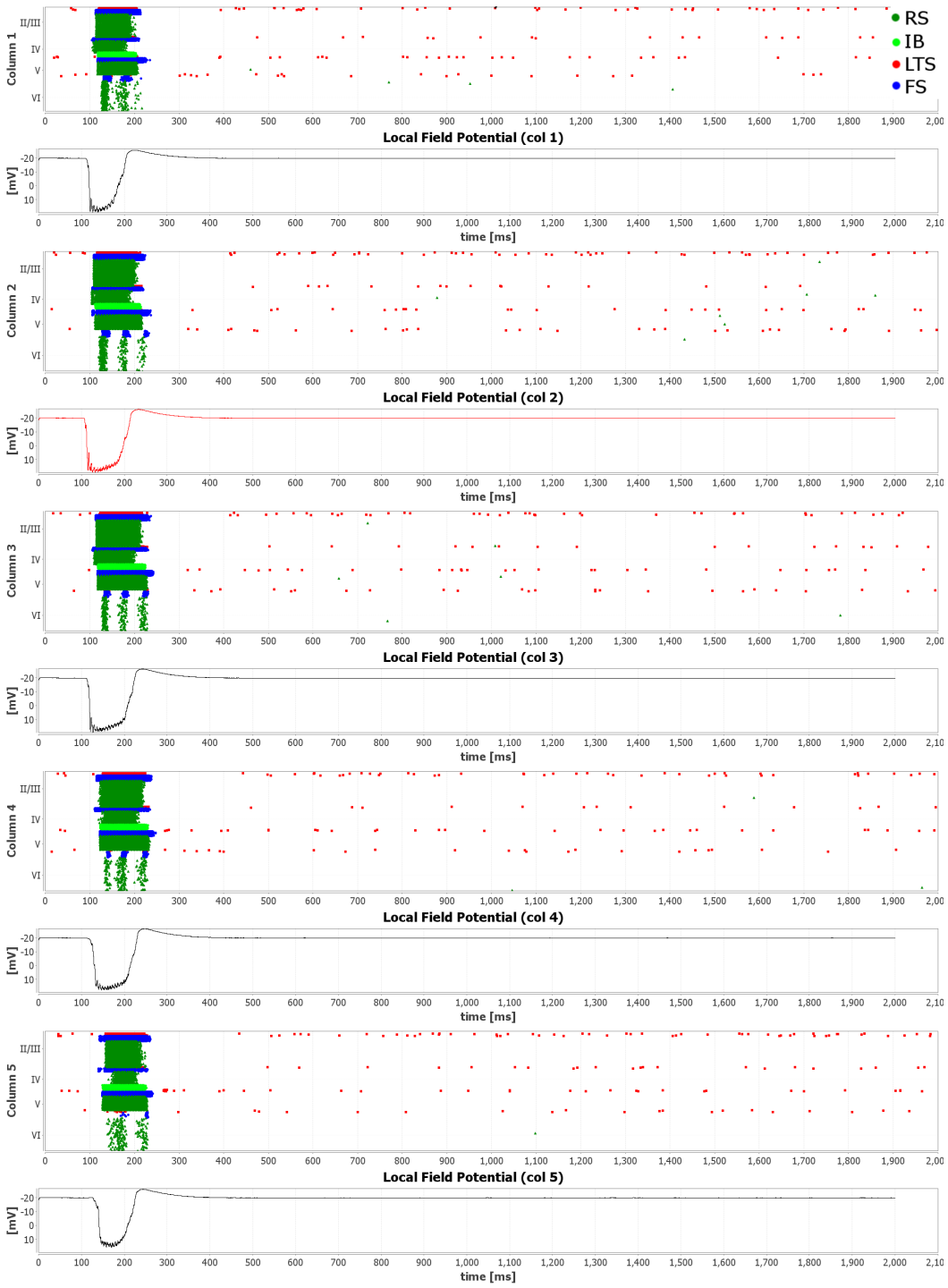

Fig. 33. Modeled condition: 50% of the inhibitory neurons, focal input to intact network.

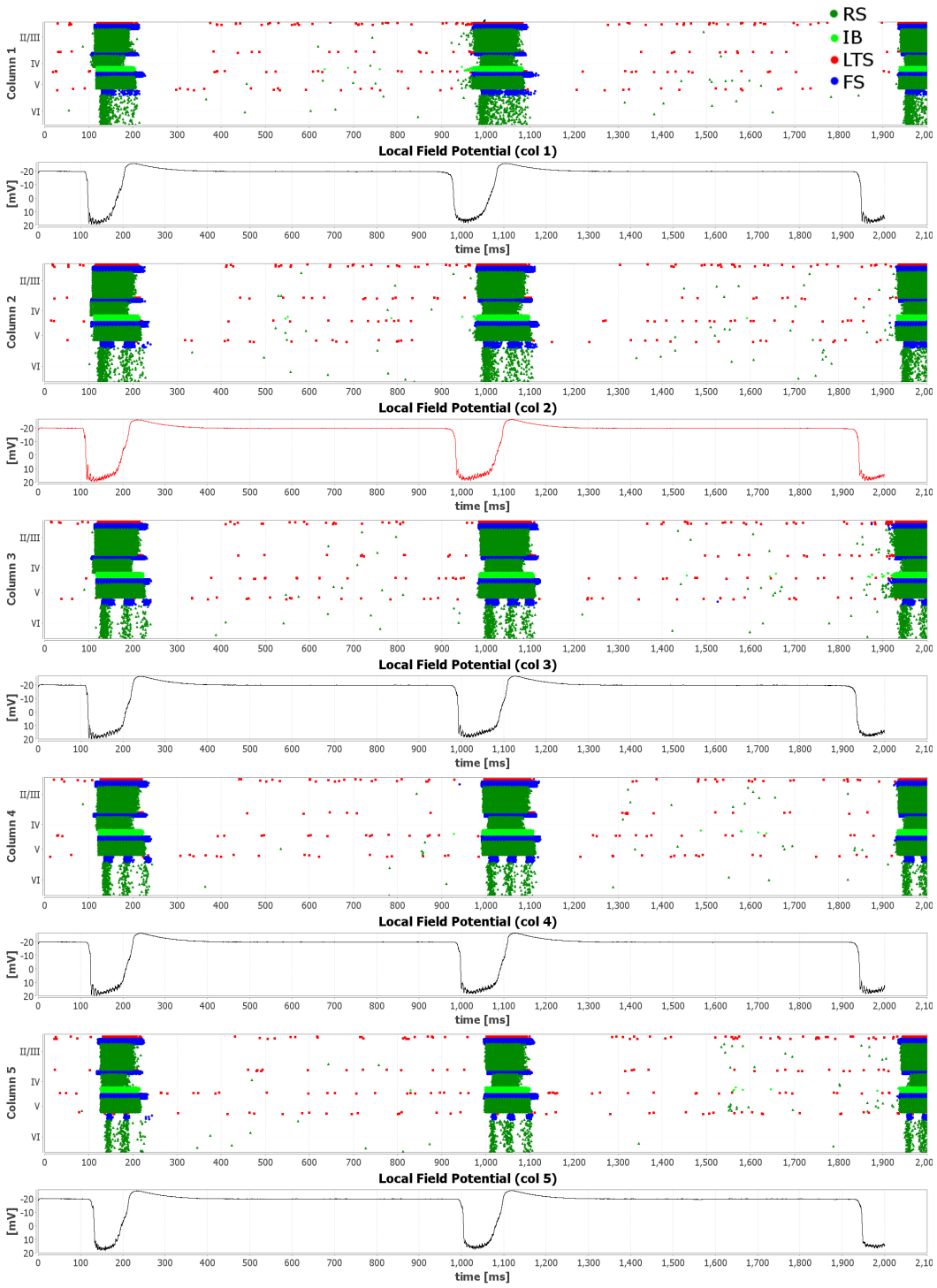

Fig. 34. Modeled condition: 80% of the inhibitory neurons, focal input to intact network.

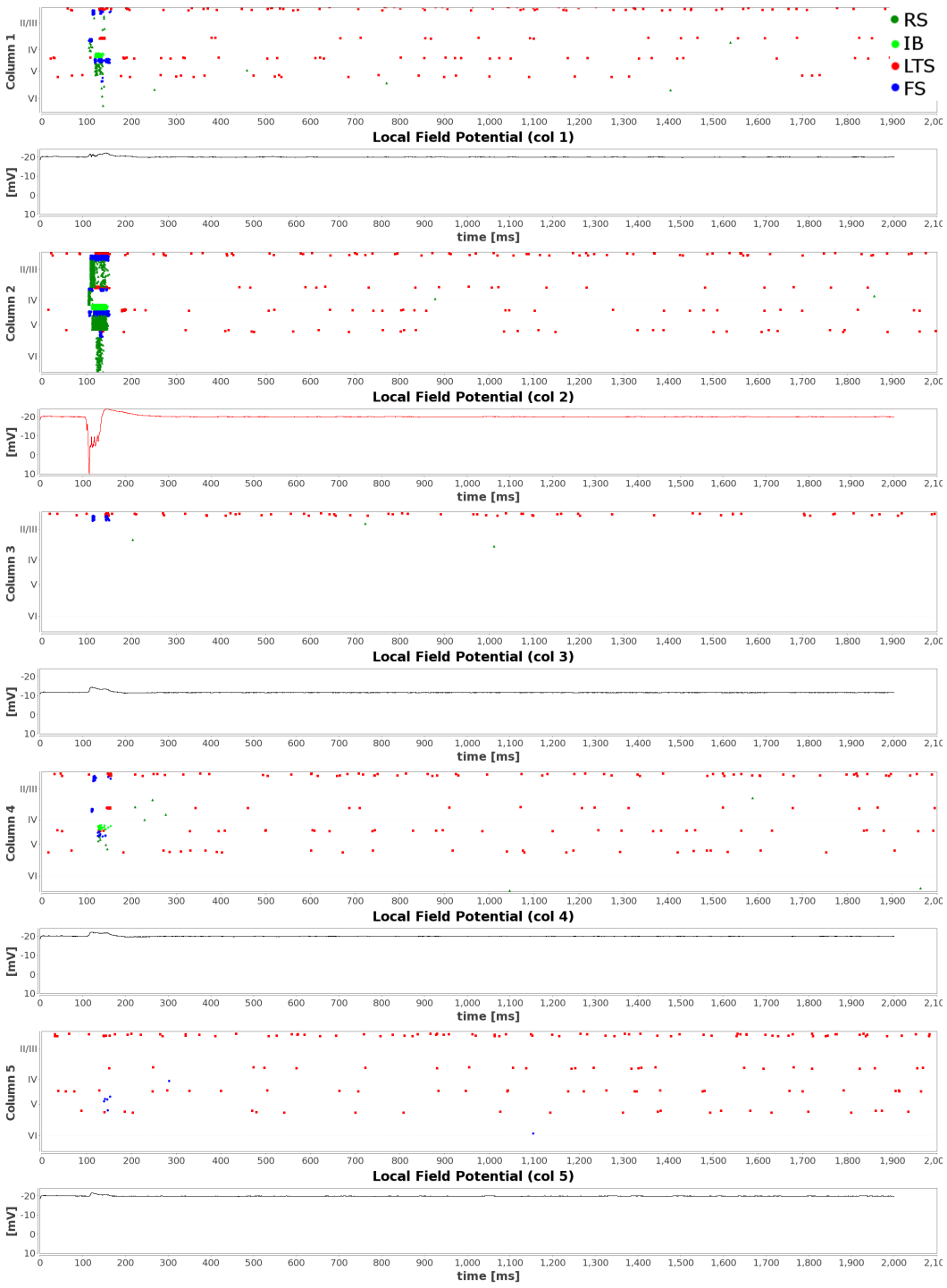

Fig. 35. Modeled condition: focal input to malformed network (removed layers IV, V, and VI from column 3).

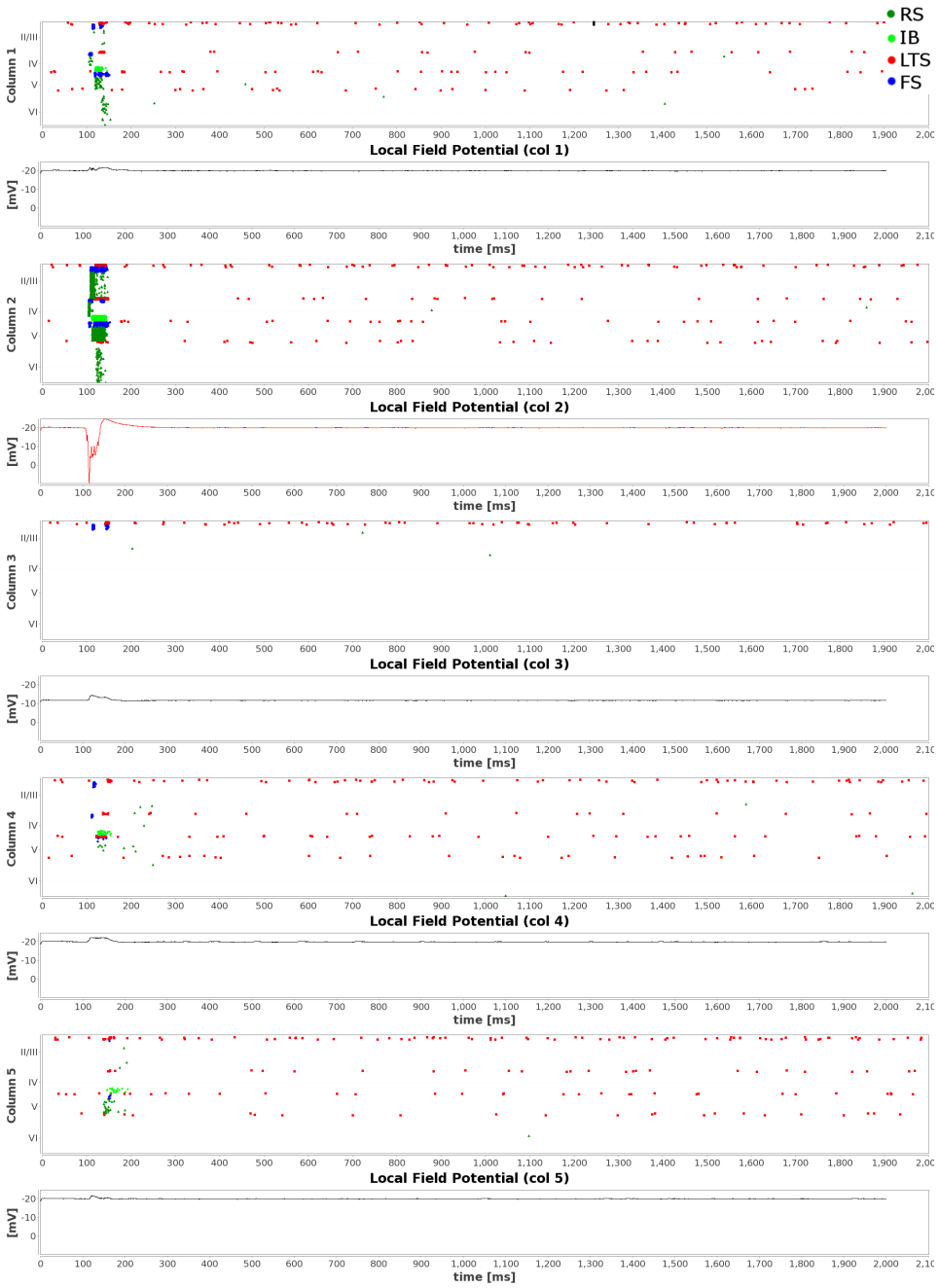

Fig. 36. Modeled condition: focal input to malformed network (removed layers IV, V, and VI from column 3) with 3X increased excitatory input to LTS neurons in columns 2-4 (see Section 6.1 for description of this condition).

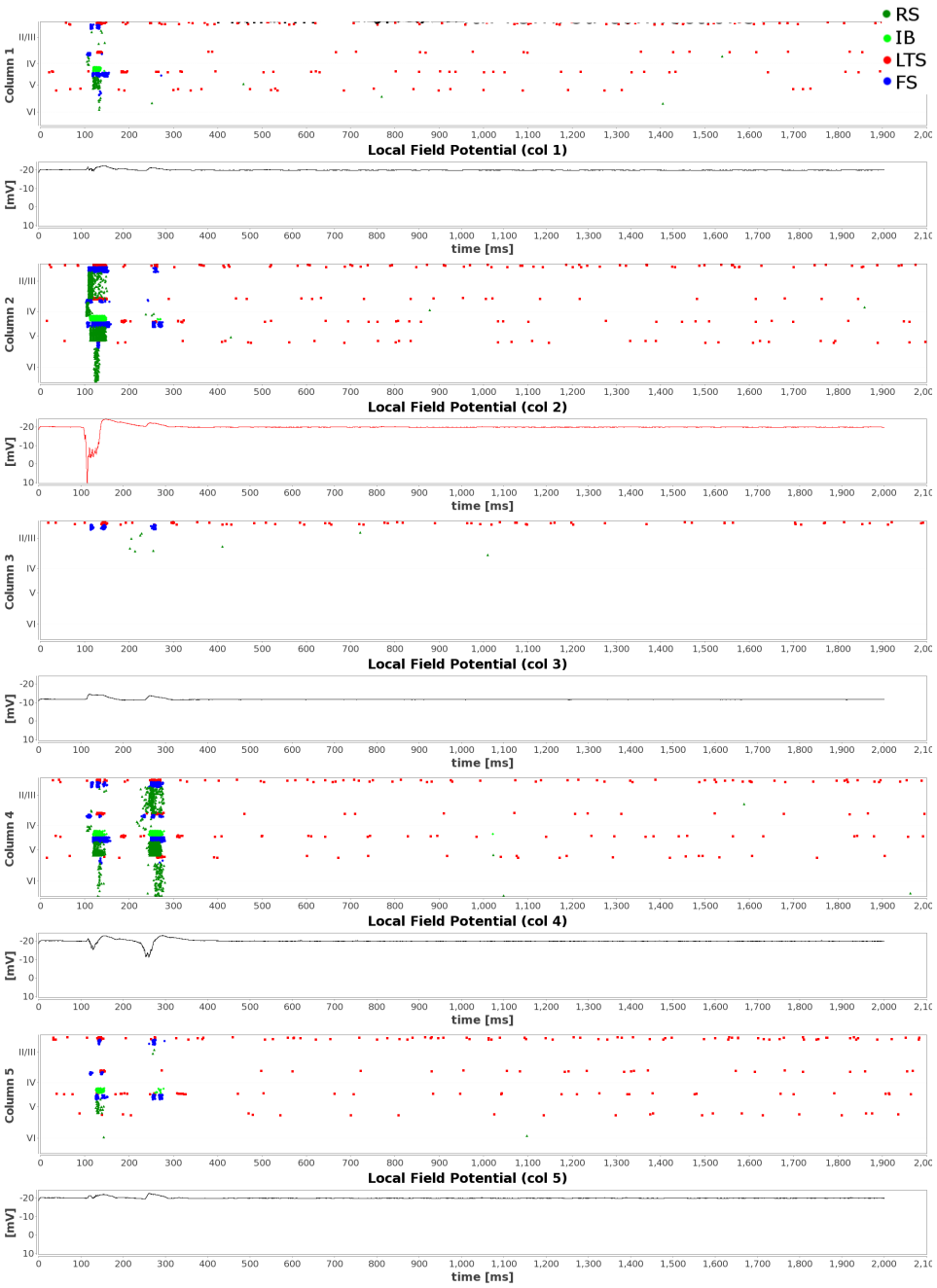

Fig. 37. Modeled condition: focal input to malformed network (removed layers IV, V, and VI from column 3) with rewired connections (see Section 6.1 for description of this condition).

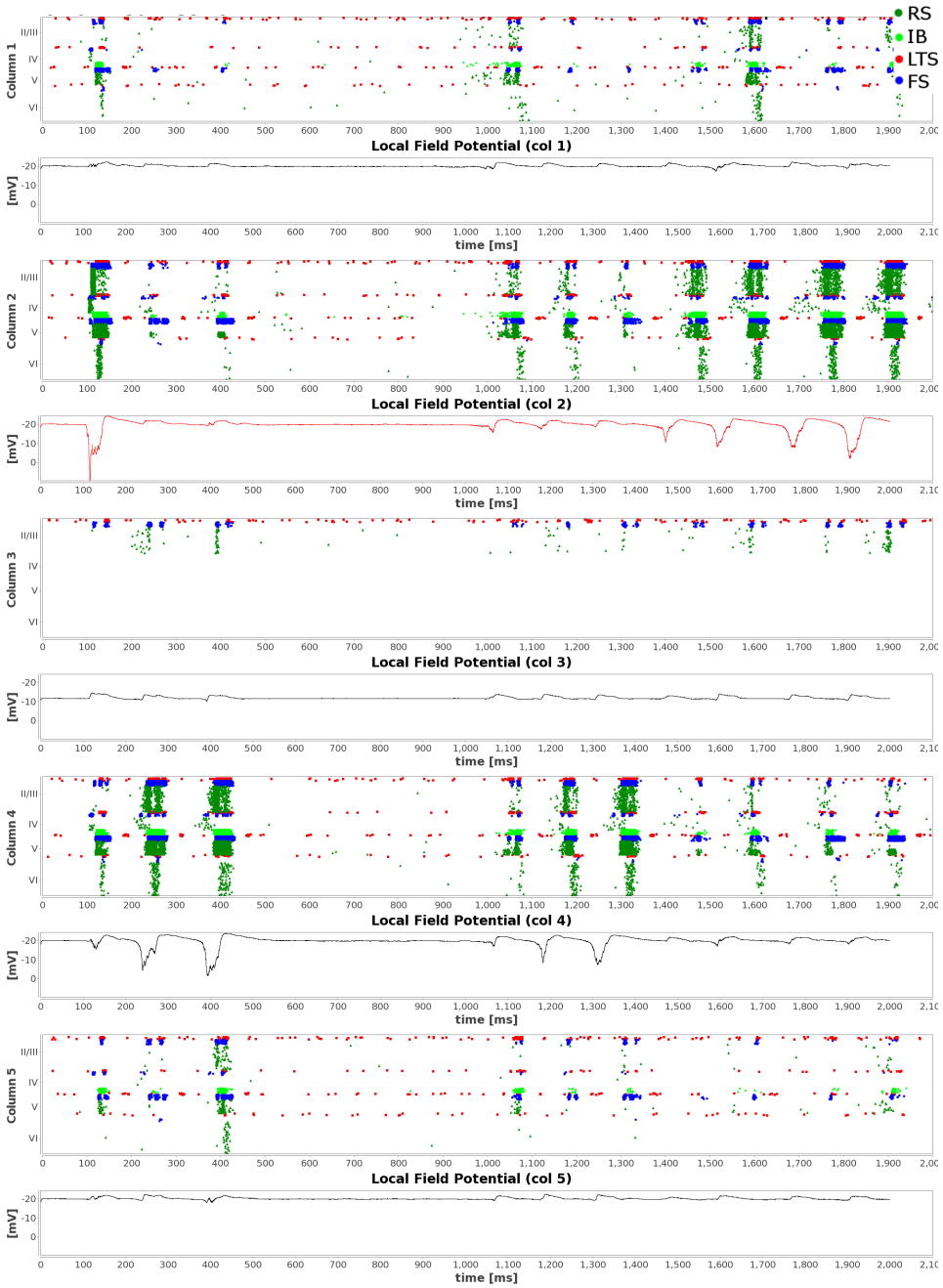

Fig. 38. Modeled condition: focal input to malformed network (removed layers IV, V, and VI from column 3) with rewired connections and 3X increased excitatory input to LTS neurons in columns 2-4 (see Section 6.1 for description of this condition).

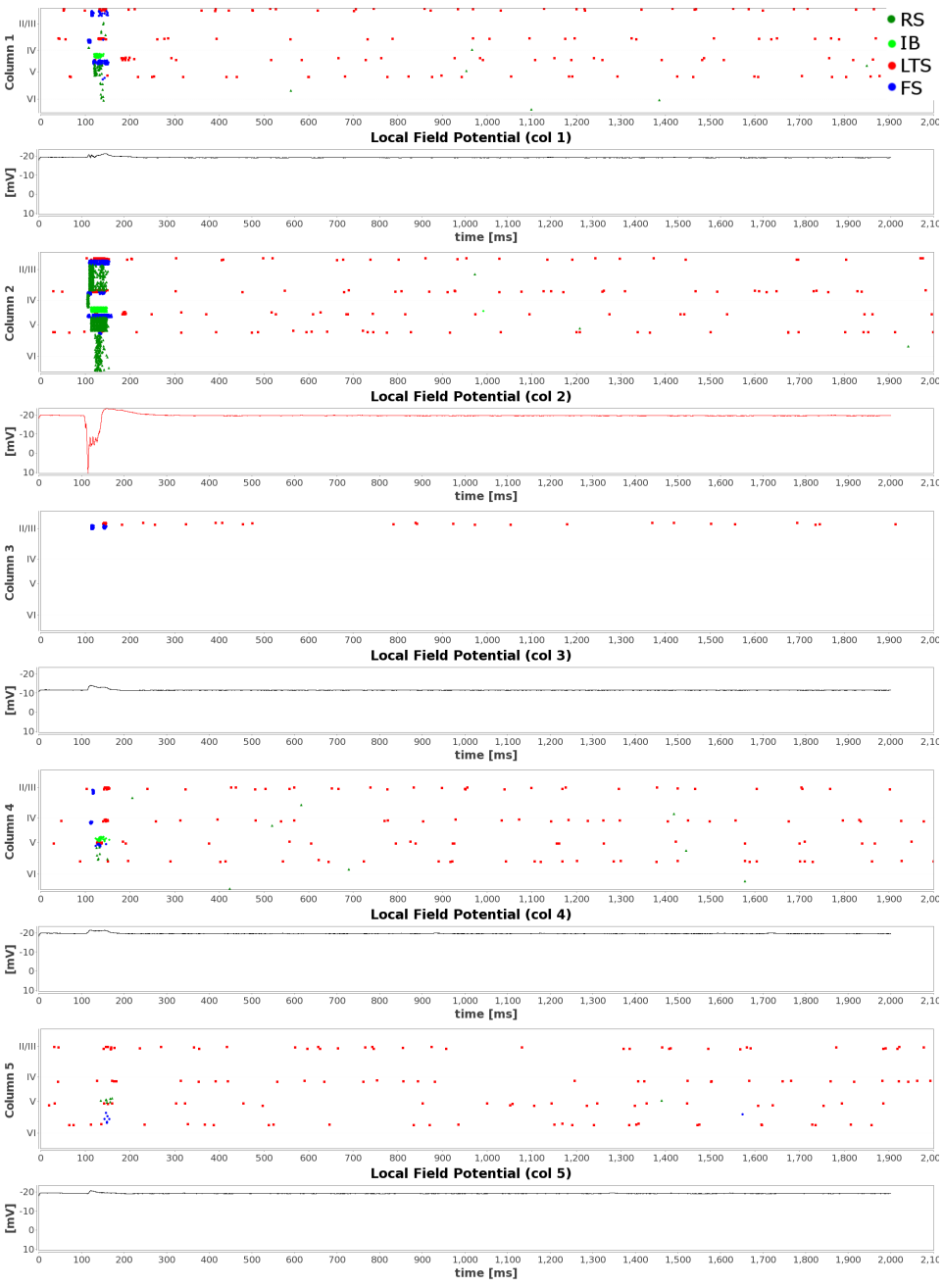

Fig. 39. Modeled condition: decrease of the number of FS neurons to 70% in columns 2-4 (see Section 6.1 for description of this condition).

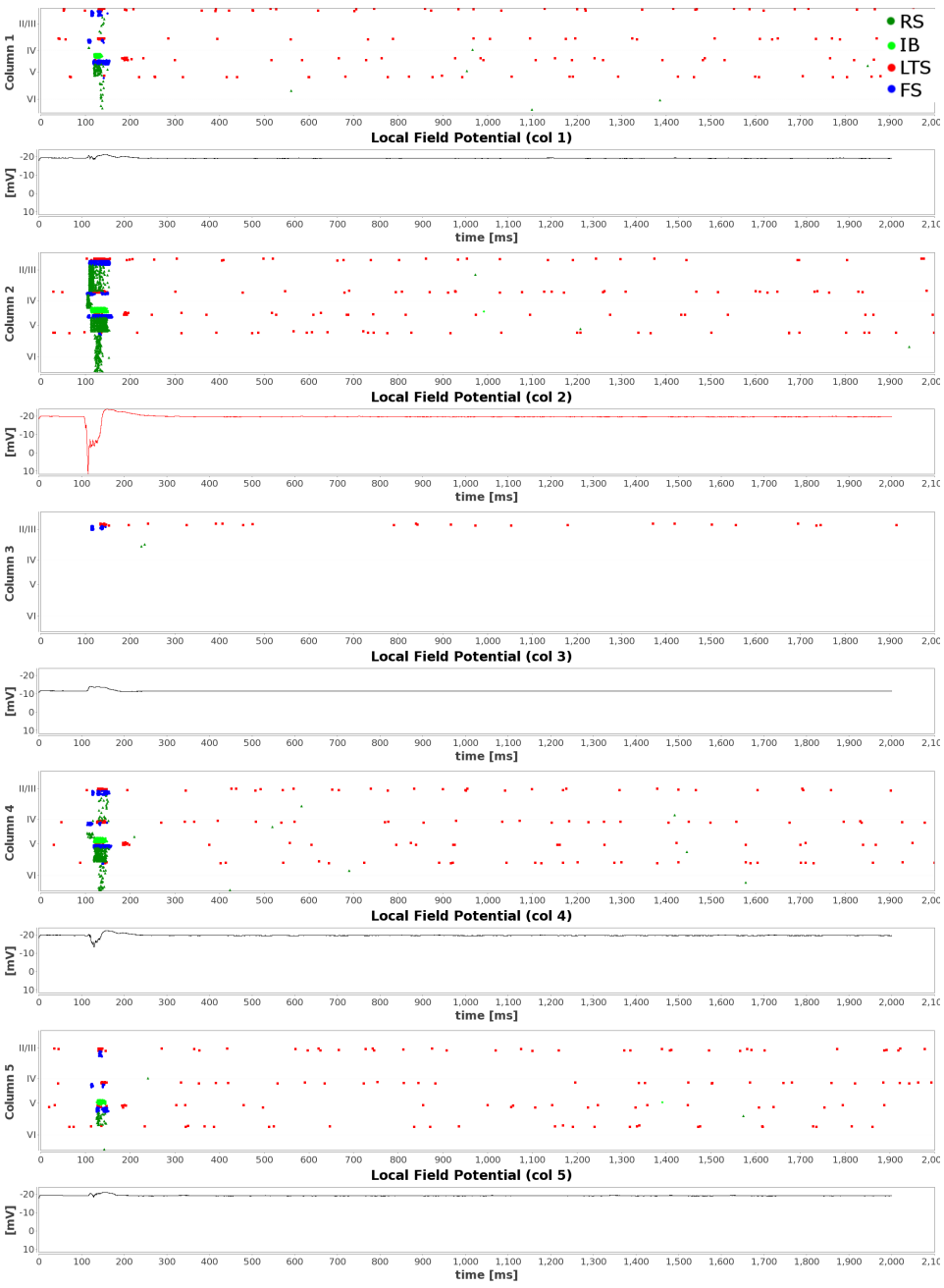

Fig. 40. Modeled condition: decrease of the number of FS neurons to 70% in columns 2-4 and rewired connections (see Section 6.1 for description of this condition).

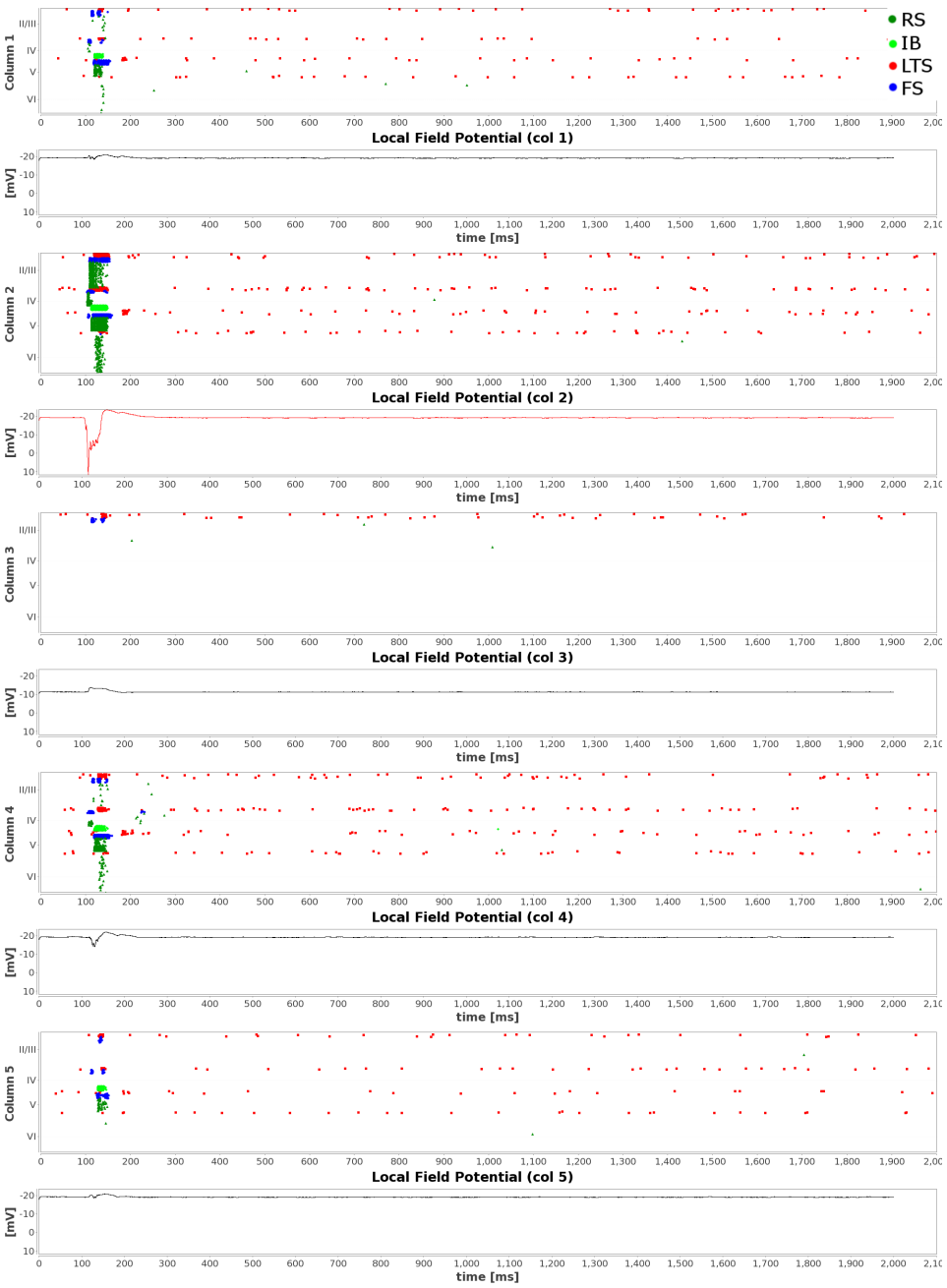

Fig. 41. Modeled condition: 30% of FS neurons in columns 2-4 replaced with LTS neurons and rewired connections (see Section 6.1 for description of this condition).

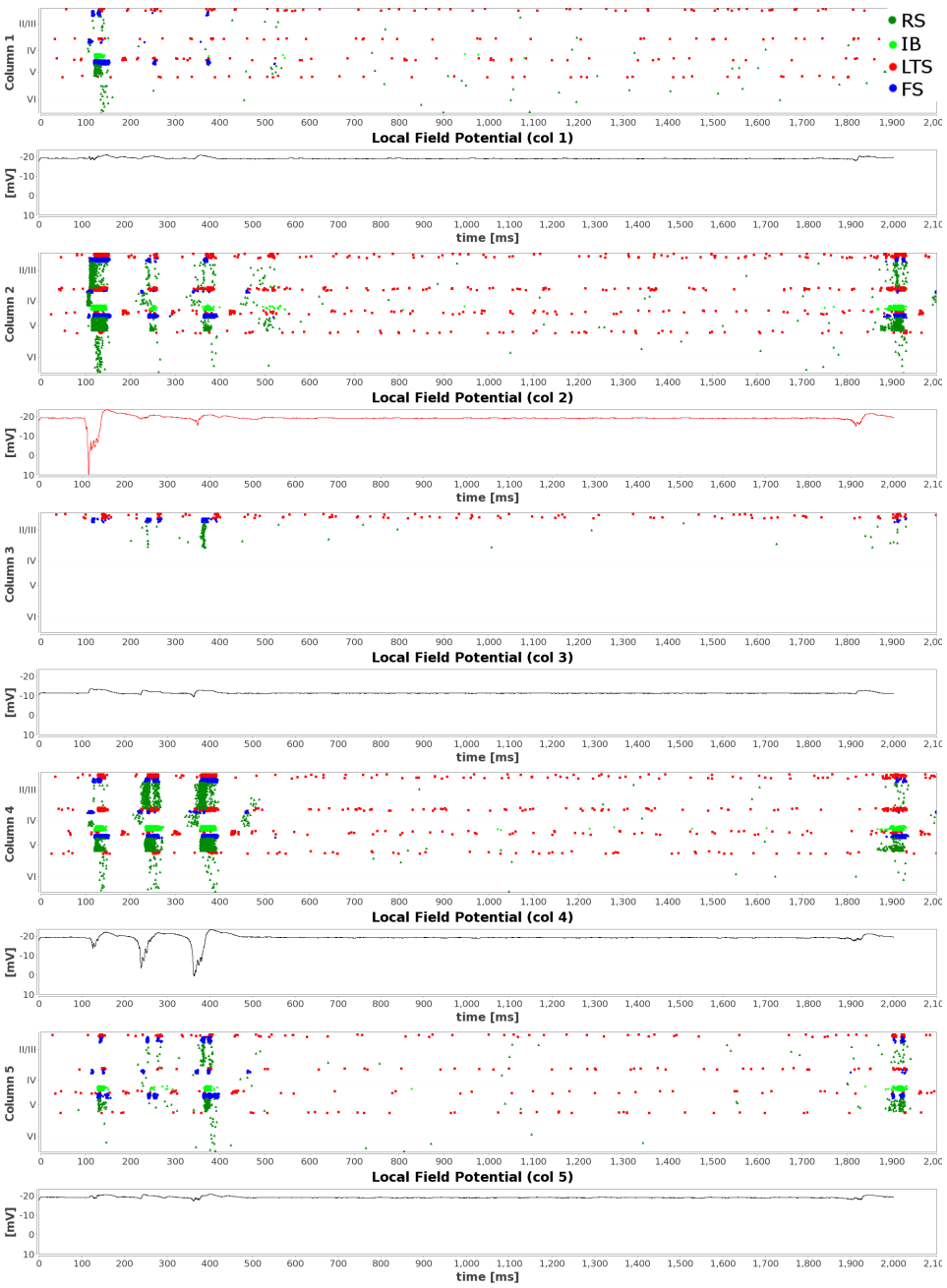

Fig. 42. Modeled condition: 30% of FS neurons in columns 2-4 replaced with LTS neurons, rewired connections and 3X increased excitation to LTS neurons (see Section 6.1 for description of this condition).

REFERENCES

Abbott, LF and SB Nelson (2000). "Synaptic plasticity: taming the beast". In: *Nat Neuroscience* 3, pp. 1178–1183.

Abbott, LF, JA Varela, K Sen, and SB Nelson (1997). "Synaptic depression and cortical gain control". In: *Science* 275, pp. 220–224.

Agmon, A. and B. W. Connors (1992). "Correlation between intrinsic firing patterns and thalamocortical synaptic responses of neurons in mouse barrel cortex." In: *J Neurosci.* 12, pp. 319–29.

Albert, PS (1991). "A Two-State Markov Mixture Model for a Time Series of Epileptic Seizure Counts". In: *Biometrics* 47, pp. 1371–1381.

Ali, A B (2003). "Involvement of post-synaptic kainate receptors during synaptic transmission between unitary connections in rat neocortex". In: *Eur J Neurosci* 17, pp. 2344–2350.

Ali, AB, AP Bannister, and AM Thomson (2007). "Robust correlations between action potential duration and the properties of synaptic connections in layer 4 interneurones in neocortical slices from juvenile rats and adult rat and cat". In: *J Physiol* 580, pp. 149–169.

Amaral, D. G. (2000). "The Anatomical Organization of the Central Nervous System". In: *Principles of Neural Science*. Ed. by E R Kandel, J H Schwartz, and T M Jessell. New York: McGraw-Hill, pp. 317–336.

Angulo, MC, J Rossier, and E Audinat (1999a). "Postsynaptic glutamate receptors and integrative properties of fast-spiking interneurons in the rat neocortex". In: *J Neurophysiol* 82, pp. 1295–1302.

Angulo, MC, JF Staiger, J Rossier, and E Audinat (1999b). "Developmental synaptic changes increase the range of integrative capabilities of an identified excitatory neocortical connection". In: *J Neurosci* 19, pp. 1566–1576.

— (2003). "Distinct local circuits between neocortical pyramidal cells and fast-spiking interneurons in young adult rats". In: *J Neurophysiol* 89, pp. 943–953.

Bacci, A., U. Rudolph, J. R. Huguenard, and D. A. Prince (2003). "Major differences in inhibitory synaptic transmission onto two neocortical interneuron subclasses." In: *J Neurosci* 23, pp. 9664–9674.

Bacci, A., J. R. Huguenard, and D. A. Prince (2005). "Modulation of neocortical interneurons: extrinsic influences and exercises in self-control." In: *Trends Neurosci.* 28, pp. 602–610.

Bannister, AP and AM Thomson (2007). "Dynamic properties of excitatory synaptic connections involving layer 4 pyramidal cells in adult rat and cat neocortex". In: *Cereb Cortex* 17, pp. 2190–2203.

Barela, AJ, SP Waddy, JG Lickfett, J Hunter, A Anido, SL Helmers, AL Goldin, and A Escayg (2006). "An epilepsy mutation in the sodium channel SCN1A that decreases channel excitability". In: *J Neurosci* 26, pp. 2714–2723.

Barkovich, A J (2010). "Current concepts of polymicrogyria". In: *Neuroradiology* 52, pp. 479–487.

Beierlein, M and B W Connors (2002). "Short-term dynamics of thalamocortical and intracortical synapses onto layer 6 neurons in neocortex". In: *J Neurophysiol* 88, pp. 1924–1932.

Beierlein, M., J. R. Gibson, and B. W. Connors (2000). "A network of electrically coupled interneurons drives synchronized inhibition in neocortex." In: *Nat Neurosci* 3, pp. 904–910.

Beierlein, M, JR Gibson, and B W Connors (2003). "Two dynamically distinct inhibitory networks in layer 4 of the neocortex". In: *J Neurophysiol* 90, pp. 2987–3000.

Bhuiyan, M.A., R Jalasutram, and T. M. Taha (2009). "Character recognition with two spiking neural network models on multicore architectures". In: *Computational Intelligence for Multimedia Signal and Vision Processing, CIMSVP '09. IEEE Symposium on*, pp. 29–34.

Binaschi, A., G. Bregola, and M. Simonato (2003). "On the role of somatostatin in seizure control: clues from the hippocampus." In: *Rev.Neurosci.* 14, pp. 285–301.

Blatow, M, A Rozov, I Katona, SG Hormuzdi, AH Meyer, MA Whittington, A Caputi, and H Monyer (2003). "A novel network of multipolar bursting interneurons generates theta frequency oscillations in neocortex". In: *Neuron* 38, pp. 805–817.

Blumcke, I, HV Vinters, D Armstrong, E Aronica, M Thom, and R Spreafico (2009). "Malformations of cortical development and epilepsies: neuropathological findings with emphasis on focal cortical dysplasia". In: *Epileptic Disord* 11, pp. 181–193.

Borgers, C, S Epstein, and NJ Kopell (2005). "Background gamma rhythmicity and attention in cortical local circuits: A computational study". In: *Proc Natl Acad Sci U S A* 102, pp. 7002–7007.

Brette, R et al. (2007). "Simulation of networks of spiking neurons: A review of tools and strategies." In: *Journal of Computational Neuroscience* 23, pp. 349–398.

Buckmaster, PS and FE Dudek (1997). "Neuron loss, granule cell axon reorganization, and functional changes in the dentate gyrus of epileptic kainate-treated rats". In: *J Comp Neurol* 385, pp. 385–404.

Buhl, EH, G Tamas, T Szilagyi, C Stricker, O Paulsen, and P Somogyi (1997). "Effect, number and location of synapses made by single pyramidal cells onto aspiny interneurones of cat visual cortex". In: *J Physiol* 500, pp. 689–713.

Bush, P and T Sejnowski (1996). "Inhibition synchronizes sparsely connected cortical neurons within and between columns in realistic network models". In: *J Comput Neurosci* 3, pp. 91–110.

Chagnac-Amitai, Y and B W Connors (1989a). "Horizontal spread of synchronized activity in neocortex and its control by GABA-mediated inhibition." In: *J Neurophysiol* 61, pp. 747–58.

— (1989b). "Synchronized excitation and inhibition driven by intrinsically bursting neurons in neocortex." In: *J Neurophysiol* 62, pp. 1149–1162.

Chagnac-Amitai, Y, H J Luhmann, and D A Prince (1990). "Burst generating and regular spiking layer 5 pyramidal neurons of rat neocortex have different morphological features." In: *J Comp Neurol.* 296, pp. 598–613.

Chakravarthy, N, S Sabesan, L Iasemidis, and K Tsakalis (2007). "Controlling synchronization in a neuron-level population model". In: *Int J Neural Syst* 17, pp. 123–138.

Chervin, RD, PA Pierce, and BW Connors (1988). "Periodicity and directionality in the propagation of epileptiform discharges across neocortex". In: *J Neurophysiol* 60, pp. 1695–1713.

Connors, B W (1984). "Initiation of synchronized neuronal bursting in neocortex." In: *Nature* 310, pp. 685–7.

Connors, BW and MJ Gutnick (1990). "Intrinsic firing patterns of diverse neocortical neurons". In: *Trends Neurosci* 13, pp. 99–104.

Connors, BW and AE Telfeian (2000). "Dynamic properties of cells, synapses, circuits, and seizures in neocortex". In: *Adv Neurol* 84, pp. 141–152.

Connors, BW, MJ Gutnick, and DA Prince (1982). "Electrophysiological properties of neocortical neurons in vitro". In: *J Neurophysiol* 48, pp. 1302–1320.

Cosandier-Rimele, D, I Merlet, F Bartolomei, JM Badier, and F Wendling (2010). "Computational modeling of epileptic activity: from cortical sources to EEG signals". In: *J Clin Neurophysiol* 27, pp. 465–470.

Cunningham, MO, MA Whittington, A Bibbig, A Roopun, FEN LeBeau, A Vogt, H Monyer, EH Buhl, and RD Traub (2004). "A role for fast rhythmic bursting neurons in cortical gamma oscillations in vitro". In: *Proc Natl Acad Sci U S A* 101, pp. 7152–7157.

Dayan, P. and L. Abbott (2001). *Theoretical Neuroscience : Computational and Mathematical Modeling of Neural Systems*. Cambridge, MA: MIT Press.

Deco, G, VK Jirsa, PA Robinson, M Breakspear, and K Friston (2008). "The dynamic brain: from spiking neurons to neural masses and cortical fields". In: *PLoS Comput Biol* 4, e1000092.

DeFelipe, J, GN Elston, I Fujita, J Fuster, KH Harrison, PR Hof, Y Kawaguchi, KA Martin, KS Rockland, AM Thomson, SS Wang, EL White, and R Yuste (2002). "Neocortical circuits: Evolutionary aspects and specificity versus non-specificity of synaptic connections Remarks, main conclusions and general comments and discussion". In: *J Neurocytol* 31, pp. 387–416.

Demirkol, A. S. and S. Ozoguz (2011). "A low power VLSI implementation of the Izhikevich neuron model". In: *IEEE 9th International New Circuits and Systems Conference (NEWCAS)*, pp. 169–172.

Douglas, R. J. and K. A. Martin (2004). "Neuronal circuits of the neocortex". In: *Journal of Computational Neuroscience* 27, pp. 419–451.

Drongelen, W van, HC Lee, M Hereld, Z Chen, FP Elsen, and RL Stevens (2005). "Emergent epileptiform activity in neural networks with weak excitatory synapses". In: *IEEE Trans Neural Syst Rehabil Eng* 13, pp. 236–241.

Drongelen, W van, HC Lee, RL Stevens, and M Hereld (2007). "Propagation of seizure-like activity in a model of neocortex". In: *J Clin Neurophysiol* 24, pp. 182–188.

Ermentrout, B and D Saunders (2006). "Phase resetting and coupling of noisy neural oscillators". In: *Journal of Computational Neuroscience* 20, pp. 179–190.

Fanselow, EE, KA Richardson, and BW Connors (2008). "Selective, state-dependent activation of somatostatin-expressing inhibitory interneurons in mouse neocortex". In: *J Neurophysiol* 100, pp. 2640–2652.

Feldmeyer, D, V Egger, J Lubke, and B Sakmann (1999). "Reliable synaptic connections between pairs of excitatory layer 4 neurones within a single 'barrel' of developing rat somatosensory cortex". In: *J Physiol* 521Pt1, pp. 169–190.

Feldmeyer, D, A Roth, and B Sakmann (2005). "Monosynaptic connections between pairs of spiny stellate cells in layer 4 and pyramidal cells in layer 5A indicate that lemniscal and paralemniscal afferent pathways converge in the infragranular somatosensory cortex". In: *J Neurosci* 25, pp. 3423–3431.

Feldmeyer, D, J Lubke, and B Sakmann (2006). "Efficacy and connectivity of intracolumnar pairs of layer 2/3 pyramidal cells in the barrel cortex of juvenile rats". In: *J Physiol* 575, pp. 583–602.

Fisher, Robert S., Walter van Emde Boas, Warren Blume, Christian Elger, Pierre Genton, Phillip Lee, and Jerome Engel (2005). "Epileptic seizures and epilepsy: definitions proposed by the international league against epilepsy (ILAE) and the international bureau for epilepsy (IBE)". In: *Epilepsia* 46, pp. 470–472.

Franaszczuk, PJ, P Kudela, and GK Bergey (2003). "External excitatory stimuli can terminate bursting in neural network models". In: *Epilepsy Res* 53, pp. 65–80.

Freeman, WJ (1978). "Models of the dynamics of neural populations". In: *Electroencephalogr Clin Neurophysiol* Suppl, pp. 9–18.

Frick, A, D Feldmeyer, and B Sakmann (2007). "Postnatal development of synaptic transmission in local networks of L5A pyramidal neurons in rat somatosensory cortex". In: *J Physiol* 585, pp. 103–116.

George, AL and KM Jacobs (2011). "Altered intrinsic properties of neuronal subtypes in malformed epileptogenic cortex". In: *Brain Research* 1374, pp. 116–128.

Gil, Z and Y Amitai (1996). "Properties of convergent thalamocortical and intracortical synaptic potentials in single neurons of neocortex". In: *J Neurosci* 16, pp. 6567–6578.

Gilbert, D, H Fuss, X Gu, R Orton, S Robinson, V Vyshemirsky, MJ Kurth, CS Downes, and W Dubitzky (2006). "Computational methodologies for modelling, analysis and simulation of signalling networks". In: *Brief Bioinform* 7, pp. 339–353.

Gilson, M, A Burkitt, D Grayden, D Thomas, and J van Hemmen (2009). "Emergence of network structure due to spike-timing-dependent plasticity in recurrent neuronal networks IV". In: *Biological cybernetics* 101, pp. 427–444.

Golden, JA and BN Harding (2010). "Cortical malformations: unfolding polymicrogyria". In: *Nat Rev Neurol* 6, pp. 471–472.

Hansel, D. and G. Mato (2001). "Existence and stability of persistent states in large neuronal networks." In: *Physical Review Letters* 86, pp. 4175–4178.

Hardingham, N R, J C Read, A J Trevelyan, J C Nelson, J J Jack, and N J Bannister (2010). "Quantal analysis reveals a functional correlation between presynaptic

and postsynaptic efficacy in excitatory connections from rat neocortex". In: *J Neurosci* 30, pp. 1441–1451.

Hauser, W and D Hesdorffer (1991). "Epilepsy: Frequency, Causes, and Consequences". In: *New York, NY: Demos.*

Haut, SR, RB Lipton, AJ LeValley, CB Hall, and S Shinnar (2005). "Identifying seizure clusters in patients with epilepsy". In: *Neurology* 65, pp. 1313–1315.

Hereld, M, R Stevebs, H Lee, and W van Drongelen (2005). "Large neural simulations on large parallel computers". In: *International journal of bioelectromagnetism* 7, p. 44.

Hereld, M, RL Stevens, HC Lee, and W van Drongelen (2007). "Framework for interactive million-neuron simulation". In: *J Clin Neurophysiol* 24, pp. 189–196.

Hodgkin, A L and A F Huxley (1952). "A quantitative description of membrane current and its application to conduction and excitation in nerve". In: *J Physiol* 117, pp. 500–544.

Hof, Patrick R., Huiling Duan, Tanya L. Page, Michael Einstein, Bridget Wicinski, Yong He, Joseph M. Erwin, and John H. Morrison (2002). "Age-related changes in GluR2 and NMDAR1 glutamate receptor subunit protein immunoreactivity in corticocortically projecting neurons in macaque and patas monkeys." In: *Brain Res.* 928, pp. 175–186.

Holmgren, C, T Harkany, B Svennenfors, and Y Zilberter (2003). "Pyramidal cell communication within local networks in layer 2/3 of rat neocortex". In: *J Physiol* 551, pp. 139–153.

Hwa, G. G. and M. Awoli (1989). "NMDA receptor antagonists CPP and MK-801 partially suppress the epileptiform discharges induced by the convulsant drug bicuculline in the rat neocortex." In: *Neurosci Lett.* 98, pp. 189–93.

Ichinose, T and T Murakoshi (1996). "Electrophysiological elucidation of pathways of intrinsic horizontal connections in rat visual cortex." In: *Neuroscience* 73, pp. 25–37.

Izhikevich, E M (2003). "Simple model of spiking neurons". In: *Neural Networks, IEEE Transactions on* 14, pp. 1569–1572.

— (2004). "Which model to use for cortical spiking neurons?" In: *IEEE Trans Neural Netw* 15, pp. 1063–1070.

Izhikevich, E M and G M Edelman (2008). "Large-scale model of mammalian thalamocortical systems". In: *Proceedings of the National Academy of Sciences* 105, pp. 3593–3598.

Jacobs, K M, M Mogensen, L Warren, and D A Prince (1999a). "Experimental microgyri disrupt the barrel field pattern in rat somatosensory cortex." In: *Cerebral Cortex* 9, pp. 733–744.

Jacobs, K M, B J Hwang, and D A Prince (1999b). "Focal epileptogenesis in a rat model of polymicrogyria." In: *Journal of Neurophysiology* 81, pp. 159–173.

Jacobs, KM and DA Prince (2005). "Excitatory and inhibitory postsynaptic currents in a rat model of epileptogenic microgyria". In: *J Neurophysiol* 93, pp. 687–696.

Jacobs, KM, VN Kharazia, and DA Prince (1999c). "Mechanisms underlying epileptogenesis in cortical malformations". In: *Epilepsy Res* 36, pp. 165–188.

Kalisman, N, G Silberberg, and H Markram (2005). "The neocortical microcircuit as a tabula rasa". In: *Proc Natl Acad Sci U S A* 102, pp. 880–885.

Kampa, BM, JJ Letzkus, and GJ Stuart (2006). "Cortical feed-forward networks for binding different streams of sensory information". In: *Nat Neurosci* 9, pp. 1472–1473.

Kandel, E R, J H Schwartz, and T M Jessell (2000). *Principles of Neural Science.* New York: McGraw-Hill.

Kapfer, C, LL Glickfeld, BV Atallah, and M Scanziani (2007). "Supralinear increase of recurrent inhibition during sparse activity in the somatosensory cortex". In: *Nat Neurosci* 10, pp. 743–753.

Kawaguchi, Y (1993). "Physiological, morphological, and histochemical characterization of three classes of interneurons in rat neostriatum." In: *The Journal of neuroscience* 13, pp. 4908–4923.

Kawaguchi, Y and S Kondo (2002). "Parvalbumin, somatostatin and cholecystokinin as chemical markers for specific GABAergic interneuron types in the rat frontal cortex". In: *J Neurocytol* 31, pp. 277–287.

Kawaguchi, Y. and Y Kubota (1996). "PPhysiological and morphological identification of somatostatin- or vasoactive intestinal polypeptide-containing cells among GABAergic cell subtypes in rat frontal cortex." In: *J Neurosci.* 16, pp. 2701–2715.

Kubota, Y and Y Kawaguchi (1994). "Three classes of GABAergic interneurons in neocortex and neostriatum". In: *Jpn J Physiol 44 Suppl* 2, S145–S148.

— (1997). "Two distinct subgroups of cholecystokinin-immunoreactive cortical interneurons". In: *Brain Res* 752, pp. 175–183.

Kuruba, R., B. Hattiangady, V. K. Parihar, B. Shuai, and A. K. Shetty (2011). "Differential susceptibility of interneurons expressing neuropeptide Y or parvalbumin in the aged hippocampus to acute seizure activity." In: *PloS one* 6, e24493.

Kwan, P and MJ Brodie (2006). "Refractory epilepsy: mechanisms and solutions". In: *Expert Rev Neurother* 6, pp. 397–406.

Latham, P.E., B.J. Richmond, P.G. Nelson, and S. Nirenberg (2000). "Intrinsic dynamics in neuronal networks. I. Theory". In: *Journal of Neurophysiology* 83, pp. 808–827.

Le Be, J V, G Silberberg, Y Wang, and H Markram (2007). "Morphological, electrophysiological, and synaptic properties of corticocallosal pyramidal cells in the neonatal rat neocortex". In: *Cereb Cortex* 17, pp. 2204–2213.

Legenstein, RF, CF Naeger, and W Maass (2005). "What can a neuron learn with spike-timing-dependent plasticity?" In: *Neural Computation* 17, pp. 2337–2382.

Lim, H. K., L. P. Keniston, J. H. Shin, B. L. Allman, M. A. Meredith, and KJ Cios (2011a). "Connectional parameters determine multisensory processing in a spiking network model of multisensory convergence". In: *Exp Brain Res* vol.213, pp. 329–339.

Lim, HK, LP Keniston, and KJ Cios (2011b). "Modeling of Multisensory Convergence with a Network of Spiking Neurons: A Reverse Engineering Approach". In: *Biomedical Engineering, IEEE Transactions on* 58, pp. 1940–1949.

Long, M A, S J Cruikshank, M J Jutras, and B W Connors (2005). "Abrupt maturation of a spike-synchronizing mechanism in neocortex". In: *J Neurosci* 25, pp. 7309–7316.

Lovelace, J. J. and K. J. Cios (2008). "A very simple spiking neuron model that allows for modeling of large, complex systems." In: *Electroencephalography and clinical neurophysiology* 20, pp. 65–90.

Lubke, J and D Feldmeyer (2007). "Excitatory signal flow and connectivity in a cortical column: focus on barrel cortex". In: *Brain Struct Funct* 212, pp. 3–17.

Lytton, WW (2008). "Computer modelling of epilepsy". In: *Nat Rev Neurosci* 9, pp. 626–637.

Lytton, WW and TJ Sejnowski (1992). "Computer model of ethosuximide's effect on a thalamic neuron". In: *Annals of Neurology* 32, pp. 131–139.

Lytton, WW, KM Hellman, and TP Sutula (1998). "Computer models of hippocampal circuit changes of the kindling model of epilepsy". In: *Artif Intell Med* 13, pp. 81–97.

Maffei, A, SB Nelson, and GG Turrigiano (2004). "Selective reconfiguration of layer 4 visual cortical circuitry by visual deprivation". In: *Nat Neurosci* 7, pp. 1353–1359.

Markram, H (1997). "A network of tufted layer 5 pyramidal neurons". In: *Cereb Cortex* 7, pp. 523–533.

— (2006). "The blue brain project". In: *Nat Rev Neurosci* 7, pp. 153–160.

Markram, H, J Lubke, M Frotscher, A Roth, and B Sakmann (1997). "Physiology and anatomy of synaptic connections between thick tufted pyramidal neurones in the developing rat neocortex". In: *J Physiol* 500, pp. 409–440.

Markram, H, M Toledo-Rodriguez, Y Wang, A Gupta, G Silberberg, and C Wu (2004). "Interneurons of the neocortical inhibitory system". In: *Nat Rev Neurosci* 5, pp. 793–807.

Mason, A, A Nicoll, and K Stratford (1991). "Synaptic transmission between individual pyramidal neurons of the rat visual cortex in vitro". In: *J Neurosci* 11, pp. 72–84.

McCormick, D. A., B. W. Connors, J. W. Lighthall, and D. A. Prince (1985). "Comparative electrophysiology of pyramidal and sparsely spiny stellate neurons of the neocortex." In: *J Neurophysiol* 54, pp. 782–806.

Mercer, A, DC West, OT Morris, S Kirchhecker, JE Kerkhoff, and AM Thomson (2005). "Excitatory connections made by presynaptic cortico-cortical pyramidal cells in layer 6 of the neocortex". In: *Cereb Cortex* 15, pp. 1485–1496.

Miettinen, R, J Sirvio, PS Riekkinen, MP Laakso, M Riekkinen, and P Jr. Riekkinen (1993). "Neocortical, hippocampal and septal parvalbumin- and somatostatin-

containing neurons in young and aged rats: correlation with passive avoidance and water maze performance". In: *Neuroscience* 53, pp. 367–378.

Migliore, M, C Cannia, WW Lytton, H Markram, and ML Hines (2006). "Parallel network simulations with NEURON". In: *J Comput Neurosci* 21, pp. 119–129.

Milton, JG, J Gotman, GM Remillard, and F Andermann (1987). "Timing of seizure recurrence in adult epileptic patients: a statistical analysis". In: *Epilepsia* 28, pp. 471–478.

Mizukawa, K, PL McGeer, SR Vincent, and EG McGeer (1987). "The distribution of somatostatin-immunoreactive neurons and fibers in the rat cerebral cortex: light and electron microscopic studies". In: *Brain Res* 426, pp. 28–36.

Monyer, H and H Markram (2004). "Interneuron Diversity series: Molecular and genetic tools to study GABAergic interneuron diversity and function". In: *Trends Neurosci* 27, pp. 90–97.

Morgan, RJ and I Soltesz (2008). "Nonrandom connectivity of the epileptic dentate gyrus predicts a major role for neuronal hubs in seizures". In: *Proc Natl Acad Sci U S A* 105, pp. 6179–6184.

Morrison, A, M Diesmann, and W Gerstner (2008). "Phenomenological models of synaptic plasticity based on spike timing". In: *Biological cybernetics* 98, pp. 459–478.

Pangratz-Fuehrer, S and S Hestrin (2011). "Synaptogenesis of electrical and GABAergic synapses of fast-spiking inhibitory neurons in the neocortex". In: *J Neurosci* 31, pp. 10767–10775.

Petersen, CC and B Sakmann (2000). "The excitatory neuronal network of rat layer 4 barrel cortex". In: *J Neurosci* 20, pp. 7579–7586.

Porter, JT, B Cauli, JF Staiger, B Lambolez, J Rossier, and E Audinat (1998). "Properties of bipolar VIPergic interneurons and their excitation by pyramidal neurons in the rat neocortex". In: *Eur J Neurosci* 10, pp. 3617–3628.

Ren, JQ, Y Aika, CW Heizmann, and T Kosaka (1992). "Quantitative analysis of neurons and glial cells in the rat somatosensory cortex, with special reference to GABAergic neurons and parvalbumin-containing neurons". In: *Exp Brain Res* 92, pp. 1–14.

Ren, M, Y Yoshimura, N Takada, S Horibe, and Y Komatsu (2007). "Specialized inhibitory synaptic actions between nearby neocortical pyramidal neurons". In: *Science* 316, pp. 758–761.

Reyes, A and B Sakmann (1999). "Developmental switch in the short-term modification of unitary EPSPs evoked in layer 2/3 and layer 5 pyramidal neurons of rat neocortex". In: *J Neurosci* 19, pp. 3827–3835.

Reyes, A, R Lujan, A Rozov, N Burnashev, P Somogyi, and B Sakmann (1998). "Target-cell-specific facilitation and depression in neocortical circuits". In: *Nat Neurosci* 1, pp. 279–285.

Richardson, MJ, O Melamed, G Silberberg, W Gerstner, and H Markram (2005). "Short-term synaptic plasticity orchestrates the response of pyramidal cells and interneurons to population bursts". In: *J Comput Neurosci* 18, pp. 323–331.

Robbins, R. J., M. L. Brines, J. H. Kim, T. Adrian, N. De Lanerolle, S. Welsh, and D. D. Spencer (1991). "A selective loss of somatostatin in the hippocampus of patients with temporal lobe epilepsy." In: *Ann.Neurol.* 29, pp. 325–332.

Robinson, H. P. and N. Kawai (1993). "Single channel properties at the synaptic site." In: *Cereb Cortex* 63, pp. 250–65.

Rosen, GD, KM Jacobs, and DA Prince (1998). "Effects of neonatal freeze lesions on expression of parvalbumin in rat neocortex". In: *Cereb Cortex* 8, pp. 753–761.

Rozov, A, J Jerecic, B Sakmann, and N Burnashev (2001). "AMPA receptor channels with long-lasting desensitization in bipolar interneurons contribute to synaptic depression in a novel feedback circuit in layer 2/3 of rat neocortex". In: *J Neurosci* 21, pp. 8062–8071.

Schwarz, P, CC Stichel, and HJ Luhmann (2000). "Characterization of neuronal migration disorders in neocortical structures: loss or preservation of inhibitory interneurons?" In: *Epilepsia* 41, pp. 781–787.

Schwindt, P. and W. O'Brien J. A.and Crill (1997). "Quantitative analysis of firing properties of pyramidal neurons from layer 5 of rat sensorimotor cortex." In: *J Neurophysiol.* 77, pp. 2484–2498.

Silberberg, G and H Markram (2007). "Disynaptic inhibition between neocortical pyramidal cells mediated by Martinotti cells". In: *Neuron* 53, pp. 735–746.

Silva, F H Lopes da, A Hoeks, H Smits, and L H Zetterberg (1974). "Model of brain rhythmic activity The alpha-rhythm of the thalamus". In: *Kybernetik* 15, pp. 27–37.

Silva, F. H. Lopes da, A. Van Rotterdam, P. Barts, E. Van Heusden, and W. Burr (1976). "Models of neuronal populations: the basic mechanisms of rhythmicity." In: *Progress in brain research* 45, pp. 281–308.

Soltesz, I. and K Staley (2008). *Computational Neuroscience in Epilepsy*. Burlington, MA: Academic Press.

Spampanato, J, I Aradi, I Soltesz, and AL Goldin (2004). "Increased neuronal firing in computer simulations of sodium channel mutations that cause generalized epilepsy with febrile seizures plus". In: *J Neurophysiol* 91, pp. 2040–2050.

Strack, B., K. M. Jacobs, and K. J. Cios (2011). "Study of inhibition influence on epileptic seizures with a network of spiking neurons." In: *Society for Neuroscience Abstracts* 37, p. 622.25.

Strack, B., K. M. Jacobs, and K. J. Cios (2013a). "Biological Restraint on the Izhikevich Neuron Model Essential for Seizure Modeling". In: *IEEE EMBS Conference on Neural Engineering*.

— (2013b). "Simulating lesions in multi-layer, multi-columnar model of neocortex". In: *IEEE EMBS Conference on Neural Engineering*.

Strogatz, SH (2001). "Exploring complex networks". In: *Nature* 410, pp. 268–276.

Suffczynski, P., S. Kalitzin, G. Pfurtscheller, and F. H. Lopes da Silva (2001). "Computational model of thalamo-cortical networks: dynamical control of alpha rhythms in relation to focal attention." In: *International Journal of Psychophysiology* 43, pp. 25–40.

Suffczynski, P, S Kalitzin, and FH Lopes da Silva (2004). "Dynamics of non-convulsive epileptic phenomena modeled by a bistable neuronal network". In: *Neuroscience* 126, pp. 467–484.

Suffczynski, P., F. Lopes da Silva, J. Parra, D. Velis, and S. Kalitzin (2005). "Epileptic transitions: model predictions and experimental validation. Journal of clinical neurophysiology?" In: *official publication of the American Electroencephalographic Society* 22, pp. 288–99.

Sunderam, S, I Osorio, M G FreiAnd, and J F 3rd Watkins (2001). "Stochastic modeling and prediction of experimental seizures in Sprague-Dawley rats". In: *J Clin Neurophysiol* 18, pp. 275–282.

Sussillo, D, T Toyoizumi, and W Maass (2007). "Self-tuning of neural circuits through short-term synaptic plasticity". In: *J Neurophysiol* 97, pp. 4079–4095.

Swiercz, W, K Cios, J Hellier, A Yee, and K Staley (2007). "Effects of synaptic depression and recovery on synchronous network activity". In: *J Clin Neurophysiol* 24, pp. 165–174.

Tamas, G, EH Buhl, and P Somogyi (1997). "Fast IPSPs elicited via multiple synaptic release sites by different types of GABAergic neurone in the cat visual cortex". In: *J Physiol* 500, pp. 715–738.

Tamas, G, P Somogyi, and EH Buhl (1998). "Differentially interconnected networks of GABAergic interneurons in the visual cortex of the cat". In: *J Neurosci* 18, pp. 4255–4270.

Tarczy-Hornoch, K, KA Martin, JJ Jack, and KJ Stratford (1998). "Synaptic interactions between smooth and spiny neurones in layer 4 of cat visual cortex in vitro". In: *J Physiol* 508, pp. 351–363.

Telfeian, A E and B W Connors (1998). "Layer-specific pathways for the horizontal propagation of epileptiform discharges in neocortex". In: *Epilepsia* 39, pp. 700–708.

— (2003). "Widely integrative properties of layer 5 pyramidal cells support a role for processing of extralaminar synaptic inputs in rat neocortex". In: *Neurosci Lett* 343, pp. 121–124.

Thomson, A. M. and J Deuchars (1997). "Synaptic interactions in neocortical local circuits: dual intracellular recordings in vitro." In: *J. Cereb.Cortex* 7, pp. 510–522.

Thomson, A. M., D. C. West, Y. Wang, and A. P. Bannister (2002). "Synaptic connections and small circuits involving excitatory and inhibitory neurons in layers 2-5 of adult rat and cat neocortex: triple intracellular recordings and biocytin labelling in vitro." In: *Cereb.Cortex* 12, pp. 936–953.

Thomson, AM (2003). "Presynaptic frequency- and pattern-dependent filtering". In: *J Comput Neurosci* 15, pp. 159–202.

Thomson, AM and AP Bannister (1998). "Postsynaptic pyramidal target selection by descending layer III pyramidal axons: dual intracellular recordings and biocytin filling in slices of rat neocortex". In: *Neuroscience* 84, pp. 669–683.

Thomson, AM and C Lamy (2007). "Functional maps of neocortical local circuitry". In: *Front Neurosci* 1, pp. 19–42.

Thomson, AM and OT Morris (2002). "Selectivity in the inter-laminar connections made by neocortical neurones". In: *J Neurocytol* 31, pp. 239–246.

Thomson, AM, J Deuchars, and DC West (1993). "Large, deep layer pyramid-pyramid single axon EPSPs in slices of rat motor cortex display paired pulse and frequency-dependent depression, mediated presynaptically and self-facilitation, mediated postsynaptically". In: *J Neurophysiol* 70, pp. 2354–2369.

Thomson, AM, DC West, and J Deuchars (1995). "Properties of single axon excitatory postsynaptic potentials elicited in spiny interneurons by action potentials in pyramidal neurons in slices of rat neocortex". In: *Neuroscience* 69, pp. 727–738.

Thomson, AM, DC West, J Hahn, and J Deuchars (1996). "Single axon IPSPs elicited in pyramidal cells by three classes of interneurones in slices of rat neocortex". In: *J Physiol* 496, pp. 81–102.

Traub, R D, J G R Jefferys, and M A Whittington (1999,). *Fast Oscillations in Cortical Circuits*. MIT Press.

Traub, R D, D Contreras, and M A Whittington (2005a). "Combined experimental/simulation studies of cellular and network mechanisms of epileptogenesis in vitro and in vivo." In: *J.Clin.Neurophysiol* 22, pp. 330–342.

Traub, R D, D Contreras, M O Cunningham, H Murray, F E LeBeau, A Roopun, A Bibbig, W B Wilent, M J Higley, and M A Whittington (2005b). "Single-column thalamocortical network model exhibiting gamma oscillations, sleep spindles, and epileptogenic bursts". In: *J Neurophysiol* 93, pp. 2194–2232.

Traub, RD, R Miles, and R K Wong (1989). "Model of the origin of rhythmic population oscillations in the hippocampal slice." In: *Science* 243, pp. 1319–1325.

Traub, RD, J Jefferys, and M Whittington (1997). "Simulation of Gamma Rhythms in Networks of Interneurons and Pyramidal Cells". In: *J Comput Neurosci* 4, pp. 141–150.

Traub, RD, MO Cunningham, T Gloveli, FE LeBeau, A Bibbig, EH Buhl, and MA Whittington (2003). "GABA-enhanced collective behavior in neuronal axons underlies persistent gamma-frequency oscillations". In: *Proc Natl Acad Sci U S A* 100, pp. 11047–11052.

Trevelyan, A. J., D. Sussillo, B. O. Watson, and R. M Yuste (2006). "odular propagation of epileptiform activity: evidence for an inhibitory veto in neocortex." In: *The Journal of neuroscience* 26, pp. 12447–55.

Trotter, SA, J Kapur, MJ Anzivino, and KS Lee (2006). "GABAergic synaptic inhibition is reduced before seizure onset in a genetic model of cortical malformation". In: *J Neurosci* 26, pp. 10756–10767.

Tsodyks, M, K Pawelzik, and H Markram (1998). "Neural networks with dynamic synapses". In: *Neural Comput* 10, pp. 821–835.

Tsodyks, M, A Uziel, and H Markram (2000). "Synchrony generation in recurrent networks with frequency-dependent synapses". In: *J Neurosci* 20, RC50.

Ullah, M and O Wolkenhauer (2007). "Family tree of Markov models in systems biology". In: *IET Syst Biol* 1, pp. 247–254.

Van Schaik, A., C. Jin, A. McEwan, and T. J. Hamilton (2010). "A log-domain implementation of the Izhikevich neuron model." In: *Proceedings of 2010 IEEE International Symposium on Circuits and Systems (ISCAS)*, pp. 4253–4256.

Voges, N, A Schuz, A Aertsen, and S Rotter (2010). "A modeler's view on the spatial structure of intrinsic horizontal connectivity in the neocortex". In: *Prog Neurobiol* 92, pp. 277–292.

von, EJ, M Eliava, AH Meyer, A Rozov, and H Monyer (2007). "Functional characterization of intrinsic cholinergic interneurons in the cortex". In: *J Neurosci* 27, pp. 5633–5642.

Wang, Y, A Gupta, M Toledo-Rodriguez, CZ Wu, and H Markram (2002). "Anatomical, physiological, molecular and circuit properties of nest basket cells in the developing somatosensory cortex". In: *Cereb Cortex* 12, pp. 395–410.

Wang, Y., M. Toledo-Rodriguez, A. Gupta, C. Wu, G. Silberberg, J. Luo, and H. Markram (2004). "Anatomical, physiological and molecular properties of Martinotti cells in the somatosensory cortex of the juvenile rat." In: *The Journal of physiology* 561, pp. 65–90.

Wang, Y, H Markram, PH Goodman, TK Berger, J Ma, and PS Goldman-Rakic (2006). "Heterogeneity in the pyramidal network of the medial prefrontal cortex". In: *Nat Neurosci* 9, pp. 534–542.

Watts, DJ and SH Strogatz (1998). "Collective dynamics of 'small-world' networks". In: *Nature* 393, pp. 440–442.

Watts, J and AM Thomson (2005). "Excitatory and inhibitory connections show selectivity in the neocortex". In: *J Physiol* 562, pp. 89–97.

Wendling, F (2008). "Computational models of epileptic activity: a bridge between observation and pathophysiological interpretation". In: *Expert Rev Neurother* 8, pp. 889–896.

West, DC, A Mercer, S Kirchhecker, OT Morris, and AM Thomson (2006). "Layer 6 cortico-thalamic pyramidal cells preferentially innervate interneurons and generate facilitating EPSPs". In: *Cereb Cortex* 16, pp. 200–211.

Whittington, MA, RD Traub, and JG Jefferys (1995). "Synchronized oscillations in interneuron networks driven by metabotropic glutamate receptor activation". In: *Nature* 373, pp. 612–615.

Whittington, MA, RD Traub, N Kopell, B Ermentrout, and EH Buhl (2000). "Inhibition-based rhythms: experimental and mathematical observations on network dynamics". In: *International Journal of Psychophysiology* 38, pp. 315–336.

Yang, KH, PJ Franaszczuk, and GK Bergey (2002). "The influence of synaptic connectivity on the pattern of bursting behavior in model pyramidal cells". In: *Neurocomputing* 44-46, pp. 233–242.

Yee, E and J Teo (2011). "Evolutionary spiking neural networks as racing car controllers". In: *11th International Conference on Hybrid Intelligent Systems (HIS)*, pp. 411–416.

Yoshimura, Y, JL Dantzker, and EM Callaway (2005). "Excitatory cortical neurons form fine-scale functional networks". In: *Nature* 433, pp. 868–873.

Zhang, L. L., P. A. Collier, and K. W. Ashwell (1995). "Mechanisms in the induction of neuronal heterotopiae following prenatal cytotoxic brain damage." In: *Neurotoxicology and teratology* 17, pp. 297–311.

Zsombok, A and K M Jacobs (2007). "Postsynaptic Currents Prior to Onset of Epileptiform Activity in Rat Microgyria". In: *J Neurophysiol* 98, pp. 178–186.

VITA

Beata Strack received her M.S. degree in Applied Mathematics in 2008 from AGH University of Science and Technology, Krakow, Poland, and then joined the Department of Applied Mathematics at AGH to conduct research in the field of spectral operator theory. Currently, she is a Ph.D. candidate at the Department of Computer Science, Virginia Commonwealth University, Richmond, U.S.A. Her research interests include computational neuroscience and data mining in medical data.